49

Multifunctional Systems With Polymer Actuators: Mechanochromism And Peristaltic Pumping

by

Melinda Joy Cromie

B.S. Mechanical Engineering 2003
University of California, Davis

Submitted to the Department of Mechanical Engineering
in Partial Fulfillment of the Requirements for the Degree of

Master of Science in Mechanical Engineering

at the
Massachusetts Institute of Technology
September 2005

Signature of Author .....

Department of Mechanical Engineering
August 1, 2005

Certified by .....

Edwin L. Thomas
Morris Cohen Professor of Materials Science and Engineering
Director, Institute for Soldier Nanotechnologies
Thesis Supervisor

Certified by .....

William A. Peters
Executive Director, Institute for Soldier Nanotechnologies
Thesis Supervisor

Certified by .....

Gareth H. McKinley
Professor of Mechanical Engineering
Thesis Reader

Accepted by .....

Lallit Anand
Professor of Mechanical Engineering
Chairman, Graduate Committee

Multifunctional Systems With Polymer Actuators:
Mechanochromism And Peristaltic Pumping

by

Melinda Joy Cromie

Submitted to the Department of Mechanical Engineering on August 1, 2005
in Partial Fulfillment of the Requirements for the Degree of
Master of Science in Mechanical Engineering

Abstract

The mission of the ISN is to explore the long-range vision of the role of nanotechnology in the future of soldier protection. Unprecedented survivability will arise from the cohesive and comprehensive coordination of the functions and interactions of each technology. The present work approaches these objectives with basic research to support the development of two multifunctional soldier survivability systems, pumping microfibers and mechanochromic pixels.

Progress was made along the two major paths of investigation towards the realization of a pumping microfiber. Polypyrrole was chemically deposited onto copolyetherester. Tubular polypyrrole actuators at the millimeter scale were electrochemically fabricated and actuated.

Mechanochromic polymers can be combined with actuating polymers to create a color changing pixel. Reflectance spectrum changes with strain in mechanochromic materials were characterized. Several pixel designs were analyzed and tested in which the polymer actuator polypyrrole induces deformation of the mechanochromic block copolymer.

Integrative studies inform the overall systems architecture of the far future battlesuit. Scoping calculations to investigate battlesuit functionality requirements were performed. The multiscale, multifunctional design solutions employed in the human body and the US Army and were studied, and the Dynamic Systems Integration Map was developed to apply the lessons learned to coordinate and leverage the many emerging survivability technologies.

Thesis Supervisor:	Prof. Edwin L. Thomas
Title:	Morris Cohen Professor of Materials Science and Engineering Director, Institute for Soldier Nanotechnologies
Thesis Supervisor:	Dr. William A. Peters
Title:	Executive Director, Institute for Soldier Nanotechnologies

Table of Contents

Acknowledgements

Prof. Thomas and Dr. Peters, thank you for being my advisors. Thank you for having confidence in me and for giving me the opportunities that you have.
Rachel 'Zim' Pytel, you have helped me in more ways than will fit on this little page. Thanks for teaching me about polymer actuators, volleyball, and life. Thanks for being the best 'driver' I could have asked for at nationals. I will miss you.
Jongseung Yoon, thanks for synthesizing the PS-PI for me, for teaching me polymer physics, and for your help with experiments.
Jocelyn Nadeau, thanks for your help with electrochemistry and the potentiostat.
Jeff Baur, thanks for many conversations and insights that helped me find direction.
Brian Pate, thanks for your help in finding direction on my research.
Matt Traum, thanks for being my Project 7.3 partner and office mate.
Melis Arslan, thanks for being my late night lab buddy. I will miss coffee shop breaks with you.
Ludovik, thanks for greeting me early in the morning with your cheerful ties.
Robin, Conor, Mike, Kathie, Adam, Dave, thanks for being such wonderful friends and understanding my sense of humor.
To Eve Downing, Charlie Dean, Lisa Shaler-Clark, Cathy Byrne, Josh Freedman, Joanne Maxwell, Marco Carega, thank you for so many contributions of insight, advice, and help in all things large and small during my time at the ISN.
To my family, I am so thankful for your love, encouragement, and help. I love you.

Thank you to Carberry's for making Heklas, to Beantowne coffee shop for blondie lattes, and to the Thirsty for good times with good friends.

Table of Figures

1. Background and Motivation

1.1. The Institute for Soldier Nanotechnologies

The Institute for Soldier Nanotechnologies (ISN) is an interdisciplinary research facility founded in March 2002 by a contract from the US Army. The mission of the ISN is to explore the long-range vision of the role of nanotechnology in the future of soldier protection. The ISN includes MIT, the US Army, and industry partners. MIT researchers from Mechanical Engineering, Chemical Engineering, Chemistry, Mathematics, Electrical Engineering, Materials Science and Engineering, and Physics collaborate on nanotechnology research projects. Incorporation of these developing technologies into a far future nano-rich battlesuit will achieve unprecedented survivability capabilities for the soldier.

1.2. Systems Architectures and Integration Project

Such a survivability system is highly complex with manifold opportunities for interactions between battlesuit technologies. The unprecedented capabilities will arise from the ability to cohesively and comprehensively coordinate and capitalize on the functions and interactions of each technology. In the technology pathway from research and development through product design, the sooner a potential interaction is found, the easier it is to turn it into an additional capability instead of a destructive mode. There are many challenges in integrating a complex system comprised largely of technologies that are still in the research and development phase. Engineers commonly design interfaces between complex subsystems. Control algorithms employed further balance the interactions between components. But can traditional processes of interface design and control algorithms be translated directly to a multiscale nanorich system such as the battlesuit?

The Systems Architectures and Integration project (ISN project number 7.3; web.mit.edu/isn) addresses the research question: What are the rules of integration for nanoscale and multiscale systems? The approach is to knit nanotechnologies together towards functional battlesuit subsystems, and to devise tools that will help plausible battlesuit system architectures to guide ISN research and further system development. In doing so, the rules of integration for multiscale systems will be observed. The stated objectives of the project are to: capitalize on diverse nanotechnologies; illuminate systems of nanotechnologies that enable multiple survivability capabilities; identify research, development and systems integration requirements; elucidate synergistic combinations of nanotechnologies; realize unprecedented functionalities. My thesis project encompasses both experimental and theoretical methods to further these objectives.

The present work encompasses both experimental and theoretical tools to further these objectives. To develop the understanding of nanocomponent integration, two subsystems enabled by polymer actuators are designed and tested: pumping microfibers and mechanochromic pixels. The lessons learned will inform the design of subsystems for the high tech battlesuit. A systems architecture tool is proposed to apply the lessons

learned to improve the basic research, tailored to the unique needs of a complex, multiscale system in early stages of development.

1.3. Pumping Microfibers

Some of the emerging ISN nanotechnologies and the subsystems into which they will be integrated will depend on fluid transport. These will depend on microfluidic systems and circuits incorporated into the battlesuit. Microfluidic circuits are currently largely based on rigid chips, but the vision for the battlesuit is a flexible textile platform.
Hollow microfibers developed by ISN industry partner DuPont have been identified as a potential platform for flexible polymer based microfluidic systems that can be interwoven with textiles. Taking inspiration from the human body, fluid circuits could enable an artificial vasculature to transport various protective elements throughout the battlesuit. Fiber circuits could be functionalized for drug delivery, local thermal control, stiffness on demand, and chemical control systems. See additional discussion of biomimetic multiscale systems in chapter 4. Soldier-mounted pumping capabilities will be required to move fluids through the fluidic circuit as described above. High pressures are required for fluid flow in small tubes, and long segments of the hollow fibers would be needed to achieve the envisioned ubiquitous network.

Chapter 2 discusses one branch of experimentation in this work, which will integrate electroactive polypyrrole actuators with hollow elastomeric microfibers toward development of a microscale peristaltic pump. Pumping microfibers are one plausible enabling technology to achieve distributed pumping power throughout a flexible microfluidic network of hollow fibers. Specifically, an actuator based on polypyrrole could be used to compress successive sections of a hollow fiber to enable a microscale peristaltic pump.

The advantage and importance of such a pump lies in its ability to provide low profile, distributed pumping power. The distributed peristaltic system conceived here would eliminate the need for a large central pump by incorporating the force generation element (the polymer actuator) into the microfiber. In addition to lowering the bulk, the distributed pumping scheme can provide redundant pumping systems.

Design concepts for a tiny peristaltic pump are postulated and experimentally investigated. The properties of polypyrrole as an electroactive polymer actuator are introduced from the literature. The properties of the elastomeric hollow fibers are described.

Key issues of integration are studied, including mechanical properties, electrical properties, and material properties. Requirements for pumping performance are calculated, including pressure requirements, power requirements, and projected flow rates. Description of the electrochemical circuit elements required for polypyrrole actuation are discussed in light of the unique challenges of achieving the pumping microfiber design. Materials interface issues are also addressed. Strong adhesion must be achieved between the deforming polypyrrole layer and the passive elastomer fiber.

The polypyrrole actuator material is polymerized electrochemically onto an electrode; it cannot be synthesized directly onto the non-conducting fiber.

Key design challenges identified were to synthesize actuator quality polypyrrole in the desired geometry, to maintain adherence of the actuating polypyrrole to the passive elastomer, to achieve sufficient electrical contact with the polypyrrole, and to incorporate the necessary ion source.

To address these key design challenges, experimental investigation into the feasibility of a pumping microfiber followed two paths simultaneously: adhesion between the polypyrrole actuator and the microfiber, and radial actuation of hollow polypyrrole tubes. Chemical and electrochemical deposition methods in the literature must be adapted to achieve actuator quality polypyrrole on a nonconductive elastomer microfiber. Chemical deposition is explored as a way to achieve a smooth, conductive layer of polypyrrole which would adhere to the fiber and serve as a working electrode for the electropolymerization of the polymer actuator. Tubular polypyrrole actuators at the millimeter scale were electrochemically fabricated and actuated. Radial actuation properties at this more manageable scale must be understood, then the micron scale can be investigated.

1.4. Mechanochromic Pixel

Chapter 3 discusses another branch of experimentation, which integrates polypyrrole actuators with mechanochromic block copolymers towards development of an on-demand color changing pixel. In a mechanochromic material, deformations cause color change. The polymer actuator, polypyrrole, swells by the incorporation of ions under electrical stimulus. Polypyrrole induces deformation of the mechanochromic block copolymer to create a color changing pixel.

Block copolymers of high molecular weight form lamellae (layers) that reflect light in the visible range. Deformations of the bulk material can change the thickness of the lamellae, which changes the color of the reflected light. Materials with this characteristic are called "mechanochromic." To properly design a mechanochromic pixel, the material must be characterized. For this work, two block polymer systems were studied, polystyrene-polyisoprene and polybutadiene-polyisoprene. The reflectance spectrum as a function of strain was measured, and the reflectance analyzed using the Transfer Matrix Method.

Design concepts for these pixels are analyzed and/or tested. Design calculations determine the necessary amounts of strain and predict the corresponding color change.

Key integration issues are force generation, strain amplification, and chemical compatibility. The relative forces transferred from the polypyrrole to the gel were analyzed for different designs. Polypyrrole can repeatably produce 1%-3% strain without degradation, while 10% strain is needed in the block copolymer to see a significant change in color (30 nm shift in wavelength). For chemical compatibility, the polypyrrole

must have an electrolyte source for actuation, and this source must not interfere with or degrade the mechanochromic material.

1.5. Systems Architectures: Inspirational Systems

The vision for the far future battlesuit is a complex system in a complex multiscale system-of-systems, incorporating various multifunctional subsystems such as the above described pumping microfibers and mechanochromic pixels. The third component of the thesis project will be part of the integrative studies of Project 7.3 to inform the overall systems architecture of the far future battlesuit. The approach will include performing scoping calculations to investigate battlesuit functionality requirements, studying inspirational systems, and developing systems architectures that tractably organize the many emerging technologies that may be integrated into the battlesuit. Inspirational design paradigms are learned from the human body, a proven, nano-rich system with multifunctional, multiscale protection systems. Lessons learned from the human skin, vasculature, and neural control systems are described. Paradigms for optimally leveraging and synergistically combining discrete elements in complex systems are informed by analogy to the Battle Command Construct described by the US Army Training and Doctrine Command (TRADOC).

1.6. Systems Architectures: Enabling Visualization Tool

To realize these paradigms in an eventual battlesuit system, the integration paradigms learned from the human body and the US Army must influence basic research and early technology development. A flexible design visualization tool is needed to inform basic research. The tool should identify and harness the capabilities of emerging technologies, and have maximum flexibility to adapt as new design requirements and new research areas emerge. The systems architectures should be an open framework that will integrate nano-enabled survivability capabilities in an informative and tractable way, with a method that fits the complexity of the system and the early stage of system development.

To this end, the Dynamic Systems Integration Map (DSIM) is proposed. DSIM is a tool to inform the systems integration aspects of basic research. The dynamic node-based taxonomy is inspired by the Resonance Hypothesis. The Resonance Hypothesis is introduced: a method to identify potentially non-intuitive areas for innovative research. DSIM also highlights system interactions between components that contribute to a particular soldier survivability capability, identifies components with similar features and functionalities, and informs innovative teaming of R&D assets, with a graphical interface that can be dynamically explored and tailored to a stakeholder's needs. DSIM maps out an open system architecture that will be user-friendly, yet competent for the high complexity of nano-components integration and the early stage of research.

1.7. Summary

Nanotechnologies have the potential to provide soldiers with a revolutionary, lighter weight battle uniform that protects them from a host of battlefield dangers and environmental threats, and administers emergency medical treatment. To translate this potential into practicality, nanotechnologies and other technologies will combine in a

comfortable, energy efficient, affordable battle suit. Several technologies will work together simultaneously or in the right sequence. This project will benefit the soldier by developing systems architectures to enable future battle suits to exploit multiple, nanotechnology-enabled survivability capabilities, e.g., threat detection, threat protection, far forward medical treatment, and performance assistance. The current approach involves top down studies to inform the design of the entire suit and bottom up investigations to design, build, and test, simple sub-systems for the suit.

2. Active Multifunctional Polymeric System: Flexible Polymer Pumping Microfibers

2.1. Introduction

As discussed in chapter 1, the vision of the ISN is to conduct basic nanotechnology research towards developing personal protective technologies that will eventually be integrated into the far-future battlesuit. Some of the emerging technologies and the subsystems into which they will be integrated will depend on fluid transport. These will depend on microfluidic systems and circuits being incorporated into the battlesuit. Microfluidic circuits are currently largely based on rigid chips, but the vision for the battlesuit is a flexible textile platform. Hollow microfibers developed by ISN industry partner DuPont have been identified as a potential platform for integration of battlesuit technologies into a textile-based battlesuit. These hollow fibers could enable flexible polymer based microfluidic systems that can be interwoven with textiles. Taking inspiration from the human body, fluid circuits could enable an artificial vasculature to transport various protective elements throughout the battlesuit. Fiber circuits could be functionalized for drug delivery, local thermal control, stiffness on demand, and chemical control systems. See additional discussion of biomimetic multiscale systems in chapter 4.

2.2. Artificial Vasculature

Soldier-mounted pumping capabilities will be required to move fluids through the battlesuit fluidic circuit as described above. High pressures are required for fluid flow in small tubes, and long segments of the hollow fibers would be needed to achieve the envisioned ubiquitous network. A design concept is postulated and experimentally investigated here to achieve distributed pumping power throughout a flexible hollow fiber enabled microfluidic network. Specifically, an actuator based on polypyrrole could be used to compress successive sections of a hollow fiber to enable a microscale peristaltic pump.

The advantage and importance of such a pump lies in its ability to provide low profile, distributed pumping power. Without such a distributed pumping scheme, a large central pump would have to provide all the pump pressure for long segments of small diameter tubing. The distributed peristaltic system conceived here would eliminate the need for the large central pump by incorporating the force generation element (the polymer actuator) into the microfiber. In addition to lowering the bulk, the distributed pumping scheme can provide redundant pumping systems. If one strand or pumping station fails, the entire fluid system does not fail. Polypyrrole has been used as both an actuator and a strain gage, so the potential exists for embedded feedback control of the flow.

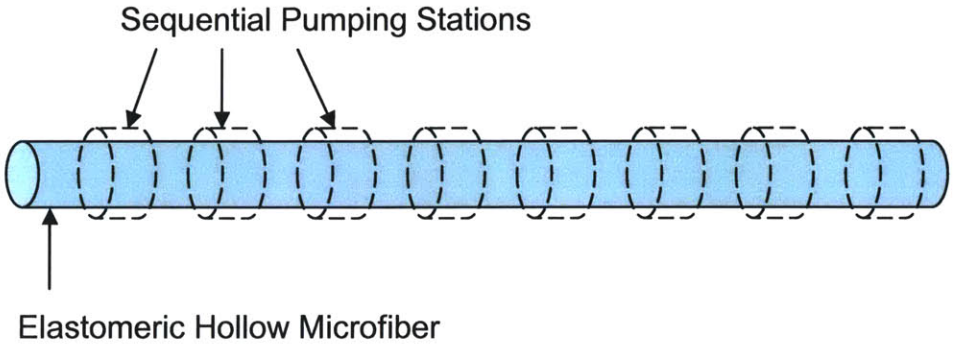

Figure 1 An actuator based on polypyrrole could be used to compress successive sections of a hollow fiber to enable a microscale peristaltic pump.

2.3. Hollow Microfibers

Many configurations of hollow microfibers are possible, including a single hollow channel per fiber or multiple hollow channels per fiber. Bicomponent fibers can be made with multiple channels in which cores and sheaths of each channel are different materials (also called islands-in-the-sea).

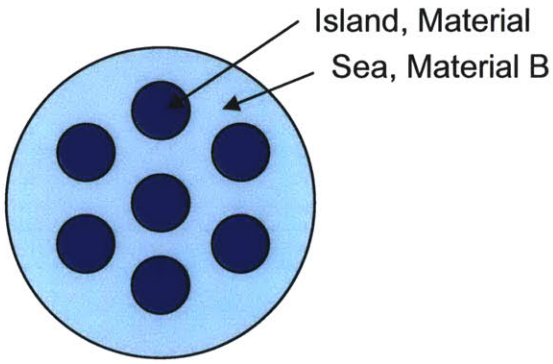

Figure 2 Bicomponent fibers can be made with multiple channels in which cores and sheaths of each channel are different materials (also called islands-in-the-sea).

The fibers are made from a melt by extrusion and post-coalescence. The melt is formed into 4 arcs as it goes through a spinneret. As the 4 sections are drawn together and down, they coalesce and are pulled down to microfiber size. Air to keep the channel inflated while it solidifies is pulled into the channel through the gap just upstream of the coalescence point. Occasional closures in multichannel fibers have been observed. The extrusion process can accommodate various polymers, such as nylons, polyesters and a thermoplastic copolyetherester. Hollow microfibers are used in commercial applications ranging from optical antisoiling fabrics to water purification to aroma-therapeutic textiles (Samuelson, 2003).

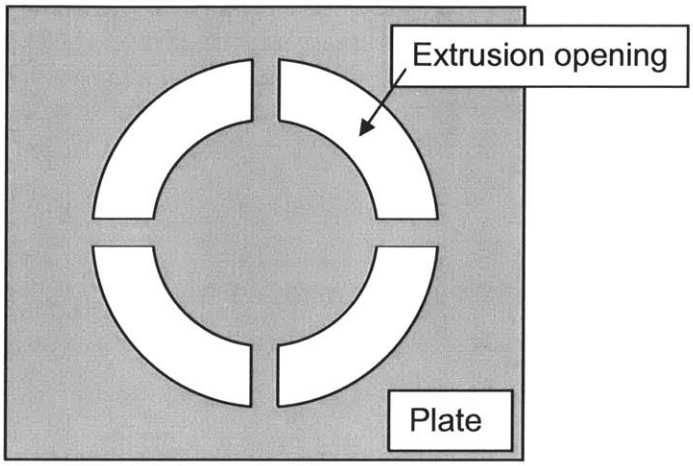

Figure 3 Schematic of spinneret

2.4. Polypyrrole

Polypyrrole has been explored for many uses: batteries, electrochromic devices, selective membranes, capacitors, microelectronics, sensors and mechanical actuators (Bar-Cohen, 2001). It's actuator properties make polypyrrole a potential enabling nanotechnology for multifunctional systems discussed in this work.

2.4.1. Synthesis

Polypyrrole is a conducting polymer. A synonym for conducting polymers is conjugated polymers. The electrons in the alternating single and double bonds along the polymer chain are delocalized, forming a conducting band. The molecular structure of polypyrrole is shown below.

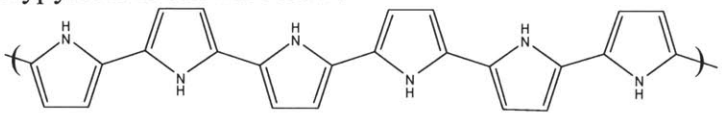

Figure 4 Molecular structure of polypyrrole (Madden, 2003)

Polypyrrole has been synthesized with chemical and electrochemical methods. Chemical methods have been used to achieve conductive surfaces on non-conductive substrates (Appel, 1996; Cheung, 1994; Fou, 1995; Nicolae, 1996; Schoch, 1995; van den Schoor, 1999; Wu, 1997), but these methods generally produces powdery polypyrrole, not robust freestanding films. In general, electrochemically synthesized polypyrrole is the preferred method for making freestanding actuators. It has higher conductivity and mechanical integrity than chemically deposited polypyrrole.

Polypyrrole is synthesized in an electrochemical cell, consisting of a working electrode, a counter electrode, electrolyte, and a reference electrode. The pyrrole monomer is mixed with the electrolyte solution. A potentiostat applies a controlled current to the cell, and the polypyrrole grows as an opaque black film onto the working electrode. The reference electrode measures the voltage in the cell and serves as part of the control feedback loop of the potentiostat.

Several factors in synthesis affect the final properties of the polypyrrole film. The working electrode must be smooth to produce a smooth film. Typical film thicknesses are 30 μm. A uniform electric field arrangement between the working and counter electrodes is important to deposit a uniform thickness. Low temperature polymerizations (-40 to -20°C) produce high conductivity (10^4 S/m) and smooth surface morphology. The voltage levels must be high enough to oxidize the monomer and cause polymerization, but low enough to not degrade the film. Typical cell voltage ranges for the current work were 0.5-1.5 V. The current determines how fast the polymerization proceeds. Typical current density values are of order 0.6 A/m^2 (with respect to the submerged working electrode surface area). Other factors such as pH, solvent, and electrolyte are discussed in Sadki (2000). The primary electrochemical polymerization procedure used in the current work is shown schematically below and described in detail in the appendix.

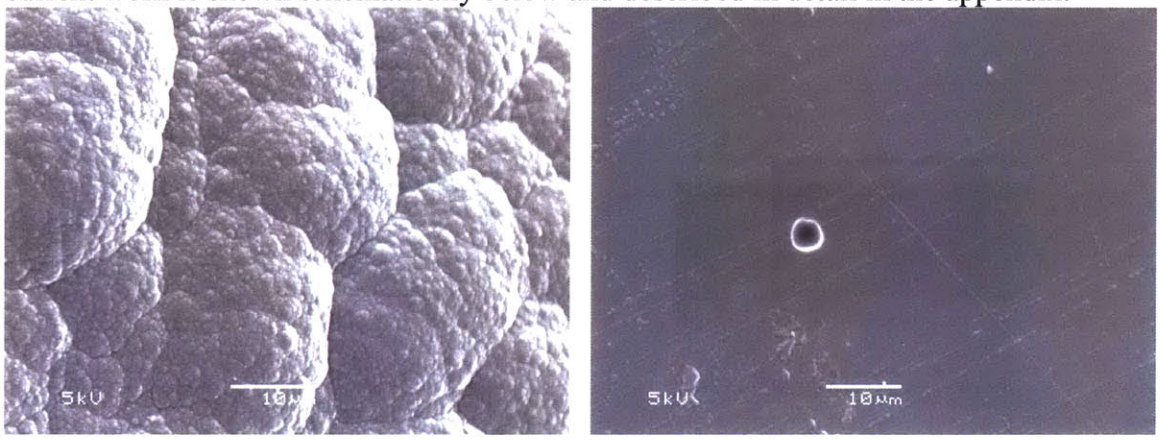

Figure 5 Bumpy and smooth morphologies of electropolymerized polypyrrole films. Low temperature polymerizations (-40 to -20°C) produce high conductivity films (10^4 S/m) with smooth surface morphology.

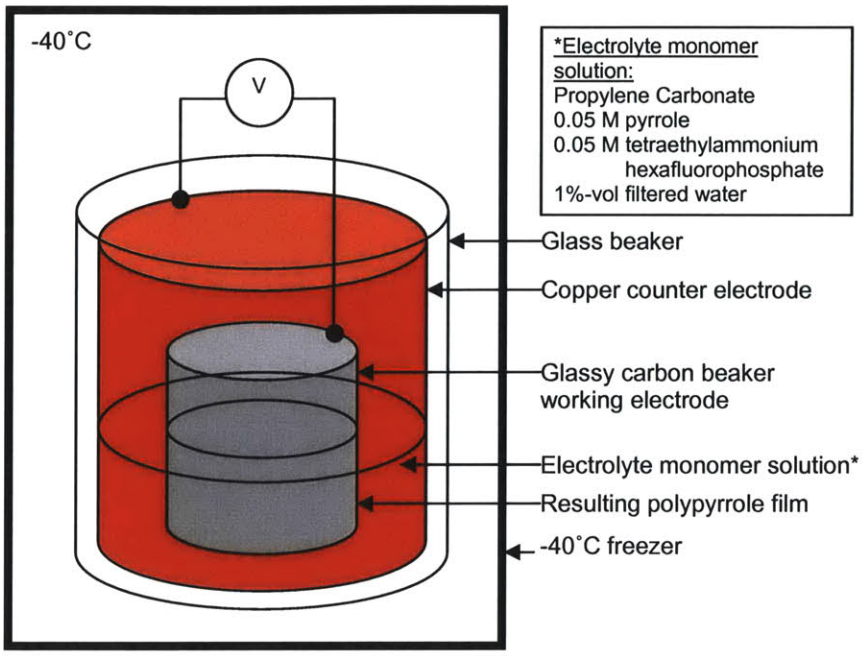

Figure 6 The primary electrochemical polymerization procedure used in the current work. Description in appendix A3.5.

2.4.2. Actuation Mechanism

The primary contributor to actuation is the exchange of ions between the polypyrrole film and the electrolyte ion source. The relative sizes of the anions and cations affect the doping type, and the amount of volume change.

Polypyrrole is electrochemically grown in the oxidized state. Anions from the electrolyte solution in which it was grown will be incorporated into the film to neutralize the charge.

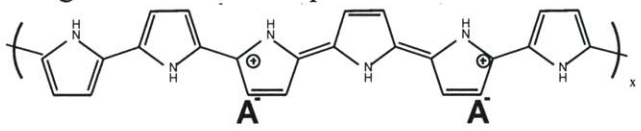

Figure 7 Molecular structure of oxidized polypyrrole. (Madden, 2003)

When the polypyrrole is reduced, the charge will be neutralized by ion transport. The nature of the associated volume change depends on the relative ion sizes.

If the film was grown in a solution with large anions or polyanions in the electrolyte, these ions will be incorporated in the film. By comparison to a smaller cation, the polyanions will be immobile. The cations will be the mobile species that dominates actuation. When the polypyrrole is reduced, cations are incorporated to balance the charge from the immobile anions, and the film expands. When the polypyrrole is oxidized, the cations are expelled to balance the additional positive charge.

If the film is grown is a solution with small anions and large cations, the anions will dominate the ion exchange. The small anion will be expelled from the film to neutralize the net negative charge when the polypyrrole is reduced because the mobility of the

cation to enter the film is lower. When the film is oxidized, the anions are again incorporated. Thus, in contrast to the above situation, the film contracts with reduction and expands with oxidation. Electrolyte systems of this type are used in the present work.

An intermediate case exists when both the anion and cation are of similar mobility (size) in the polypyrrole. Upon reduction, the anions are expelled and the cations are incorporated, resulting in a small net volume change. Upon oxidation, the cations are expelled and the anions incorporated, again resulting in a small net volume change. A summary of the three situations is shown in the table below. Examples of mobile cation and mobile anion electrolyte systems are also listed.

Figure 8 Actuation of polypyrrole with electrolyte systems of differing relative ion sizes

Electrolyte System	Incorporated at Deposition	Mobile Species	Reduction	Oxidation
small cation, large anion	large anion	small cation	cation enters film expands	cation released film contracts
large cation, small anion	small anion	small anion	anion released film contracts	anion enters film expands
equivalently sized ions	anion	both cation and anion	cation enters anion released small net change	cation released anion enters small net change

Figure 9 Examples of mobile cation and mobile anion electrolyte systems for use in polypyrrole actuation.

Mobile Cation Electrolyte Systems	Mobile Anion Electrolyte Systems
lithium perchlorate (Spinks, Madden, Sapp) sodium nitrate (Spinks) potassium nitrate (Spinks) Magnesium nitrate (Spinks) lower strain Barium nitrate (Spinks) lower strain Cadmium nitrate (Spinks) lower strain sodium dodecylbenzenesulfonate (Smela, Bay) sodium polyvinylsulfate (Spinks) sodium chloride (Bay)	tetraethylammonium hexafluorophosphate (Madden) (used in present work) tetrabutylammonium hexafluorophosphate (Rocchia, Spinks, Hara) 1-butyl-3-methyl-imidazolium hexafluorophosphate (Rocchia) 1-butyl-3-methyl-imidazolium tetrafluoroborate (Schmid thesis) tetraethylammonium chloride (Spinks)

In practical terms, the actuation of polypyrrole requires an electrochemical cell with working electrode, counter electrode, electrical input, and electrolyte (ion source). The working electrode connects to the polypyrrole, delivering electrical inputs. The electrical input is generally a sawtooth wave or square wave of approximately ±1-2V. Higher voltages can degrade the polypyrrole, as evidenced by wisps of black residue emerging into the electrolyte solution. Cycling frequency ranges from several Hz to 0.05 Hz or slower. The electrolyte is generally a dissolved salt solution in which the polypyrrole is submerged (acetonitrile, propylene carbonate, and water are common solvents) or a gel

layered with the polypyrrole (Schmid, 2003; Sapp, 1996; Madden, 2000). The electrolyte should be selected to have ions with unequal mobilities, according to the criteria above. High conductivity in polypyrrole will increase the uniformity of oxidation and reduction throughout the film which will lead to more uniform actuation. The electric field around the polypyrrole also affects the oxidation and reduction, and is important in controlling the actuation.

The volume change in polypyrrole has been exploited in a variety of geometric arrangements. Films have been studied under lengthwise contraction, such as in a Dynamic Mechanical Analyzer under load. Bending has been achieved in bilayer and trilayer stacks (Madden, 2000). In a bilayer, a polypyrrole film is layered with an ion source (gel) and a non-actuating layer. Expansion and contraction of the inactive layers produces bending in the structure. A trilayer consists of two polypyrrole layers sandwiching an electrolyte layer to produce bending. One film is oxidized while the other is reduced which results in net bending. Another variation of the trilayer is capabile of linear extension and contraction. The two polypyrrole layers are synthesized with opposite doping. Thus, in opposite oxidation states, both films extend or contract together. Tube geometries have also been synthesized. The axial actuation of these has been studied, but the radial behavior is left largely undescribed (Hara, 2004; Rocchia, 2003). This is in part because of the difficulties associated with creating a radial electric field and measuring the resulting forces and deformations. Fibers coated with polypyrrole have also been studied in contraction (Spinks, 2002). Thin films of polypyrrole (1 μm thick) have demonstrated high anisotropic deformations, achieving up to 30% swelling in thickness as measured with AFM (Smela, 1999). Further anisotropy is studied by stretch alignment of the films. Conductivity is increased along the direction of chain alignment while actuation and creep are increased perpendicular to the chains (Yaumura, 1989).

Figure 10 Polypyrrole performance metrics (Madden, 2003)

PROPERTY	MIN.	TYP.	MAX.	LIMIT
Strain (%)		2	12	> 20
Stress (MPa)		5	34	200
Work Density (kJ/m^3)		100		1000
Strain Rate (%/s)		1	12	10,000
Modulus (GPa)	0.2	0.8	3	
Tensile Strength (MPa)		30	120	400
Applied Potential (V)		1.2	10	
Conductivity (S/m)		10,000	45,000	

2.4.3. Summary: Primary Design Tradeoffs

The design of a multifunctional system with polypyrrole is governed by the above described properties and requirements. Some key design tradeoffs are summarized here.

The rate limiting factor in polypyrrole actuation is ion transport. Thin films can actuate faster due to the shorter time required for mass transport of the ions. The diffusion time constant, τ_D, is proportional to the second power of a characteristic length (thickness)

over the diffusion constant of the ions. Relative sizes of the ions are important: one must be less mobile than the other, whether by its bulk or by being otherwise constrained, such as in an electrolyte gel. Thicker films take longer to actuate but can generate greater total force. If the ion source only contacts the polypyrrole on one face, the diffusion time constant is increased by a factor of 4.

$$\tau_{D,2\,faces} = \frac{L^2}{4D}$$

Equation 1 Diffusion time constant for ion transport from both surfaces of a film. L=thickness, D=diffusion constant (Deen, 1998; Madden, 2003)

$$\tau_{D,1\,face} = \frac{L^2}{D}$$

Equation 2 Diffusion time constant for ion transport from one surface of a film. (Deen, 1998; Madden, 2003)

The ion transport is driven by the oxidation and reduction of the polymer. The applied voltage must overcome internal resistance to evenly propagate and cause uniform actuation. Higher conductivity and increased electrical contact points make the actuation more uniform. Higher driving voltages can be applied to increase actuation and cause faster switching between states. At an upper limit of a few volts polypyrrole can be irreversible oxidized and the film begins to degrade. Though the actuation over a few cycles is increased, the lifespan is extremely limited. Speed of actuation can be increased with the input voltage cycling rate, but higher strains are achieved with slower cycling.

2.4.4. Motivation for Current Work

Polypyrrole was selected as an actuator to be studied for use in the pumping microfiber design. Tubular shaped actuators on the millimeter scale, and fiber actuators on the micron scale had all been studied in axial actuation, but not in radial actuation. The anisotropic high strain response reported by smela raised the question of radial actuation.

2.5. Design Concepts

Two preliminary design schematics were created to guide experimentation, one based on a single channel hollow fiber, and another based on a multichannel fiber. A general fabrication scheme was envisioned for each which informed the direction of the experimentation.

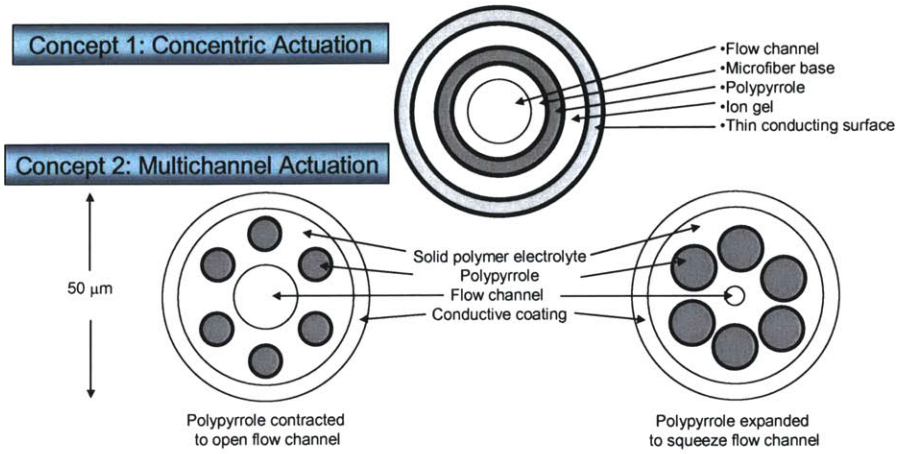

Figure 11 Two preliminary design schematics were created to guide experimentation, one based on a single channel hollow fiber, and another based on a multichannel fiber.

The single channel design was selected to dictate experimentation, since the construction of the pumping components outside the hollow fiber seemed easier to perform and evaluate. The single channel fiber would be processed by extrusion according to the established methods. Then a conductive treatment would be made to the surface of the fiber and the actuator quality polypyrrole would be electropolymerized onto that. At this point characterization studies could be done in an electrolyte bath without the gel or integrated counter electrode. An electrolyte gel layer could be applied, and finally a conductive counter electrode would form the outermost layer. Spaces would be left in the outer layer at regular intervals to allow for electrical contact to the underlying polypyrrole.

The multichannel design concept was rejected for initial study due to the difficulty of polymerizing in the tiny channels and making electrical contact to the polypyrrole in those channels. The inner diameters of the multichannel fibers (10 μm) are smaller than those of the single channel fibers (25 μm). A process postulated for the multichannel design would involve incorporation of ions into the microfiber, either extruded with it in the melt or diffused into the matrix after fabrication, perhaps with the aid of a swelling solvent. Then actuator quality polypyrrole would be electropolymerized into the channels, and multiple electrical contacts must be made with them to complete the circuit for actuation. Finally a counterelectrode would cover the surface.

2.6. Integration Issues

2.6.1. Mechanical

Scoping calculations demonstrated the feasibility of a polypyrrole actuator generating enough power and strain to compress a hollow microfiber and pump fluid through a small diameter tube. The stress generated by the polypyrrole was compared to the stress required to compress an elastomeric tube and the pressure required to move water through a tiny pipe. The geometric basis of the calculations was an elastomeric hollow fiber with 50 μm outer diameter, 25 μm inner diameter, and 2 MPa elastic modulus (DuPont, 2001).

A primary concern in the feasibility study was the question of whether the polypyrrole can generate sufficient force to compress the elastomeric microfiber. Standard equations for thick-walled pipes (wall thickness larger than 10% of radius) under uniform external pressure were used (Roark, 1975).

$$\Delta a = \frac{-qa}{E}\left(\frac{a^2+b^2}{a^2-b^2}-\nu\right)$$

$$\Delta b = \frac{-q}{E}\left(\frac{2a^2 b}{a^2-b^2}\right)$$

a= outer radius (25 μm)
b= inner radius (12.5 μm)
q= external pressure (5 MPa)
E= elastic modulus (2 MPa)
ν= Poisson's ratio (0.45)

Equation 3 Deformations of thick-walled pipes under uniform external pressure. (Roark,)

Using these typical values for polypyrrole stress generation and copolyetherester elastic modulus, the above relations gave nonsensical results, indicating decreases in radii larger than the actual radii. Clearly this was not possible, and buckling would have occurred first. The equations above break down in this limit, but this analysis showed that the forces generated by the polypyrrole will not be limiting factor in the compression of the tube; instead the strains generated will be the limiting factor.

Hollow polypyrrole tubular actuators have been reported to decrease in radius by 20% (Rocchia). Rearranging the above equations to solve for the external pressure, it was estimated that 0.8 MPa of stress will be required to induce a 20% change in the outer radius of the copolyetherester fiber. This is below the typical value of stress obtained from polypyrrole (5 MPa).

$$q = \frac{-E\frac{\Delta a}{a}}{\left(\frac{a^2+b^2}{a^2-b^2}-\nu\right)} = 0.8MPa$$

Equation 4 Stress required to induce 20% change in radius.

However, 20% is a high strain to achieve in uniform compression of a soft tube. It is highly likely that radial symmetry will be lost in the real actuation process. The microscope images below show thin slices of microfiber cross sections. The soft sections have deformed under cutting and handling. The post-coalescence process by which the microfibers are made can be used to design bending points in the microfiber walls. The fibers shown here were extruded from a spinneret. The points of post-coalescence have a slightly reduced wall thickness and create preferential bending points. These points can be controlled by changing the shape of the spinneret.

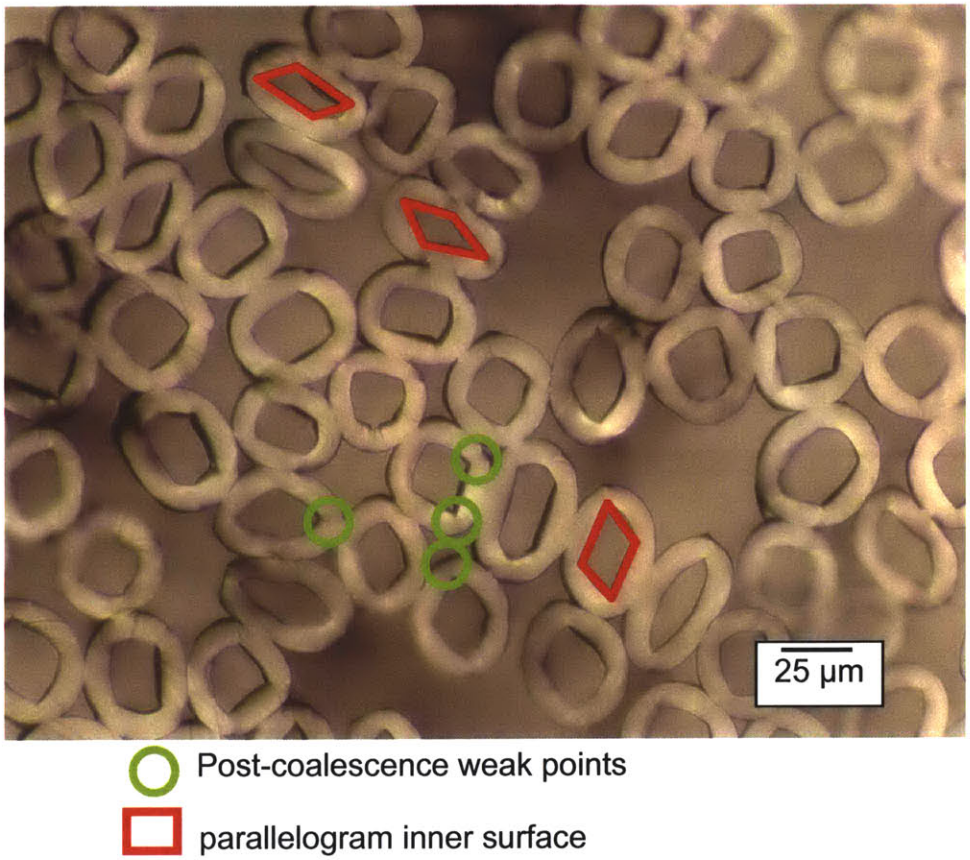

Figure 12 The post-coalescence process by which the microfibers are made can be used to design preferential bending in the microfiber walls. (optical micrograph courtesy V. Samuelson)

In peristaltic pumping, the nature of the shape change is not as important as the net decrease in cross sectional area. The microfiber images above can be approximated geometrically to estimate the deformations needed to achieve a 36% decrease in cross sectional area (for comparison to the above estimations of purely radially symmetric deformations). The needed strain will be found from the constraints of a 36% decrease in cross sectional area while the perimeter remains constant. One geometric construct would be to consider the deformation of a circle into an ellipse. However, the inner surface of a fiber in the micrograph is somewhere between an ellipse and a rhombus. As discussed above, the post-coalescence points in the melt stream create preferential bending points in the microfiber walls, creating 4 'corners' instead of a rounded ellipse. The simpler geometry of a square becoming deformed into a rhombus was selected for the estimation.

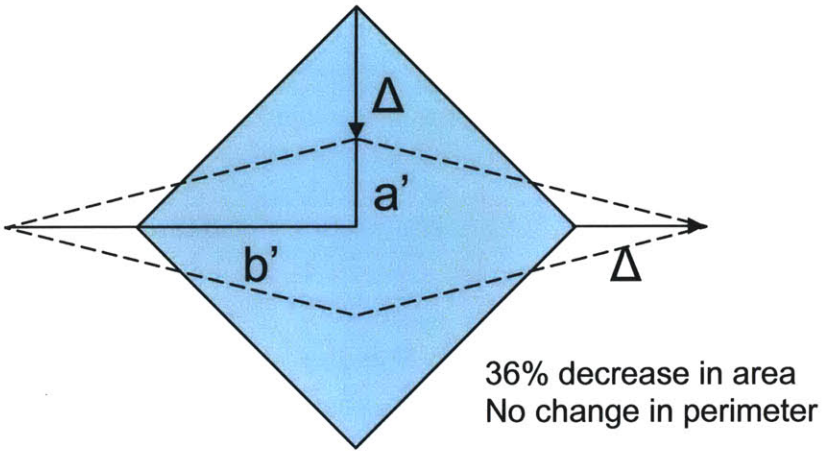

Figure 13 The microfiber cross sections can be approximated geometrically to estimate the deformations needed to achieve a 36% decrease in cross sectional area (for comparison to the estimations of purely radially symmetric deformations).

To determine the amount of strain in this geometry necessary achieve an equivalent 36% area reduction, constraining area and perimeter equations were constructed for the neutral and deformed cross sections. In the neutral state, the sides are of equal length, r, and the lines from center to corner of inner cavity (a,b) are also equal. To maintain constant perimeter of the inner surface, the decrease in length of a must equal the increase in length of b. Simple geometric relations show that Δ required to achieve 36% decrease in area is 60% of the original length a.

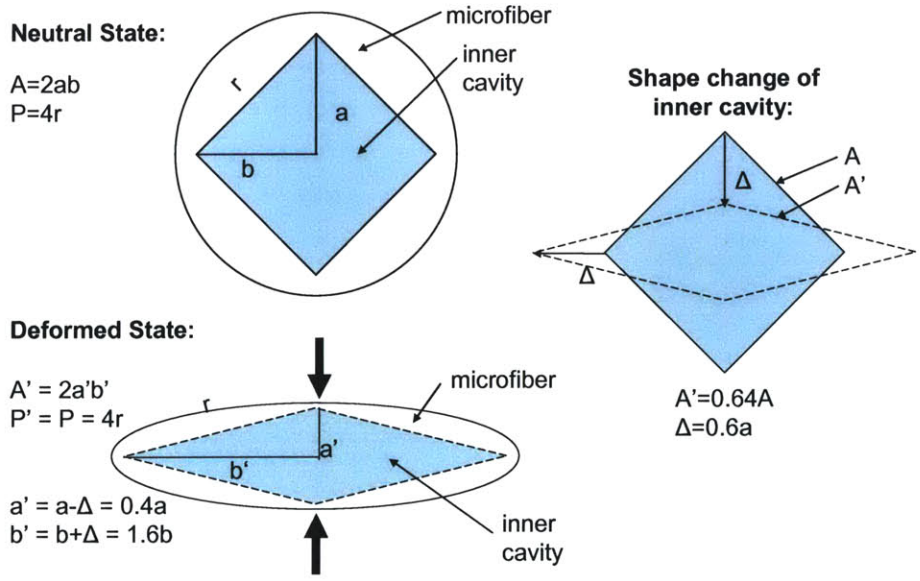

Compressed area is 64% of the original area:
$A'=0.64A$
Area of internal cross section:
$A=2ab$
$A'=2a'b'$
Change in lengths a and b due to compression:
$a'=a-\Delta$
$b'=b+\Delta$
Substitute identities for the compressed state:
$0.64(2ab)=2(a-\Delta)(b+\Delta)$
$-0.36ab=\Delta(a-b)-\Delta^2$
$a=b$
solve for compression needed:
$\Delta=0.6a$

Figure 14 To determine the amount of strain in this geometry necessary achieve an equivalent 36% area reduction, constraining area and perimeter equations were constructed for the neutral and deformed cross sections.

Relating this geometric approximation back to the actuator system at hand, the starting values a and b can be considered to be equal to the internal radius 12.5 μm. Deformations of 7.5 μm would be required. The ability of polypyrrole to perform this deformation depends on the design. A 40 μm thick film could produce this strain by

swelling 20% in thickness. Even at 1% linear strain repeatably achieved in a linear actuator, a film less than 1 mm would supply enough displacement. A 2 mm wide, 20 μm thick film achieved 1% strain over an actuation length of 6 mm, a displacement of 60 μm at 0.05 Hz (data taken 3 Mar 2005). A plausible design to implement a linear actuator to induce this deformation is shown below. The forces required will depend on the bending strength of the thinned section of the hollow microfiber, a function of modulus, size, and geometry. Importantly, the bending forces required would be less than the forces required for uniform radial compression as calculated above.

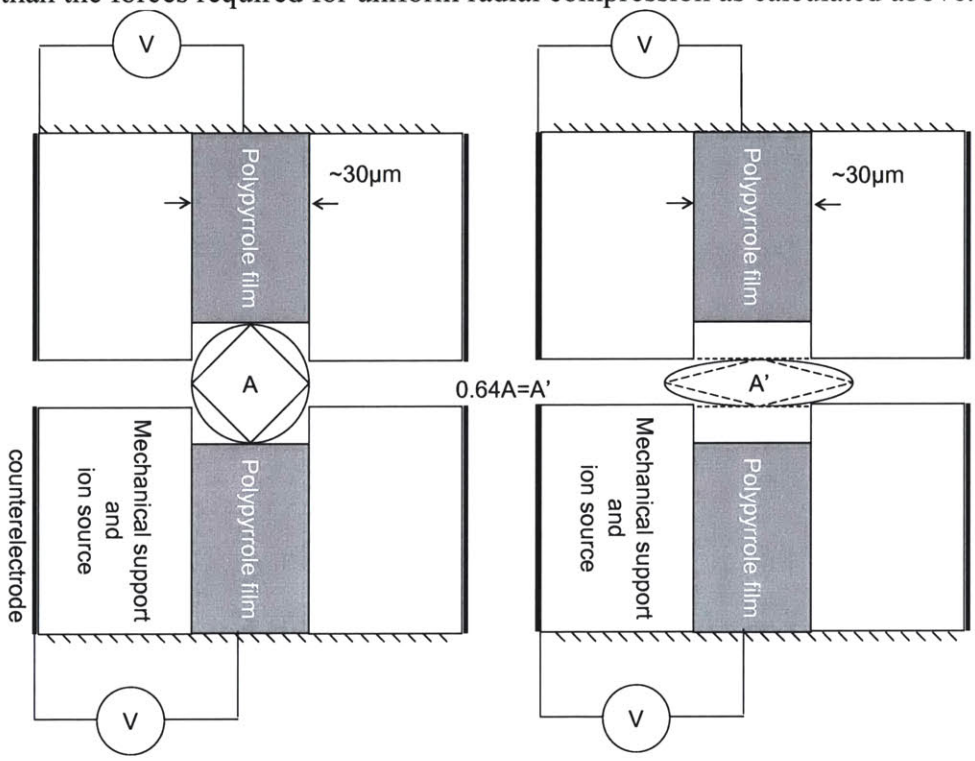

Figure 15 A plausible design to implement a linear actuator to induce microfiber. The bending forces required would be less than the forces required for uniform radial compression.

In addition to compressing the hollow fiber, the polypyrrole must generate pressure to pump the fluid through the hollow channel. To estimate the pressure required, the system was modeled as a simple pipe. Fluid was selected to be water at room temperature. Poiseuille flow, no-slip velocity profile, and smooth walls were assumed. The Poiseuille estimation was justified by the Womersley number Wo<1 (Vogel, 1981). The Womersley number is used to describe unsteady flow inside circular cylinders, such as the pulsing pressure gradients in peristaltic pumping. For Wo<1, the flow profile is quasi-steady, meaning the velocity profile matches the applied pressure without a significant time lag. The resulting pressure relation is shown below.

$$Wo = d_i\sqrt{\frac{\omega}{\nu}} = 0.16$$

$$\Delta P = \frac{f\rho V^2 l}{2d_i} = 0.04Pa$$

Equation 5 For Wo<1, the flow profile is quasi-steady, meaning the velocity profile matches the applied pressure without a significant time lag. The resulting pressure difference is ΔP.

Wo = Womersley number
d_i = inner diameter (25 μm)
ω = frequency of pulse (1 Hz = 2π s^{-1})
ν = kinematic viscosity of water ($1 \cdot 10^{-6}$ m^2 s^{-1})
ΔP = required pressure differential
f = friction factor, smooth walls (64/Re)
ρ = density of water (10^3 kg m^{-3})
V = average fluid velocity (17 μm s^{-1})
l = length of pipe section (50 μm)

Adding together the pressure required to compress the microfiber and the pressure required to pump the fluid, the total requirement is less than 1 MPa. This is very moderate compared to the 5MPa-34MPa range that can be generated by the polypyrrole.

The velocity for the above equation was found in the following way. Decrease of radius by 20% translates to 36% decrease in volume. Typical actuation frequency of 1 Hz was assumed (Madden, 2003). The average fluid velocity V is shown below.

$$\dot{Q} = A_i l \varepsilon \omega = 8.6 \cdot 10^3 \mu m^3 / s$$

$$V = \frac{\dot{Q}}{\text{Area}} = 17.5 \mu m^3 / s$$

Equation 6 Volumetric flow rate, average fluid velocity equations.

$\dot{Q}$ = volumetric flow rate
A_i = inner diameter (490 μm^2)
l = length of pipe section (50 μm)
ε = volume decrease (36%)
ω = frequency of pulse (1 Hz)
V = average fluid velocity

2.6.2. Electrical

Power consumption is an important metric for soldier-mounted systems. From the calculations above and an estimated 50% pumping efficiency, the predicted power consumption will be:

$$\frac{Power}{Length} = \frac{\dot{Q} \cdot P}{l \cdot \eta_{pump} \cdot \eta_{ppy}} \approx 1.17 W / m$$

Equation 7 Power consumption estimate for pumping microfibers.

$\dot{Q}$ = volumetric flow rate
P = pressure delivered by the pump (34MPa)
l = length of pipe section (50 μm)
η_{pump} = estimated pump efficiency (50%)
η_{ppy} = polypyrrole efficiency (1%) (Madden, 2003)

Approximately 5.1 meters of pumping microfiber network could be operated with 6 Watts. In comparison to biological systems, this is a small fraction of the human vasculature, which has ~100,000 km in blood vessels. The human heart delivers 8 W during exercise (Vogel, 1981). Additional pumping power in the veins (returning blood to the heart) is supplied parasitically by the surrounding muscles. For further discussion of this phenomenon and potential for biomimetic designs, see chapter 4 of this thesis.

The electrochemical circuit for actuation of the polypyrrole must be integrated into the microfiber. As discussed previously, polypyrrole connects to the working electrode and requires an electrolyte and a counter electrode. Electrical contact must be made to the thin, small diameter polypyrrole sheath and to the counter electrode. Contact resistance can be significant. The electrodes set the electrical field direction which will determine

the shape-change behavior of the polypyrrole. The counter electrode must set the needed radial electric field without interfering with actuation. The connections to the polypyrrole must be resistant to the chemical environment and not significantly inhibit ion exchange at the surface of the film.

Later product design stages must address additional design issues, such as active feedback control and mitigation of creep. Within even the first several cycles, the full amount of displacement is not recoverable. The plot below shows this in a typical strain curve during actuation of a polypyrrole film. Modeling and control investigations have been performed on polypyrrole that could eventually be adapted to alternate geometries and polypyrrole in devices (Madden, 2002; Bowers, 2004). Polypyrrole has been used as both an actuator and a sensor (P. Madden, 2003) and thus gives the potential for the future development of embedded sensing for feedback control within the pumping microfiber.

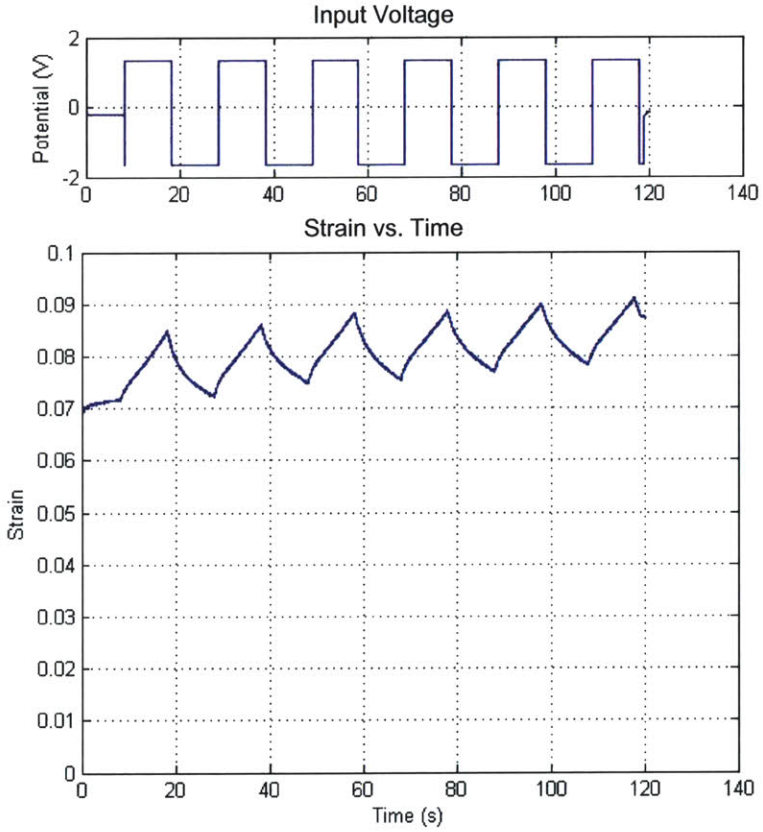

Figure 16 Actuation behavior of a polypyrrole film: input potential and output strain vs. time. Film dimensions 2 mm wide x 20 μm thick x 6 mm long (actuation direction).

2.6.3. Materials/Chemical

As discussed previously, polypyrrole cannot be processed in a melt. It has a virtually nonexistent glass transition temperature and it will degrade before it melts. Therefore it cannot be directly processed into a hollow tube in the extrusion method used for the hollow microfiber manufacturing.

Actuator quality polypyrrole is synthesized electrochemically. Since this necessarily involves polypyrrole forming on the electrode, polypyrrole cannot be electropolymerized directly onto a nonconducting substrate such as the elastomeric fiber. The polypyrrole-elastomer interface is at risk for delamination, where the actuating material is mated with non-actuating material. Hypotheses to achieve actuator quality pyrrole with good adhesion to the copolyetherester are discussed later in this chapter. Better understanding of polypyrrole in its various actuation modes will aid the evolution of this design. The anisotropic actuation properties and processing relationships are still under investigation by many researchers, and it is not immediately obvious how these properties will manifest in a tubular, radial design (Rocchia, 2003; Smela, 1999).

The material of the hollow fiber must be soft enough to be deformed by the polypyrrole actuator, and must fit the criteria for fiber processing. The microfiber extrusion and post-coalescence procedure can accommodate a wide range of materials, but the viscosity of the material will put lower limits on fiber size and wall thickness. (Samuelson, 2003) The fiber material must also be resistant to the chemical system which it is transporting.

Providing the ion source and the counter electrode to the polypyrrole in a tubular geometry will be a particular challenge in this system. The ion source must contact the polypyrrole and the counter electrode. The configuration of the counter electrode and ion source will dictate the direction of shape change within the polypyrrole.

The relationships between processing and properties of these very different polymers is critical. The effects of the processes on the other components of the system must also be understood.

2.6.4. Future Multiscale Integration Issues

For the battlesuit to benefit from the integration of a ubiquitous network of pumping microfibers, an economical and efficient way to interconnect them must be devised. Pumping microfibers will not be the only means of fluid transport within the battlesuit, but they will augment systems by providing low rate pumping in small scale conduits. They will not be optimal for large volume transport, but good for local ubiquitous distribution. This requires mating with larger scale fluidic systems and other subsystems that will be served by the network. This will be a unique product design challenge for each subsystem. The fluid and electrical circuits must be designed with redundancy to avoid a single point of failure. It would be unacceptable to have a design in which the failure of one "pumping station" rendered the entire length useless (as in failures of strands of lights connected in series).

2.7. Designs and Experiments

The issues described above are compounded by the small scale, which makes handling difficult. The overall design problem was broken into two branches of experimental work. One focused on the materials interface, evaluating hypotheses for integrating

copolyetherester with polypyrrole. The other focused on the synthesis and characterization of polypyrrole, to investigate its radial actuation properties.

This division of the experimentation into 2 parts was the result of initial experiments in chemical deposition of polypyrrole onto fibers (as distinct from electrochemical deposition). Using recipes from the literature for chemical deposition onto non-conducting woven fibrous substrates, polymerization directly onto nylon and polyester fibers was attempted. The resulting fiber coverage was non-uniform, as shown. See procedural details in A3.1.

Figure 17 Optical microscope image of non-uniform polypyrrole coverage from chemical deposition on hollow microfiber.

A variation of the chemical deposition recipe was performed with polypyrrole polymerized onto copolyetherester fibers from the vapor phase. The hypothesis was that if a uniform coating of the other ingredients in the polymerization were achieved on the fibers, then the vapors from the pyrrole monomer would uniformly surround the fibers and polymerize into a smooth, even coating. As seen in these micrographs, the polypyrrole coverage was irregular and disconnected. The fiber conductivity varied within 2 orders of magnitude, 0.1 - 10 S/m. See details in A3.1.

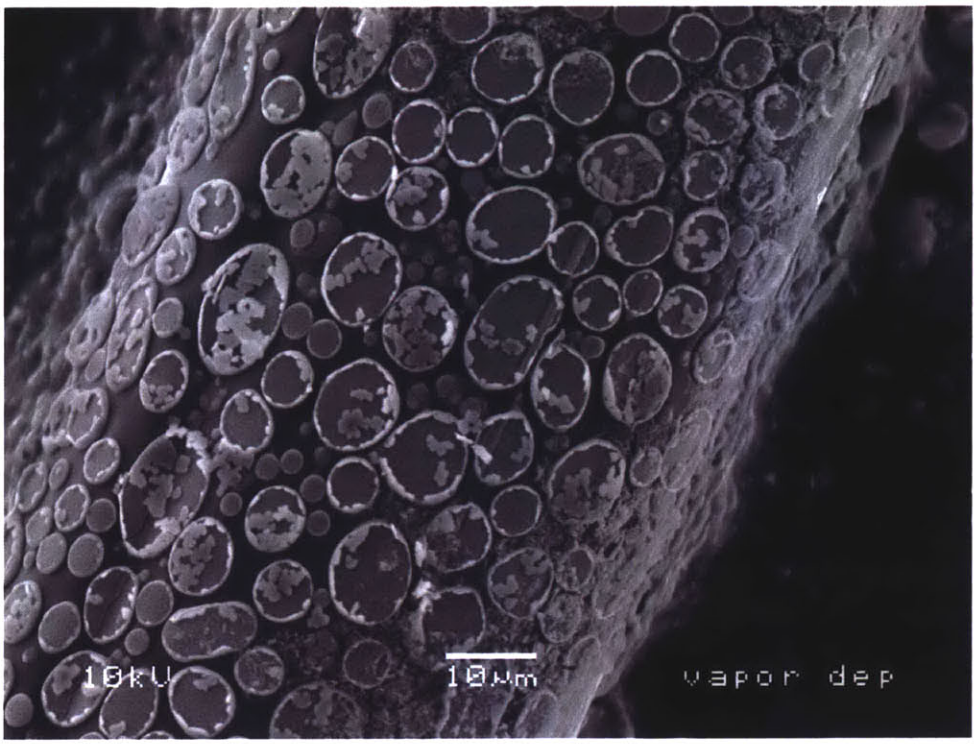

Figure 18 Irregular, disconnected coverage of polypyrrole vapor deposited on microfibers.

These experiments demonstrated the importance of chemical and materials issues to this design problem and the experimental difficulty of handling and separating the microfibers. In addition, experience was needed in polypyrrole actuation. Thus the two part investigation was devised to separate materials interface investigations from actuation investigations.

2.8. Materials interface studies

A thermoplastic copolyetherester from DuPont was selected for a microfiber material based on the stiffness and processing requirements. The polymer is a copolyetherester described in U.S. Patent number 4,906,729 with the specific composition given in U.S. 6,548,166, Column 23, Lines 61-65.

The next step was to investigate ways to strengthen its interface with the actuating polypyrrole. Since the microfiber geometry was difficult to handle and characterize, the experiments were primarily done on film samples.

One option considered was to sputter coat gold onto copolyetherester, and then to electropolymerize polypyrrole onto the gold layer. The synthesis may have been possible, but delamination problems were anticipated from the gold layer flaking off during synthesis and especially during actuation. Also, the method developed should be easily adaptable to the cylindrical geometry, and it can be difficult to evenly sputter coat onto a fiber.

Chemical deposition methods have been reported to achieve conductive layers of polypyrrole. It was hypothesized that better adhesion could be achieved between the copolyetherester and polypyrrole by first chemically depositing a conductive layer that would bond strongly to the copolyetherester and then electrodepositing actuator-quality polypyrrole onto the chemically deposited conductive layer.

The chemical polymerization method involved mixing equal parts of two solutions. Solution 1 included the pyrrole monomer (0.02 M) and the naphthalene disulfonic acid (0.006 M), and Solution 2 contained the ferric chloride (0.46 M) (Spinks, 2003).

The first experiments achieved noticeable polymerization and some adherence to the substrates. However the coverage was not uniform or continuous, and the adherence was not strong. Handling with gloved fingers caused the polypyrrole to flake off. By swelling the matrix of the copolyetherester with Solution 1 and then adding solution 2 to complete the polymerization, the objective was to create a gradient from pure copolyetherester to pure polypyrrole that would not delaminate. Copolyetherester pellets were swollen with Solution 1, then Solution 2 was added. The polypyrrole polymerized within the matrix of the copolyetherester. But these sample shapes could not be easily tested for conductivity because of their small size and irregular geometry. See details in A3.2. Some thin films were also treated by the same chemical methods. Copolyetherester films were cast onto glass slides and then swollen with drops of the Solution 1, then an equal amount of Solution 2 was added. Again polymerization was observed, however the thin films buckled and folded under the swelling with the solvent and other chemicals, which led to conductivity which was uneven and difficult to measure. See details in A3.3.

A parameter for the measurement of immiscibility of polymers is known as χ (chi). There is likely a large χ between the copolyetherester and polypyrrole since they are chemically dissimilar, which would cause phase separation. It would be difficult to ensure a continuous network of polypyrrole necessary for conductivity throughout the film.

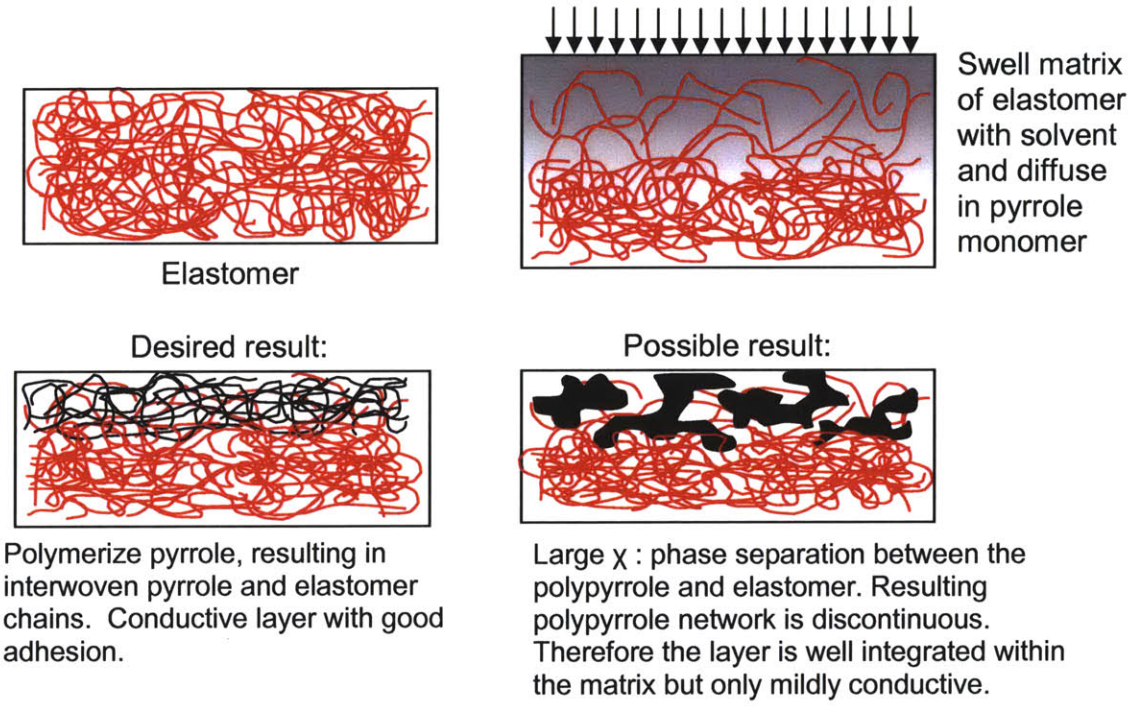

Figure 19 Schematic representation of experiments and results of chemical polymerization of polypyrrole within the copolyetherester matrix.

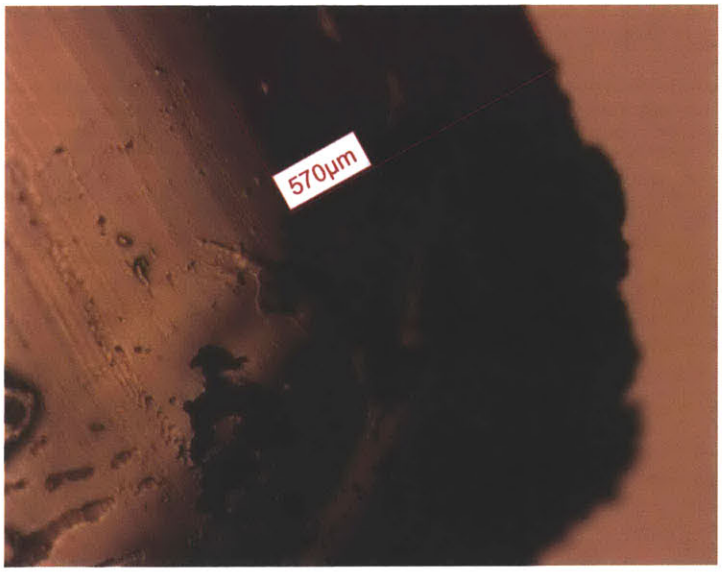

Figure 20 Optical microscope image of polypyrrole chemically polymerized within copolyetherester matrix. Penetration depth 0.5 mm

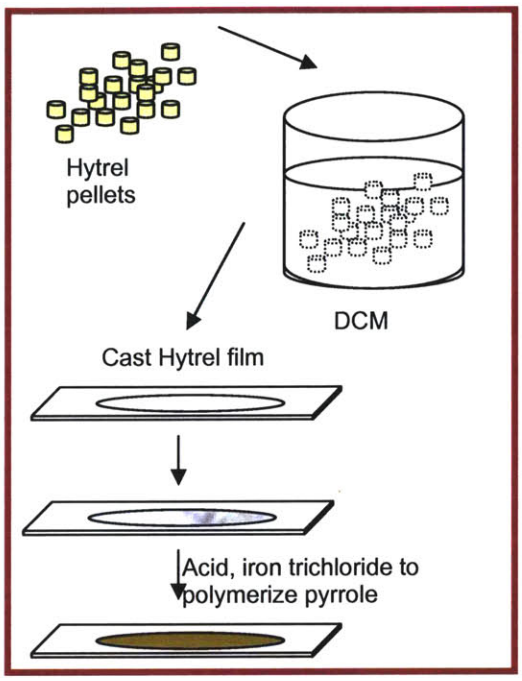

Figure 21 Schematic representation of chemical polymerization of polypyrrole within copolyetherester films.

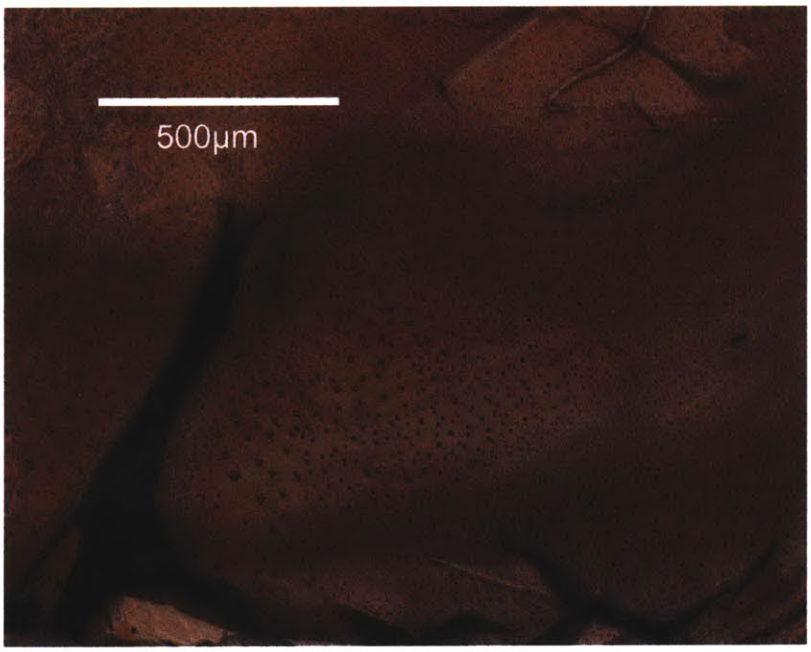

Figure 22 Optical microscope image of chemically polymerized polypyrrole within copolyetherester film. Film buckled and folded due to solvent swelling.

Another experiment was to chemically deposit polypyrrole onto the copolyetherester while stretching the copolyetherester. This was to determine whether the stretch-aligned copolyetherester chains would induce some alignment in the polypyrrole chains and result in higher conductivity. Polymerization occurred, but surface coverage was not

uniform, and adhesion was not strong. The film slipped in the dynamic mechanical analyzer grips before plastic deformation occurred, so we did not attempt to measure alignment in the copolyetherester chains. Conductivity of the stretched film was lower than in the unstretched control film. See details in A3.4. A combination method of swelling and stretching simultaneously while polymerizing was considered, but the copolyetherester film was not anticipated to survive the process intact.

2.8.1. Conclusions

Conductive layers with limited adhesion were achieved through chemical deposition methods. Progress was made towards the polymerization of polypyrrole within the copolyetherester matrix, but the resulting copolyetherester/polypyrrole films were not conductive enough or uniform enough to serve as working electrodes for the electrodeposition of actuator quality polypyrrole. Further study is needed in this significant materials interface part of the design.

2.9. Radial Actuation Studies

The second branch of experiments investigated polypyrrole actuation. Radial actuation of tubular shaped polypyrrole actuators is only briefly mentioned in the literature. Several papers discuss tubular actuators, but these are used axially as push rods as an improvement over films, which cannot generate compressive force (Ding, 2003; Hara, 2004; Hutchison, 2000). Rocchia (2003) briefly mentions a 20% change in radius but does not discuss the experiment or the measurement in detail. Further discussion of the importance of the experimental arrangement, especially of the electric field, follows in a subsequent section.

To gain experience with the materials and methods, procedures found in the literature were repeated, with similar results in conductivity and actuation. See details in A3.5. The ASTM standard two-configuration four point probe test was used to measure conductivity (reference). First films made showed bumpy morphology, but subsequent films polymerized at low temperature and low current density were smooth.

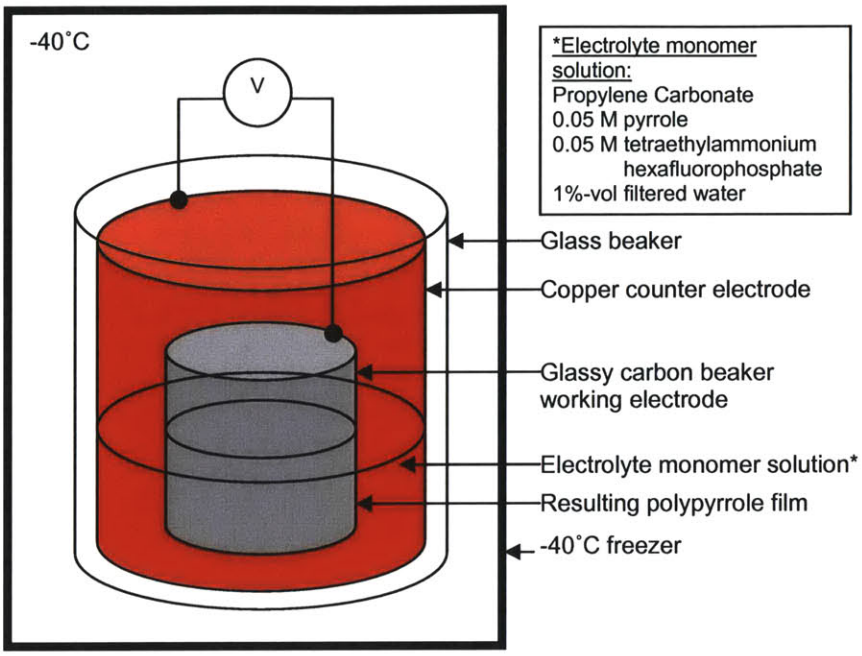

Figure 23 Schematic diagram of electropolymerization procedure

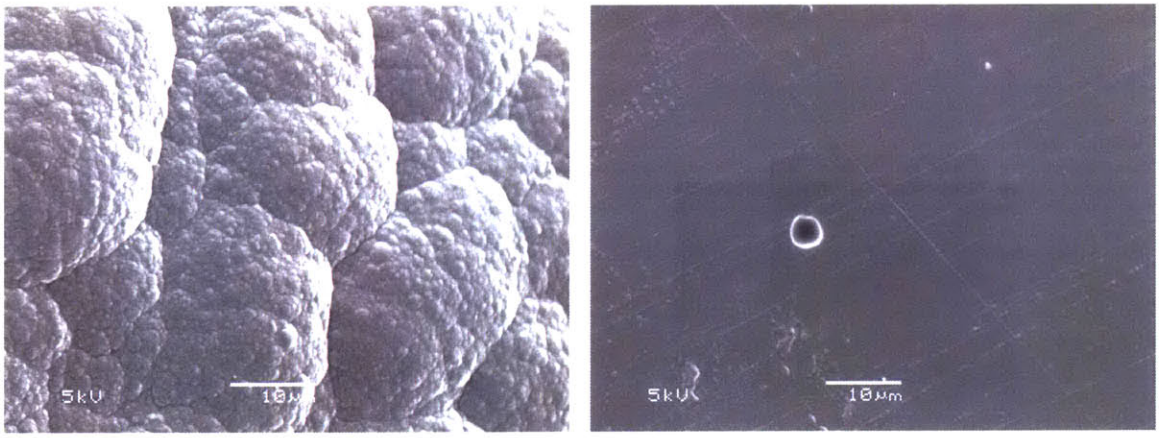

Figure 24 Bumpy and smooth morphologies of electropolymerized polypyrrole films. Low temperature polymerizations (-40 to -20°C) produce high conductivity films (10^4 S/m) with smooth surface morphology.

To design an effective micron-scale peristaltic pump, the radial actuation properties of polypyrrole in a tubular shape must be understood. Some millimeter scale polypyrrole tubes were electropolymerized. The tubes were much larger than those needed for micropumps, but this was done for ease of fabrication and measurements. A similar recipe including the low temperature was used to electropolymerize polypyrrole tubes onto 18 gage copper wire (D = 1 mm). The polypyrrole tube was gently pulled from the wire with gloved fingers and tweezers. The conductivity of these tubes could not be measured with the 4 point probe because it would be crushed or penetrated by the probes. The use of the same recipe that yielded conductive polypyrrole and the subsequent observation of actuation indicate conductivity. See details in A3.6.

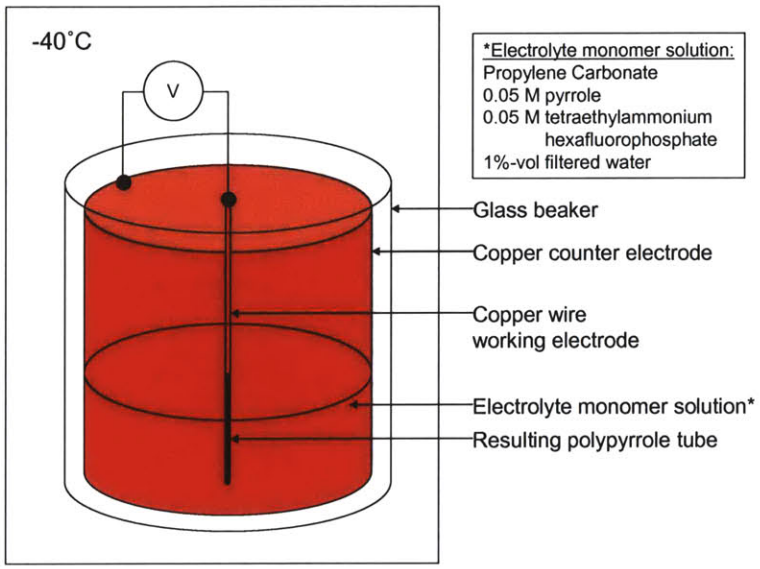

Figure 25 Schematic showing low temperature electropolymerization procedure for 1 mm diameter polypyrrole tubes.

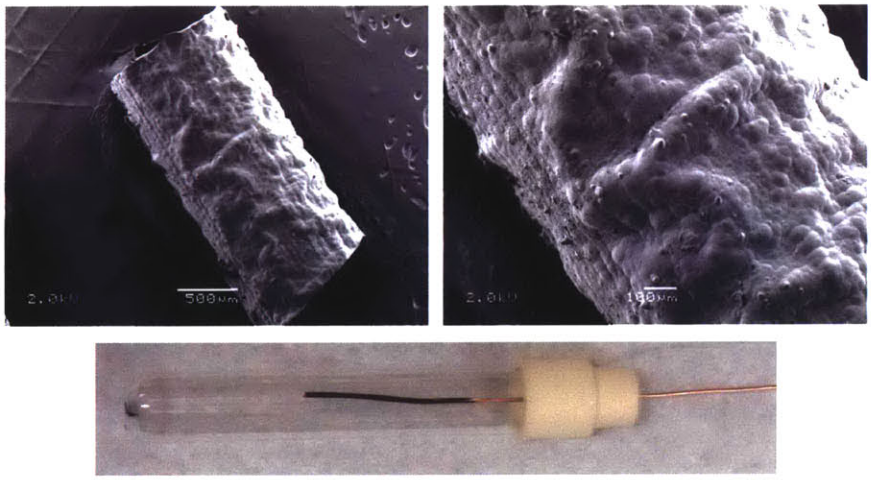

Figure 26 Scanning electron micrographs and digital picture of 1 mm polypyrrole tube

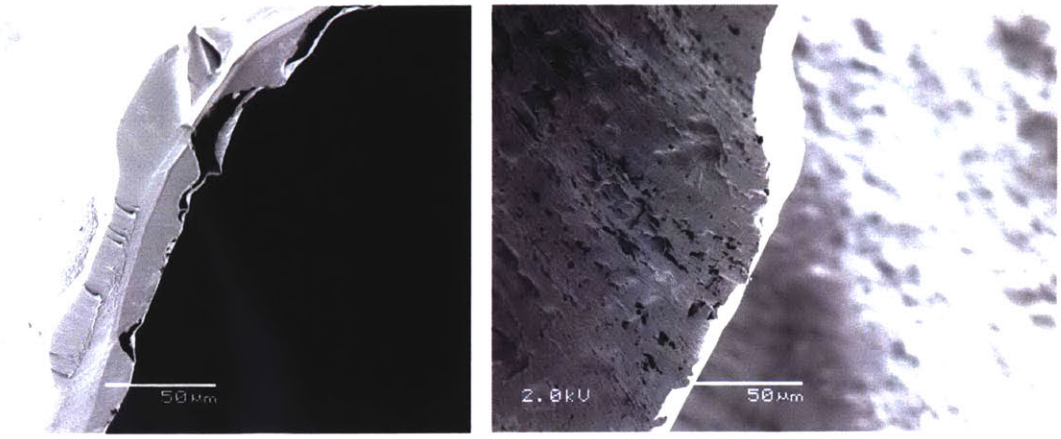

Figure 27 Scanning electron micrograph of tube edge cut with razor blade.

The importance of the electric field configuration in the electrochemical actuation cell was demonstrated by actuation experiments with these tubes. A 1 mm copper wire was inserted a short distance (1 cm) into the polypyrrole tube, leaving the majority of the tube hollow. The two were attached with colloidal silver liquid. Then this assembly was suspended horizontally in an electrolyte bath with a stainless steel sheet counter electrode on the floor of the bath. With slow square wave inputs (0.05 Hz, ±3 V to ±5 V), the tube was observed to bend upwards and return to horizontal with the cycling. See details in A3.7. This was found to correspond to the shape of the electric field. Qualitative analysis of the general shape and relative strength of the electric field accounted for the non-uniformity of the actuation. The electric field lines go from the working electrode to the counter electrode. The strongest field was then vertically downwards from the polypyrrole tube to the working electrode. Along the length of the tube, resistance in the material caused the voltage to decrease with distance from the electrical contact point. Oxidation of the polypyrrole (and consequently actuation) was greatest where the field is strongest: on the bottom of the tube at the end nearest the electrical contact. As the end of the tube rose, the field weakened with distance from the counter electrode. The curvature diminished along the length of the tube. The dual effect explains the curling and raising of the tube that was observed: the point of greatest actuation pushed and curled the tube upwards. This demonstrated the importance of the arrangement of the electric field for actuation properties, especially for a design such as the pumping microfiber in which the geometry of the actuator is not a flat film.

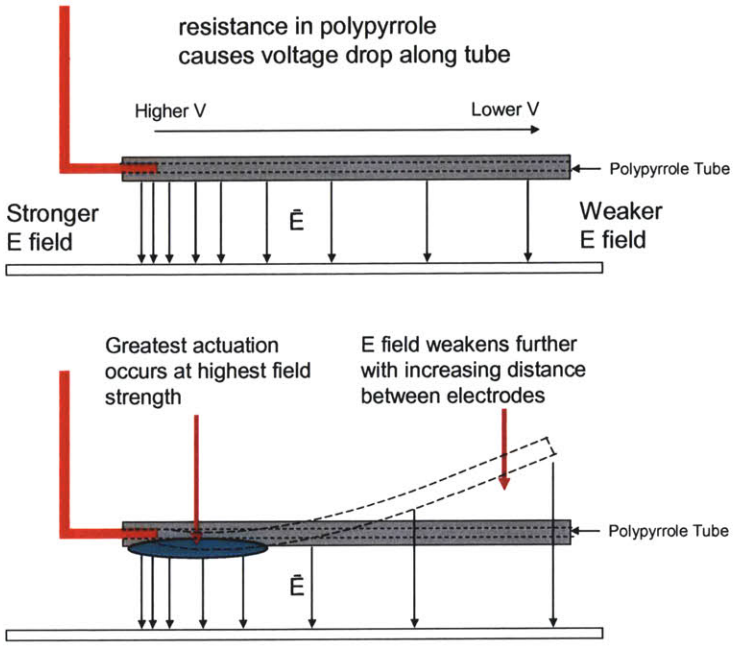

Figure 28 Actuation experiments with polypyrrole tube demonstrating the importance of the electric field orientation.

The next set of experiments centered around creating a cylindrical electric field in which to radially actuate and observe a polypyrrole tube. It was desired to do this under a microscope to more accurately observe and measure the resulting actuation. A ring of stainless steel foil was bent into a circular cylinder to create an even electric field to induce radial actuation, and placed in an electrochemical bath. To observe the cross sectional changes under the microscope, a short piece of the tube was used as an actuation sample. A small shape change in the cross section of a tube was observed. The shape change was a slight expansion and contraction of free ends near a defect in the tube edge. The material used to make electrical connection to the tube had covered some of the surface and blocked the ion transfer at much of the surface.

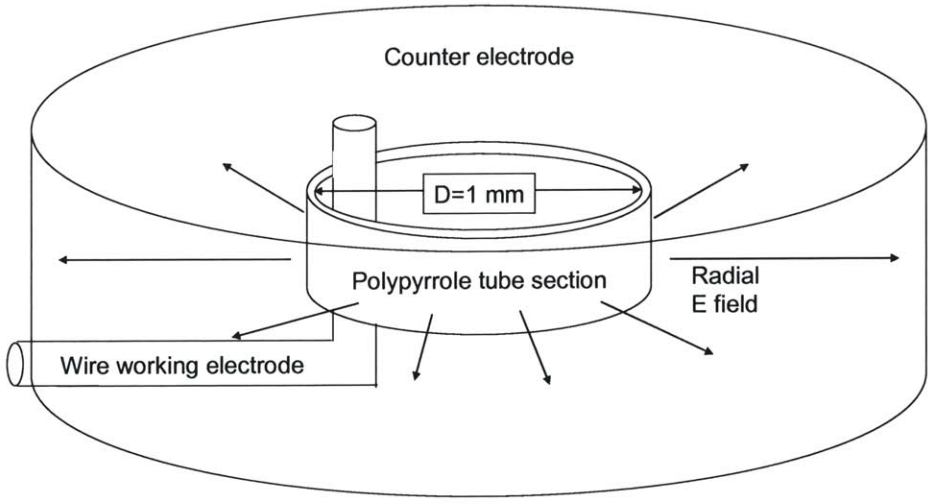

Figure 29 Schematic diagram of radial actuation experimental setup with radial electric field

This illustrates a particular challenge in setting up the measurement, which was the electrical connection to the tube. The small 1 mm diameter of the tube made it difficult to achieve electrical connection without interfering with the observation or the actuation. The 1 mm copper wire could not be used for the electrical interconnect because the 1 mm wire would resist the contraction of the tube and also obstruct the view of the microscope. Instead a thinner wire was used, and attached with colloidal silver liquid or Electrodag® (graphite based). Some of the connection materials tried did not withstand the propylene carbonate environment, and electrical contact could not be maintained. The iteration described above in which a larger quantity of colloidal silver liquid was used provided better electrical contact and some actuation was observed, but it covered too much of the tiny surface and blocked the transfer of ions throughout most of the sample surface area.

2.9.1. Conclusions

Further characterization of the radial actuation properties of polypyrrole is needed to develop a pumping microfiber. Significant design efforts are needed to develop a method to measure strains in a radial actuation setup. A useful design may involve tiny clamps (millimeter scale parrot clips) that could make electrical contact with a range of sizes of polypyrrole tubes, maintain contact in the solvent solution, and not interfere with optical measurement of strain. The radial actuation test configuration must be compatible with microscope observation so that a reliable digital measurement method can be used. The ability to measure radial stresses would also be useful.

2.10. Conclusions and Future Work

Progress was made along the two major paths of investigation towards the realization of a pumping microfiber. The two branches explored the chemical deposition of a smooth, conductive layer of polypyrrole onto copolyetherester which would adhere to the copolyetherester and serve as a working electrode for the electropolymerization of actuator quality polypyrrole. Investigations into the interface of the two materials (copolyetherester and chemically deposited polypyrrole) resulted in polypyrrole layers with conductivity or integration within the copolyetherester. Further development is needed to simultaneously achieve both conductivity and adhesion in this case where one material is deforming the other, and also to improve smoothness and mechanical integrity. Tubular polypyrrole actuators at the millimeter scale were fabricated and actuated. Radial actuation properties at this more manageable scale must be understood and then the micron scale can be investigated. The importance of a radial electric field was shown and a set of requirements was developed for a test setup to further characterize radial actuation.

Future work towards the development of a pumping microfiber should focus on the radial actuation of polypyrrole. If polypyrrole cannot be made to generate sufficient strain and stress to deform the hollow fibers, then the pump as conceived here will not work and the surface adhesion problem will not be important. Polypyrrole as an actuator is still the subject of much research. Radial actuation is all but omitted in the literature. As its structure-property relationships are better understood, the ability to harvest those

properties in useful devices will grow. Anisotropic properties in polypyrrole can be manipulated by stretch alignment and electric field effects, and it is not obvious how these properties, studied primarily in films, will manifest themselves in a radial actuator of small diameter.

Another reason to focus future experimentation on radial polypyrrole actuators is that the problems of electrical contact and electrical circuit development can be addressed independently of the adhesion problem. Polypyrrole has been used as both an actuator and a sensor (Spinks, 2003; P. Madden, 2003). Some polypyrrole tube segments could be actuators deforming the elastomeric fiber and functioning as pumping stations, while other tube segments would measure the pulses felt through the elastomeric tube. Thus the pumping microfiber has the potential for the future development of embedded sensing for feedback control. The feedback system could be applied locally over just a few segments, in keeping with the biomimetic distributed control paradigm discussed in chapter 4. Much more research would be needed to characterize the gage parameters and time responses of polypyrrole as a strain sensor, and to correlate those data to the internal flow.

Far future integration of pumping microfibers into functional circuits, including soldier protection systems for the battlesuit, will require efficient ways of connecting the pumping microfibers with macro, micro, and nanoscale components. This challenge will have a different design solution for each subsystem in which it is used. The economic and robust manufacture of the pumping microfibers would also be necessary to field large numbers of battlesuits with the ubiquitous artificial vasculature envisioned.

2.11. Appendix

A3.1. Chemical Deposition of Polypyrrole onto Polymer Microfibers

Objective
To evaluate the conductivity and adhesion of existing methods to chemically polymerize polypyrrole onto microfibers. Adapted from Madden or Antequil (theses in hunter group).

Procedure
1. Nylon 66 and 2GT polyester hollow microfibers were obtained from DuPont.
2. Solution 1 was 0.02 M pyrrole and 0.006 M Naphthalenedisulfonic acid (Naphth.) in water. Solution 2 was 0.046 M ferric chloride ($FeCl_3$) in water.
3. Equal volumes of the solutions were mixed in a vial and the fibers submerged.
4. Vial sealed and covered with aluminum foil and chilled in refrigerator.

Results and Analysis
Polypyrrole polymerized onto the fibers and in the bulk of solution. Polypyrrole adhered to the surfaces, but the adhesion was not resistant to even handling of the fibers. Coatings were uneven. See microscope image in chapter.
Vapor depositions were performed from a similar recipe by soaking fibers in 0.046 M $FeCl_3$ in ethanol. After removal from the ethanol solution, fibers were exposed to pyrrole vapor in a sealed jar. The resulting coatings were non-uniform. See micrographs in chapter. A likely contributing factors to this irregular coverage was the reduction of the iron from Fe^{3+} to Fe^{2+} by the ethanol, which would stop the ions' ability to polymerize the polypyrrole.

A3.2. Chemical Deposition of Polypyrrole onto Copolyetherester Pellets

Objective
To determine if adherence can be achieved between a significantly conductive polypyrrole layer and an elastomeric copolyetherester layer by the polymerization of pyrrole within the surface of the copolyetherester substrate.

Pellets of the copolyetherester were received from DuPont. On average, pellets were roughly circular cylinders with diameter and length 2 mm. Pellets are opaque and light peach colored. Polymerization was adapted from Spinks 2003, Madden 2003.

Procedure
1. Pellets immersed in tetrahydrofuran (THF) until swollen to ~8 times original volume and translucent. This was done to open the polymer matrix to increase pyrrole monomer diffusion into the copolyetherester matrix.
2. Pellets removed from THF and submerged in pure pyrrole monomer overnight. Vial was sealed, covered with aluminum foil and left in a refrigerator to protect pyrrole from

excessive oxidation. As controls, some pellets were left in an open vial to dry and some were sealed in a vial after removal from THF.
3. Pellets removed from pyrrole monomer bath and placed into aqueous or THF solutions to polymerize the pyrrole.
4A. Equal parts of the following 2 solutions were added to the pyrrole-THF swelled pellets and refrigerated 1 hr.
0.006M Naphthalenedisulfonic acid (Napth.) in water
0.046M ferric chloride ($FeCl_3$) in water
4B. To another group of pyrrole-THF swelled pellets, equal parts of the following 2 solutions were added, then refrigerated 1 hr.
0.006M Naphthalenedisulfonic acid (Naphth.) in THF
0.046M ferric chloride ($FeCl_3$) in THF
4C. As a control, a some pyrrole-THF swelled pellets were sealed in a vial and refrigerated 1hr.
5. Pellets removed from solutions and sliced into cross-sections to view in optical microscope. Some were sliced parallel to the cylindrical face and others were sliced perpendicular to it.

Results and Analysis
In both the aqueous and THF polymerization solutions, pellets had a 0.5 mm thick black section at the edge of the pellet. See microscope image in chapter. No color change was observed in any of the control groups. The black section was polypyrrole which had been polymerized within the matrix of the copolyetherester. Conductivity measurements could not be made due to the geometry of the samples.

A3.3. Chemical Deposition of Polypyrrole onto Copolyetherester Films

Objective
To repeat polymerization within matrix of copolyetherester and measure resulting conductivity.

Procedure
1. Copolyetherester films were cast from dichloromethane (DCM) solution onto Teflon-coated slides from 3 wt% solution of copolyetherester in DCM.
2. After drying, drops of solution A put on to film to swell matrix and allow diffusion of pyrrole into the copolyetherester.
Solution A: 0.02 M pyrrole, 0.006 M Naphth. in THF
3. Equal drops solution B put onto film.
Solution B: 0.046M $FeCl_3$ in THF
4. Samples were not refrigerated or protected from air or moisture.

Results and Analysis
Polymerization proceeded quickly. Polypyrrole was observed throughout the treated areas of the film. The thin films buckled and folded from the swelling. Conductivity was

found to be on average 10^{-6} S/m, but was highly variable due to the buckling and folding of the film.

A3.4. Chemical Deposition of Polypyrrole onto Copolyetherester Films While Stretching

Objective
To determine if alignment of polypyrrole chains (and consequently increased conductivity) can be achieved in chemically deposited polypyrrole by stretch alignment of the underlying substrate while polymerizing.

Procedure
1. Copolyetherester film was solvent cast into a glass dish from 5 wt% solution of copolyetherester in DCM.
2. Small strip of film loaded into Dynamic Mechanical Analyzer (DMA) with chemical bath.
3. Equal parts of following solutions put into chemical bath.
0.02M pyrrole and 0.006M Naphth in water
0.046M $FeCl_3$ in water
4. Film stretched at 35 kPa/min during chemical polymerization.
5. As a control, a section of the same film was polymerized in the same solution without stretching.

Results and Analysis
Polymerization of polypyrrole was observed on the stretched and unstretched films. The film slipped in the DMA grips as it neared the yield point.

Film	Average conductivity
Stretched	4.9 S/m
Unstretched	26.8 S/m

Thus, the stretching apparently did not increase conductivity of the polypyrrole. The polypyrrole layer had weak adhesion to the copolyetherester film in both stretched and unstretched films. The and polypyrrole have a large chi between them. The motion of the copolyetherester surface and the large χ between the polymers probably kept the polypyrrole from adhering, thus resulting in a lower conductivity. The copolyetherester film did not reach plastic deformation before it slipped. Permanent chain alignment that occurs in plastic deformation may give increased alignment in the polypyrrole.

A3.5. Electrochemical Deposition of Polypyrrole Films onto Glassy Carbon

Objective
To polymerize actuator quality polypyrrole by accepted procedures in the literature. references: Spinks 2003, Madden 2000.

Procedure

1. Electrochemical cell consists of glassy carbon beaker (Sigradur) as working electrode, copper sheet counter electrode, Ag/Ag^+ in propylene carbonate reference electrode and the following monomer/electrolyte solution.
2. Propylene Carbonate monomer/electrolyte solution contains:
0.05 M tetraethylammonium hexafluorophosphate (TEAP)
0.05 M pyrrole, distilled
1 vol% Millipore water
3. Polypyrrole deposited onto glassy carbon at -40°C galvanostatically at 0.6 A/m^2 for 6 hrs. Cell potential during deposition was 1V.

Results and Analysis
Average film conductivity was $1.2 \cdot 10^4$ S/m. Actuation performed with DMA in 0.05 M TEAP solution under 1 MPa applied tensile stress. Open cell potential (OCP) for actuation was -0.37 V. Summary of representative actuation data:

Sawtooth Wave (around OCP)	Frequency	Strain
±1.5V	0.5 Hz	0.2%
±1.5V	0.1 Hz	0.4%
Square Wave (around -0.2V)		
±1.5V	0.05 Hz	1%
±2.0V	0.05 Hz	2%
±2.0V	0.02 Hz	5%
±3.0V	0.02 Hz	8% until degradation of film after a few cycles

Films with cauliflower surface morphology were polymerized using the above procedure, with three exceptions: water was omitted, current density was 3 A/m^2, and polymerization was carried out at room temperature.

A3.6. Electrochemical Deposition of Polypyrrole Tubes onto Copper Wires

Objective
To electropolymerize freestanding actuator quality polypyrrole tubes. (Ding, 2003; Hara, 2004; Hutchison, 2000)

Procedure
1. Electrochemical cell consists of 1 mm diameter copper wire as working electrode, copper sheet counter electrode, Ag/Ag^+ in propylene carbonate reference electrode and the following monomer/electrolyte solution.
2. Propylene Carbonate monomer/electrolyte solution contains:
0.05 M tetraethylammonium hexafluorophosphate (TEAP)
0.05 M pyrrole, distilled
1 vol% Millipore water
3. Polypyrrole deposited onto glassy carbon at -40°C galvanostatically at 5.2 A/m^2 for 5.5 hrs. Cell potential during deposition was 0.34 V.

Results and Analysis
Tubes were fabricated and gently slid from the copper wire electrodes with gloved fingers and tweezers. Conductivity could not be measured with the four point probe due to the cylindrical geometry. Using a multimeter, some current could be passed through the length of the tube, but conductivity could not be measured reliably or repeatably. See actuation data below.

A3.7. Electrochemical Actuation of Polypyrrole Tube with Parallel Counter Electrode

Objective
To investigate the actuation properties of tubular polypyrrole actuators and to investigate the importance of electric field alignment within the actuation cell.

Procedure
1. Actuation cell consists of copper wire working electrode inserted into the hollow end of the horizontally positioned tube, stainless steel foil counter electrode horizontally along bottom of bath, Ag/Ag^{+} in propylene carbonate reference electrode, and 0.1 M TEAP in propylene carbonate electrolyte solution. Cell is in an open glass dish. Electrical contact between polypyrrole tube and wire electrode was made by close fit and colloidal silver liquid applied at the junction. Tube internal diameter is 1 mm and length is 3.5 cm.

2. Voltage was applied by a potentiostat in square waves about the OCP (-0.17V) and resulting actuation observed qualitatively by naked eye.

Results and Analysis
Summary of qualitative actuation data. All voltages are square waves at 0.05 Hz.

Voltage	Qualitative description of actuation
±1.0V	no visible actuation
±2.0V	no visible actuation
±3.0V	free end of tube points slightly upward during positive voltage. (roughly 5° angle from horizontal)
±4.0V	tube begins to smoothly curl upwards during positive voltage cycle, with tightest radius of curvature near the fixed end. Free end angle is roughly 10° from horizontal. Tube goes almost back to horizontal during negative voltage cycle.
±5.0V	tube curls more steeply while positive voltage applied, free end angle is near 30° from horizontal. Some wisps of black emanating from the tube after 2 cycles indicate degradation of polypyrrole.

3. Active Multifunctional Polymeric System: Mechanochromism in Block Copolymers Exploited by Electroactive Polymer Actuators

3.1. Introduction

The ability to dynamically change the reflectivity spectrum of a surface could have multiple applications to the soldier, including analog sensing and display technologies. Mechanochromic block copolymers can be combined with actuating conjugated polymers to achieve a relevant active nanoenabled system. In a mechanochromic material, deformations cause color change. The previously described polypyrrole is an actuator that changes shape under electrical stimulus. The polypyrrole induces deformation of the mechanochromic block copolymer to create a color changing pixel.

3.2. Mechanochromic Polymers

The color changing pixel is based on the mechanochromic properties of two block copolymers (BCP). A block copolymer of polystyrene and polyisoprene (PS-PI) has been synthesized to have high molecular weight (synthesized by W. Lee and J. Yoon). Polystyrene is the hard glassy block with a higher refractive index (n_H=1.59) and polyisoprene is the soft rubbery block with the lower refractive index (n_L=1.51). The PS-PI is plasticized with a nonvolatile, nonselective solvent, dioctyl phthalate (DOP). The molecular weight is 840,000 g/mole (480,000 for polystyrene, 360,000 for polyisoprene) measured by gel permeation chromatography (GPC) relative to a polystyrene standard. The other is high molecular weight polyisoprene-polybutadiene (PB-PI) (synthesized by A. Avgeropolous). The polybutadiene block is 600,000 g/mole and the polyisoprene block is 400,000 g/mole. Both PB and PI are rubbery; no plasticizer is necessary. The refractive index mismatch for the polybutadiene-polyisoprene (PB-PI) is small: 0.008 for 550 nm light. Refractive indices of the corresponding PB and PI homopolymers were measured by spectroscopic ellipsometry. At 550 nm, the approximate midpoint of the visible spectrum, the refractive indices are 1.5242 and 1.5163 for PB and PI, respectively.

Mechanochromic Polystyrene-b-Polyisoprene

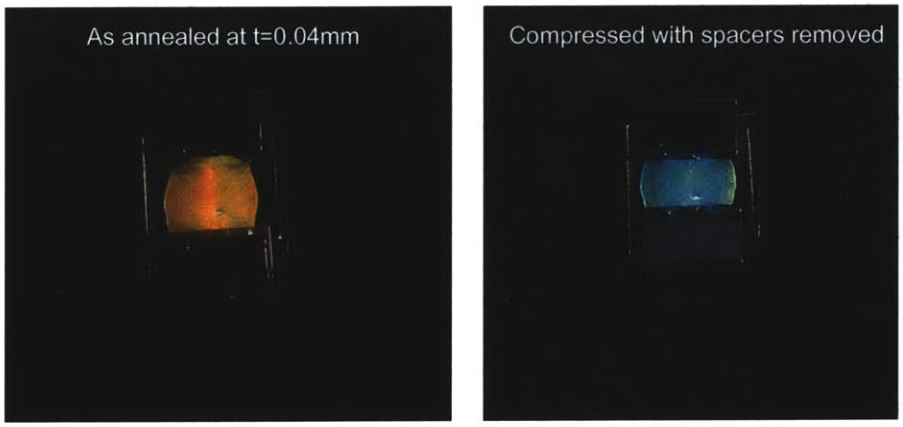

Figure 30 Top view of mechanochromic film of polystyrene-b-polyisoprene in experimental compression fixture. Film annealed at 0.04 mm thickness is orange. Film compressed with spacers removed is green-blue.

3.2.1. Block Copolymer Microstructure

The microstructure of a block copolymer is a result of competing enthalpic and entropic effects. There is a positive enthalpy of mixing the two different polymers. To lower the free energy of the system, the polymers will separate into distinct regions. The interaction parameter (χ) measures the degree to which the two polymer types will try to phase separate. The covalent bonding limits the degree to which they can phase separate. A range of phase separated microstructures are possible. The formation of separate domains stretches the polymer chains from the random coil, increasing the entropy of the system. The interfaces have higher enthalpy than the bulk polymer, so the domains will form a shape that minimizes the surface of interface. For volume fractions nearly equal, the balance of minimizing enthalpy and maximizing entropy results in a lamellar (layered) microstructure.

Different relative amounts of each polymer result in different equilibrium microstructures. The block copolymers used for this work form lamellae as described above. If the concentration is not completely equal in weight percent of each domain, the resulting microstructure in the as-synthesized BCP is different, for example cylinders of polystyrene in polyisoprene. Polystyrene homopolymer can be added which mixes with the polystyrene block of the BCP until the total weight percents of the two blocks are nearly equal. This results in the polystyrene-polyisoprene lamellar structure described above.

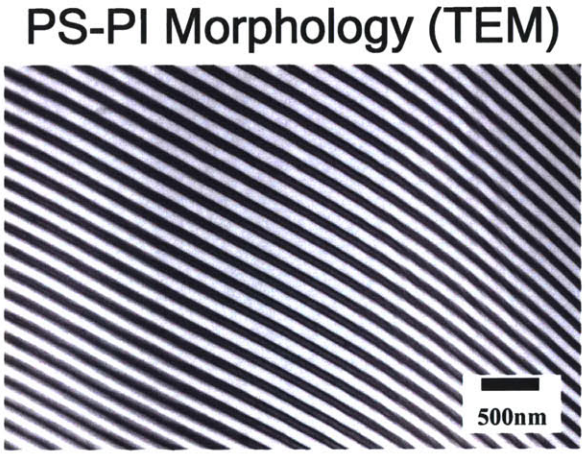

Figure 31 Transmission Electron Microscope (TEM) image of lamellar morphology for PS-PI. Domain spacing: 100 nm. Sample cast from toluene solution, thin sliced with a microtome. PI block stained with osmium tetroxide (OsO_4)

3.2.2. Mechanochromism

Both polystyrene and polyisoprene are transparent in the visible region (wavelength 400-700 nm). The visible color arises from the different wavelengths of light reflected at each interface between the layers of differing refractive index. The transparency and

refractive indices of the polymers are important for photonic bandgap applications. Transparency is important to minimize absorbed and diffused light, and the refractive index contrast must be maximized to optimize reflectance (that is, to create a robust bandgap).

The reflected wavelength (λ) depends on the optical thicknesses of the layers. The product of the index of refraction (n) and the actual thickness (d) is called the optical thickness. For the polystyrene-polyisoprene block polymer, the lamellae are 100 nm thick. Thickness depends on molecular weight and solvent swelling. The refractive indices for polystyrene and polyisoprene are 1.59 and 1.51, respectively. The center wavelength of reflected light can be estimated by the quarter-wave stack model. In a quarter-wave stack, the optical thickness of each layer is one quarter of the wavelength of peak reflectance.

$$\frac{\lambda}{4} = n_i d_i \qquad \text{(Edrington, et al.)}$$

Equation 8 Quarter wave stack.

As seen in the equation above, changing the thickness of the lamella changes the wavelength (color, in the visible range) of the reflected light. Narrowing the thicknesses of the layers (by uniaxial compression or biaxial stretching) shortens the reflected wavelength. This relationship between deformation and color change is known as mechanochromism.

A simple estimation of the mechanochromic effect can be calculated assuming constant indices of refraction, same thickness in all lamellae, uniform modulus in both domains, and incompressibility of the BCP. Poisson's ratio (ε_x = uniaxial strain parallel to the lamellae, ε_z = strain normal to the lamellae) combined with the reflected wavelength equation approximated for layers of equal thickness results in a linear relationship between strain and reflected wavelength with a slope m. For the PS-PI under investigation, m=-310 nm (units: wavelength per strain). This means that for 10% uniaxial strain (extension) parallel to the layers, the reflected wavelength will shorten by 30 nm. Alternatively, relating the color change to strain normal to the lamellae, the reflected wavelength will shorten by 30 nm with only 5% strain (compression).

$$\nu = \frac{-\varepsilon_x}{\varepsilon_z} = 0.5$$

Equation 9 Poisson's ratio

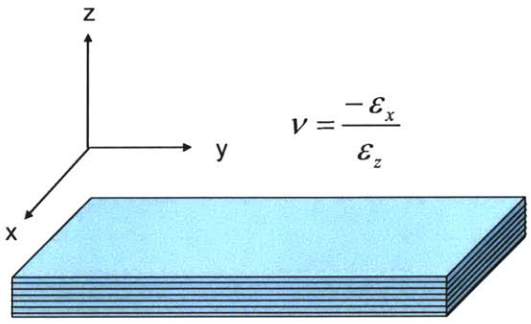

Figure 32 Definition of axes for lamellar block copolymer

$$\lambda = 2(n_1 + n_2)d$$

Equation 10 Quarter wave stack approximation for equal lamellar thicknesses

$$m = -(n_1 + n_2)d$$

Equation 11 Estimated wavelength change per strain.

3.2.3. Effects of Mechanical Properties on Mechanochromism

The mechanical properties of the layers in mechanochromic materials affect the color change. The mechanochromic effect depends on the change in optical thickness (nd). Changes in the true thickness of the high index layer affect the optical thickness more than changes in the low index layer. The stiffer layer will deform less and will also constrain the softer material. The ideal mechanical properties for a mechanochromic polymer would be moderately soft, uniform elastic modulus in both layers. The layers of polystyrene and polyisoprene have dissimilar elastic moduli, and a plasticizer is needed to soften the polystyrene. The result is a viscoelastic polymer with a long recovery time (on the order of several hours). The polybutadiene-polyisoprene is more elastic, with similar moduli in both layers (2 MPa). To achieve repeatable color change, a restoring force and displacement must bring the gel back to its original shape, whether by using an intrinsically elastic mechanochromic polymer or an elastomeric substrate.

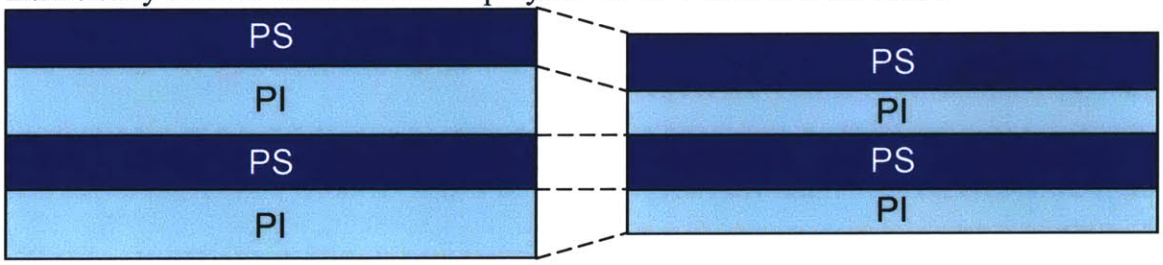

Figure 33 Changes in the true thickness of the high index layer affect the optical thickness more than changes in the low index layer. The stiffer layer will deform less and will also constrain the softer material.

3.2.4. Comparison to Mechanochromism in Co-Extruded Films

Similar mechanochromic effects in the visible spectrum have been achieved by others in elastomeric multilayer films. The structures were thin co-extruded layers of polymers (Schrenk, 1988, 1990, 1992). The tradeoffs between the two mechanochromic polymer systems are in processing and flexibility of design.

The two types of mechanochromic polymers require different processing techniques. An advantage of the block copolymers is that they self-assemble into the lamellar structure. To achieve optical thicknesses that reflect in the visible spectrum, high molecular weight copolymers must be synthesized. Once the polymerization takes place, it can be processed to self-assemble into the lamellar microstructure. High molecular weight molecules increase the entanglements of the polymer molecules, but the addition of a solvent allows the molecules freedom to move. At low polymer concentrations (~5%), the polystyrene and polyisoprene domains separate, forming the microstructure. The incorporation of a solvent (such as dioctyl phthalate) swells the microdomains and increases the wavelength of reflected light (redshift).

The co-extruded polymer layers require an elaborate co-extrusion setup, which is easier to achieve in a larger scale commercial situation than in a benchtop laboratory setting. The two (or three) polymers selected for co-extrusion are narrowly restricted. In addition to having high transparency and high index difference, the coextruded polymers must have similar viscosities so that they can be co-extruded without flow instabilities in the melt. They must be sufficiently immiscible that distinct interfaces form between layers, but they must not be so immiscible that the layers delaminate or dewet (Schrenk, 1988). Some examples of such materials are polytetramethylene glycol ether thermoplastic polyurethanes, polyadipate ester thermoplastic polyurethanes, polyether block amides, and flexible copolyesters (Schrenk, 1990).

The two types of mechanochromic polymers have different optical and mechanical properties that may be suited to different applications. The block copolymers self-assemble into lamellae of thicknesses dependant on the molecular weight. Distribution of the solvent can affect uniformity of the lamellar thicknesses. The thicknesses throughout the sample will be nearly uniform. This results in a smaller band of reflected wavelengths, resulting in purer color and lower intensity of reflected light for a given number of layers. Adding homopolymer or solvent blends with the polymer layers tunes the wavelength of reflectivity by increasing domain size. See additional analysis and discussion following characterization of mechanochromic films.

The co-extrusion technique allows precise control over the thickness of the individual elastomer layers within a stack. This makes it easier to achieve a wider range of reflected wavelengths, from infrared, through the visible spectrum, to ultraviolet. This control over layer thickness has been exploited to create a gradient in layer thicknesses. This can create a wide, tailored range of reflected wavelengths, and increase the intensity of reflected light. Co-extrusion also allows for the easier integration of a third polymer layer to control the constructive and destructive interactions, in order to control the higher order reflectance (Schrenk, 1988).

The mechanical properties of these both co-extruded and self-assembled systems are tailorable depending on the materials selected for the layers and solvent content. The

materials span the range of polymer material properties, from gels that flow easily to rubbery elastomers that recover their shape easily.

3.3. Characterization of Mechanochromic Films

In order to design an integrated pixel, the mechanochromic properties must be quantified. Specifically, the reflectance spectrum as a function of wavelength and strain was measured. This can be coordinated with elastic modulus to understand the forces required, and with confocal microscopy images to understand the relationships between microstructure changes, bulk strain, and reflectance.

3.3.1. Spectroscopic Measurements as a Function of Strain

The reflectance spectrum was measured as a function of uniaxial compressive strain by compressing the sample to a series of discreet thicknesses and measuring the spectrum at each. Samples of the block copolymer (PS-PI with DOP) were cast from toluene solution in a small crucible. Samples were then removed and compressed between a glass slide and cover glass. Steel spacers (metric feeler gauges, McMaster-Carr) were used to set the sample thickness. Sample below was annealed at 0.10 mm spacing. Spectral measurements were taken with an Axioskop microscope (Zeiss) equipped with a fiber optic spectrometer (StellarNet EPP2000). The numerical aperture of the microscope is 0.3, which corresponds to a half-angle of collected light of 17.5°. Reference for the 100% reflectance level over the visible range was a silver coated mirror.

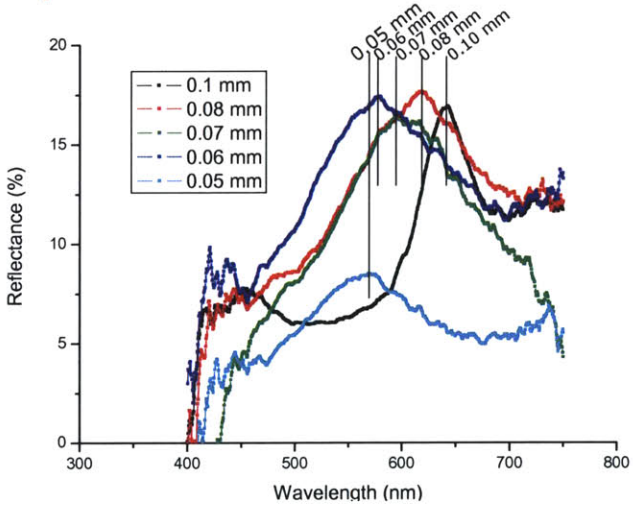

Figure 34 The reflectance spectrum was measured as a function of uniaxial compressive strain by compressing the sample to a series of discreet thicknesses and measuring the spectrum at each. Microscope used in reflectance mode and equipped with fiber optic spectrometer.

3.3.2. Results

The mechanochromic properties are quantified here of a representative film of PS-PI with DOP. With uniaxial compression in the bulk sample, the lamellae are deformed causing a blueshift with increasing compression. For most of the compression states, the reflectance is around 17%. The peak wavelength is directly proportional to bulk sample thickness. The peak is the sharpest for the 0.10 mm because the sample was annealed in the above experimental setup at this thickness for 48 hours in 40°C toluene vapor

environment. With each compression (~10% each time), disorder of the microstructure was increased and the peak broadened.

The results from the PS-b-PI film are compared to co-extruded elastomer multilayer stack (Schrenk, 1990). The specific sample is not described, only that the index contrast is 0.05 or 0.06, there are from 100 to 700 layers, and the layer thicknesses range from 0.05 μm to 0.1μm. There may be a gradient of layer thicknesses in the sample. The sample can be reasonably compared to the PS-b-PI film; the index contrast is similar, and the bulk sample and layers are of comparable thicknesses.

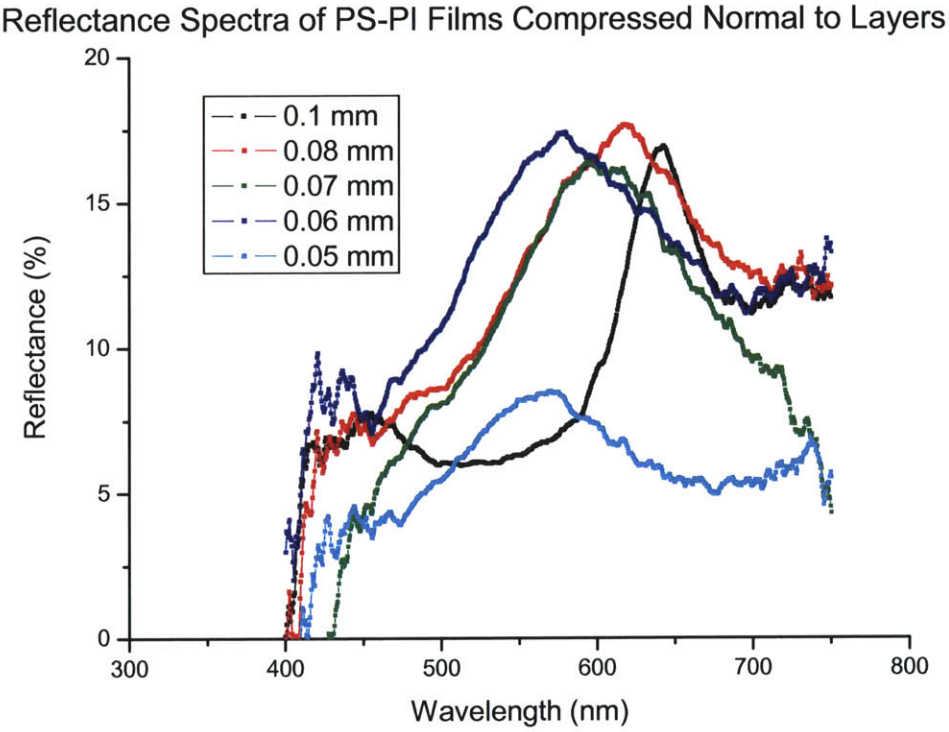

Figure 35 Reflectance Spectra of PS-PI Films Compressed Normal to Layers. Thicknesses of film at each measurement are shown in inset box.

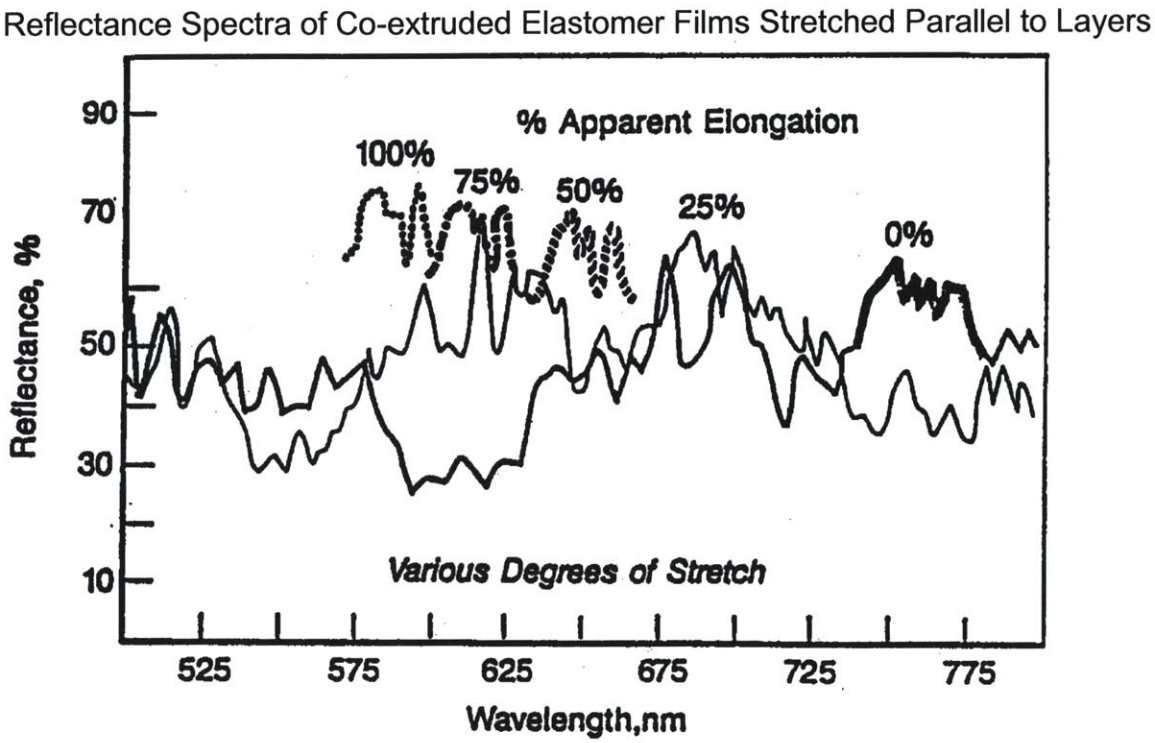

Figure 36 Reflectance Spectra of Co-extruded Elastomer Films Stretched Parallel to Layers. (Schrenk, 1990)

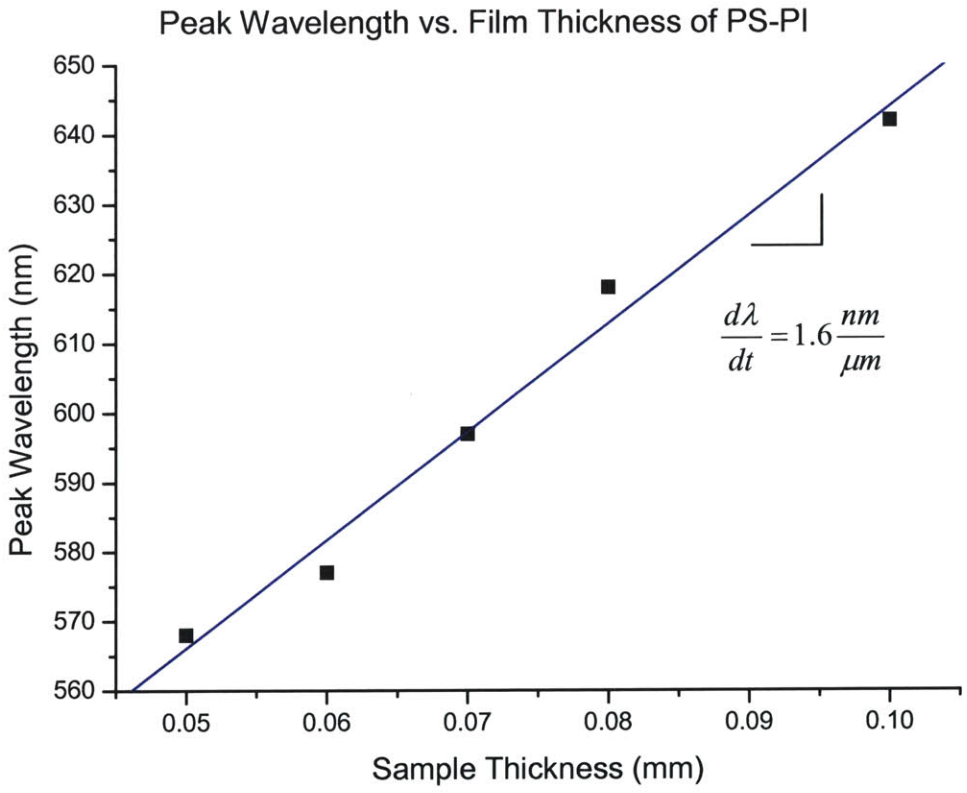

Figure 37 Peak Wavelength vs. Film Thickness of PS-PI

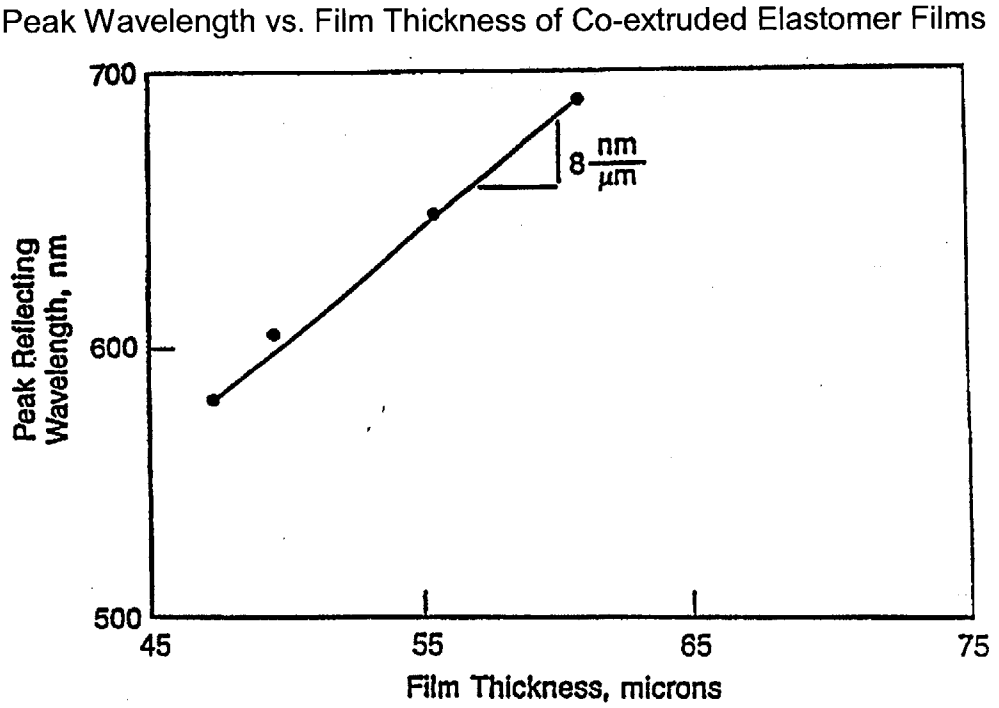

Figure 38 Peak Wavelength vs. Film Thickness of Co-extruded Elastomer Films. (Schrenk, 1990)

The co-extruded film has higher reflectivity, and a wider, more irregular bandgap than the PS-b-PI. Though the specific number of layers was not reported, it is likely that the co-extruded film had more layers than the BCP which could produce the higher reflectivity for similar index contrast (0.06 for the coextruded film, 0.08 for the BCP). The co-extrusion process likely produces higher order in alignment in the layers than self assembly does in the microdomains of the PS-b-PI. The broader, more irregular peak in the co-extruded film may be due to a gradient of layer thicknesses. Layers of different optical thicknesses have different bandgaps. A gradient of layer thicknesses within the stack can tune the bandgap to cover a range of frequencies. The bandgap of the PS-b-PI is narrower, due to the more uniform domain size produced by self assembly. Some irregularities in BCP domain thickness may occur if the DOP is not evenly distributed. Dioctyl phthalate is a nonselective good solvent for both PS and PI, but may not be uniformly distributed throughout the sample.

The slope of peak wavelength vs. sample thickness is of the same order of magnitude for both the co-extruded film and the BCP. The slope for peak wavelength (nm) vs. sample thickness (μm) for the BCP is 1.6 nm/μm and for the co-extruded film is 8 nm/μm. Mechanical properties and layer orientation could contribute to this difference, and to differences between predicted and measured center wavelength of the bandgaps. See discussion below.

3.3.3. Analysis of Peak Wavelength

To analyze the mechanochromic behavior of the PS-b-PI film, a quarter-wave stack is used to predict the center wavelength of the spectrum. The optical thickness of each domain is assumed to equal one quarter the peak reflected wavelength. The maximum reflectance occurs when the incident and reflected waves interfere constructively (are in phase). The points chosen for this analysis were from the linear fit to the data. The "initial" thickness was taken to be 0.10 mm and the "final" thickness 0.08 mm.

$$d_{H,i} = \frac{\lambda_i}{4 \cdot n_H} = 101.7nm$$

$$d_{L,i} = \frac{\lambda_i}{4 \cdot n_L} = 107.1nm$$

λ_i=647 nm
n_H=1.59 (PS)
n_L=1.51 (PI)
$d_{H,i}$=initial thickness of high-index layer (PS)
$d_{L,i}$=initial thickness of low-index layer (PI)

Equation 12 Quarter wave stack

If the sample is uniformly compressed, each actual thickness will be compressed by the same ratio as the whole sample.

$$r = \frac{t_f}{t_i} = \frac{d_{H,f}}{d_{H,i}} = \frac{d_{L,f}}{d_{L,i}}$$

$$d_{H,f} = 79.6nm(PS)$$

$$d_{L,f} = 83.9nm(PI)$$

r=compression ratio
n_H=1.59 (PS)
n_L=1.51 (PI)
$d_{H,f}$=final thickness of high-index layer (PS)
$d_{L,f}$=final thickness of low-index layer (PI)

Equation 13 Mechanochromic peak wavelength shift analysis

Then the final peak reflected wavelength can be predicted.

$$\lambda_f = 4(n_H d_{H,f}) = 4(n_L d_{L,f})$$

$$\lambda_f = 507nm(predicted)$$

$$\lambda_f = 612nm(measured)$$

Equation 14 Predicted wavelength shift

3.3.4. Discussion

Thus for a bulk compression of 20% (0.10 to 0.08 mm), the predicted change in center wavelength is 140 nm blueshift but the measured result is 35 nm blueshift.

Two important aspects of polymer physics can account for the differences between the reflectance measured and the reflectance predicted by the models: mechanical deformations and microdomain orientation.

3.3.5. Mechanical Deformations

The layers of polystyrene and polyisoprene have dissimilar elastic moduli. The addition of dioctyl phthalate softens the polystyrene domain, but since it is a non-selective good solvent for both polystyrene and polyisoprene, some relative modulus difference will likely remain. The mechanochromic effect depends on the change in optical thickness (nd). If the high index material deforms less, the overall wavelength shift is diminished. If the contrast in elastic moduli (ΔE) of the co-extruded elastomers is smaller than the ΔE

of the plasticized PS and PI, the layers could maintain their relative spacing and maximize wavelength blueshift. This effect contributes to the difference in $d\lambda/dt$ observed between the co-extruded and self-assembled film.

3.3.6. Microdomain Orientation

Even with annealing, the orientation of the microdomains of the PS-PI is not perfectly parallel to the substrate. In thicker samples, the surface effects do not propagate throughout the bulk of the material and alignment decreases in the bulk of the film. Compression of the sample tends to align the lamellae horizontally. As the microdomains rotate from grazing incidence to normal incidence, there is a resulting redshift. This redshift opposes the desired blueshift that results from microdomain compression. The measured peak wavelength of reflectance is then larger than the quarter wave stack prediction.

The PS-PI samples measured had lower magnitude of reflectance peak shift with strain than the coextruded layer stack. The coextruded layers were likely more uniformly aligned than the self-assembled lamellae of the BCP. Thus the bulk deformations transferred more directly to deformations of the lamellae (which causes the desired blueshift) instead of domain reorientation (which causes opposing redshift). In block copolymers, the alignment will be easier to achieve in thin films where surface effects (the tendency of the microdomains to be parallel to the surface) will dominate bulk effects.

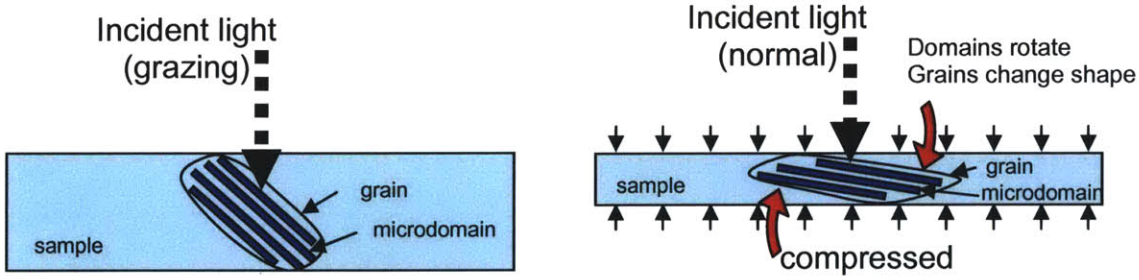

Equation 15 Orientation of microdomains during compression detracts from desired blueshift.

3.3.7. Analysis of Reflectance Intensity with the Transfer Matrix Method

The intensity of light reflected from a stack of dielectric layers can be calculated using the transfer matrix method. For further explanation see Hecht, 1997. A relationship between the magnitude of the electric and magnetic fields at one interface and the magnitude of the fields at the next interface can be established by a matrix relationship. To calculate the intensities being reflected from a stack of layers, the matrices for each layer are multiplied together to calculate the total reflectance.

Ambient light is non-polarized, which in general is a linear combination of transverse electric (TE) and transverse magnetic (TM) polarized light. This derivation considers only TE polarized light. Transverse electric is light in which the electric fields are perpendicular to the plane of incidence. The plane of incidence is perpendicular to the surface and contains the wave vector of the incident light (**k**).

There are two primary elements on which the derivation is based. The boundary conditions at the interfaces are that the magnitudes of the electric fields must be continuous and the magnitudes of the magnetic fields must be continuous. The phase shift of the light as it passes through the layer one time is $\delta=k_0 n_1 d\cos\theta_{i2}$.

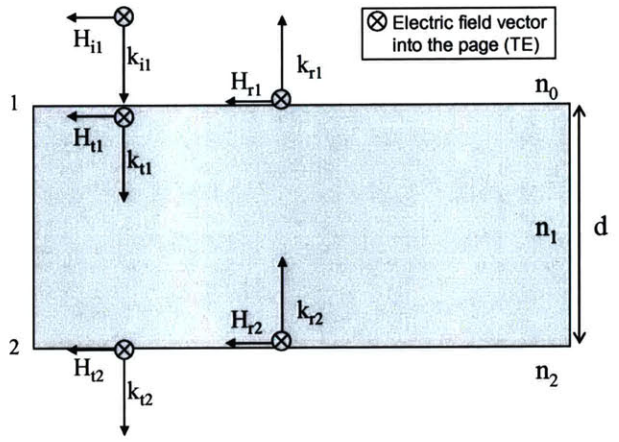

Figure 39 Layer of a dielectric stack used for derivation of transfer matrix method

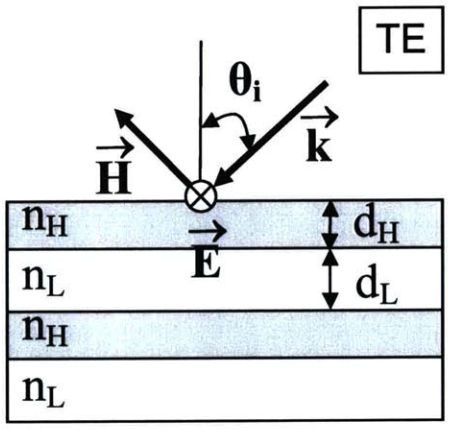

Figure 40 Multilayer reflecting stack with transverse electric polarization.

Equating magnitudes of fields at each boundary, including the relationship between electric and magnetic fields in nonmagnetic media, and substituting in the phase shift in the wave as it transverses the medium, yields two equations relating the fields at adjacent interfaces. See Hecht, 1997. These can be combined in the following matrix form:

$$\begin{bmatrix} E_1 \\ H_1 \end{bmatrix} = \begin{bmatrix} \cos\delta & i\sin\delta/Y \\ iY\sin\delta & \cos\delta \end{bmatrix} \begin{bmatrix} E_2 \\ H_2 \end{bmatrix}$$

$$\delta = k_0 nd\cos\theta_{i2}$$

$$M \equiv \begin{bmatrix} \cos\delta & i\sin\delta/Y \\ iY\sin\delta & \cos\delta \end{bmatrix}$$

$$Y = \sqrt{\frac{\varepsilon_0}{\mu_0}} n_1 \cos\theta_{i2}$$

Equation 16 Transfer Matrix for a single layer

The power of this method is the convenience with which it can be extended to stacks of multiple layers. ***M*** is the transfer matrix for TE polarized light interacting with one layer.

To calculate the fields E_1 and H_1 for a stack of many layers, the transfer matrices for the layers can be calculated and multiplied together:

$$\begin{bmatrix} E_1 \\ H_1 \end{bmatrix} = M_1 M_2 \cdots M_N \begin{bmatrix} E_N \\ H_N \end{bmatrix}$$

Equation 17 Transfer Matrix Method for multilayer stack

Using this method, the reflectance spectrum can be calculated for a multilayer stack of the PS-PI system studied. The relationship between number of layers and reflectance can be studied. For stacks with small index mismatches between layers, the R(λ) peak (bandgap) will be narrow and more layers will be required to reach a given desired reflectance.

The number of layers of PS-PI needed to achieve sufficient reflectance can be found by the Transfer Matrix Method. With 130 total layers (65 periods), over 90% reflectance can be achieved if the layers are well-ordered. This would correspond to a film 13 μm thick. If only 70%-80% reflectance was required, a 50 layer film would be sufficient (thickness 5 μm). A thinner mechanochromic film would more easily achieve higher order in the layers due to greater surface effects. It would also require less total deformation for a given strain. Thus a design tradeoff between film thickness (and corresponding deformations required) and total reflectance will be required for the design of a pixel. The measured PS-PI films were 100 μm thick, which corresponds to >>130 layers, but the reflectance was not as high as predicted. Disorder (random arrangement of lamellae within the sample) causes deviations from the ideal case predicted by the perfectly aligned layers modeled in the TMM calculation.

The PB-PI system has on order-of-magnitude smaller gap between the refractive indices (Δn=0.008 for PB-PI, Δn=0.08 for PS-PI). The physical result is that the bandgap (range of wavelength of light which cannot pass through) is narrower, and at each layer less light is reflected. Thus for the same number of layers, the smaller bandgap material has a much lower reflectance. Equivalently, many more layers are required to achieve similar reflectance levels. Both the magnitude of reflectance and the range of wavelengths reflected are important and depend on the index contrast. The plot below shows the magnitude of reflectance for incident light normal to the surface.

$$R = \left[\frac{1 - \left(\frac{n_2}{n_1} \right)^{2N}}{1 + \left(\frac{n_2}{n_1} \right)^{2N}} \right]^2$$

$$n_2 > n_1$$

Equation 18 Magnitude of reflectance depends on index contrast and number of layers. (Edrington, 2001)

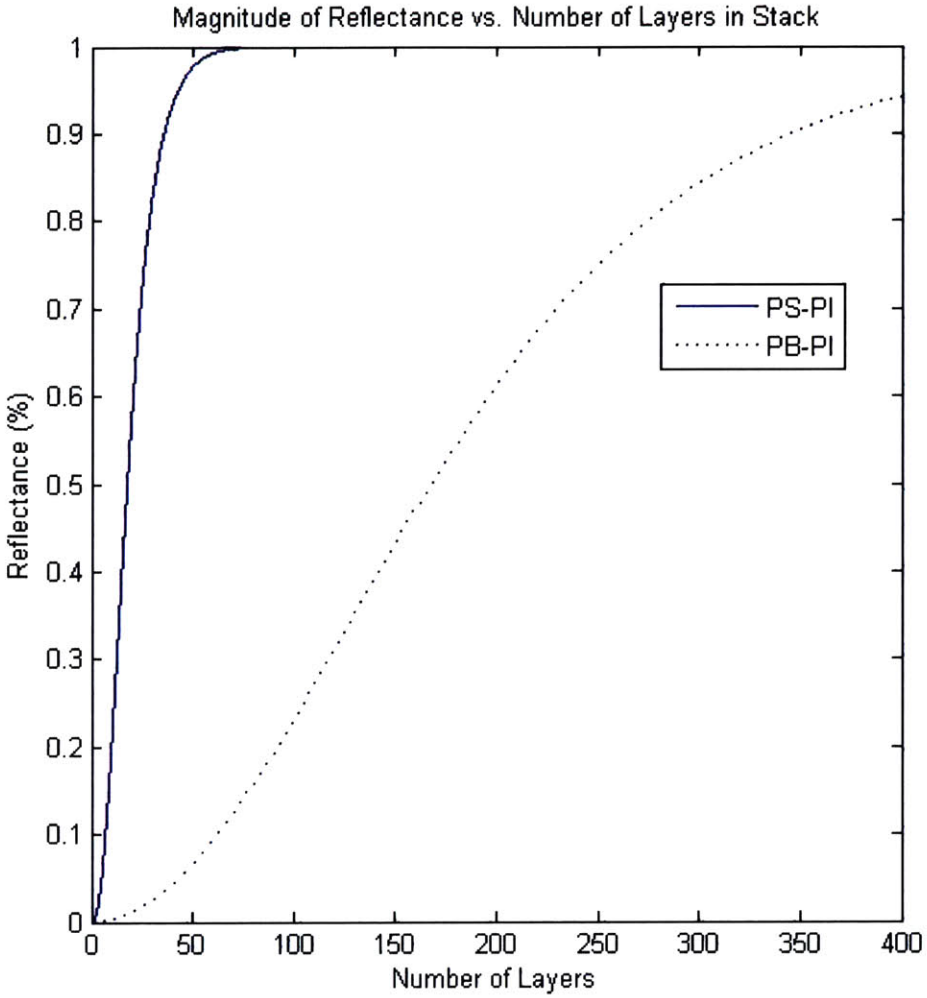

Figure 41 Magnitude of reflectance for incident light normal to the surface. Δn(PS-PI)=0.08; Δn(PB-PI)=0.008. For the same number of layers, the smaller index contrast stack has a much lower reflectance.

The range of wavelengths reflected are also important. The plots below show the spectrum predictions for a PB-PI multilayer stack based on the Transfer Matrix Method for light at normal incidence. The same lamellar thicknesses are assumed as in the PS-PI calculations above. For 130 layers, the PS-PI is predicted to achieve over 90% reflectance, but the 130 layer PB-PI stack can achieve only 25%. To reach 70%, 450 layers of well-ordered PB-PI are necessary (45 μm thick film), and at 550 layers the reflectance is below 90%. Regardless of number of layers, the bandgap is narrow for the PB-PI system. The plots below are all for light of normal incidence.

Figure 42 Predicted Reflectance Spectrum for Polystyrene-Polyisoprene: 50 layers

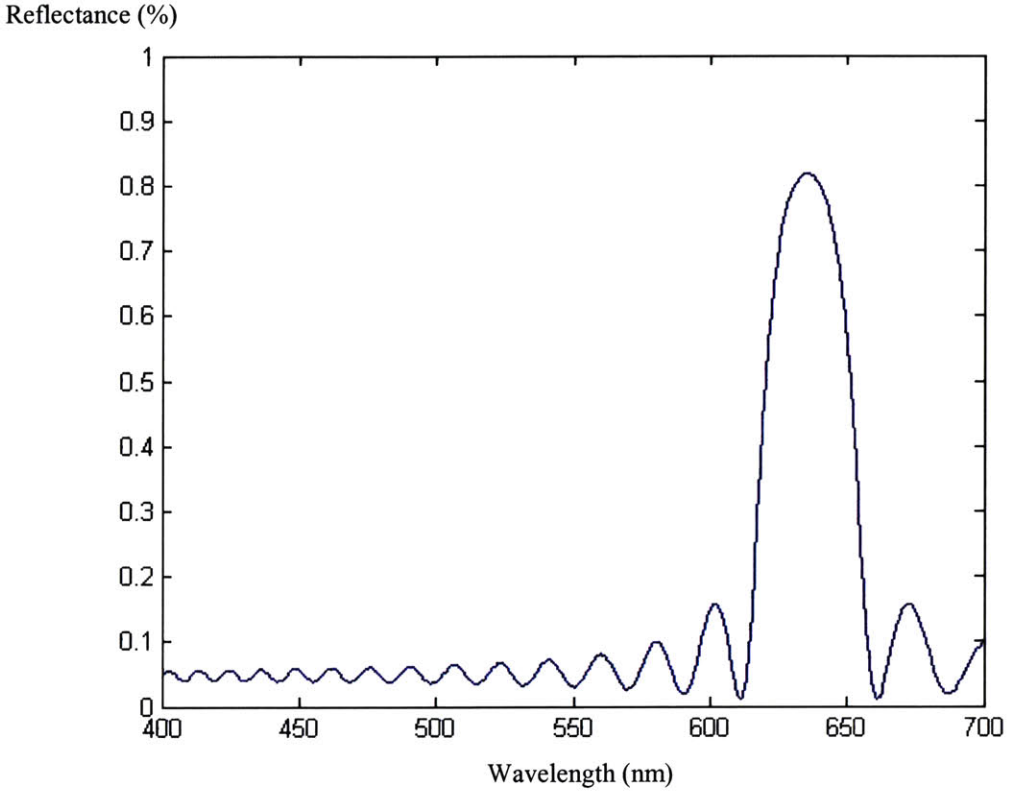

Figure 43 Predicted Reflectance Spectrum for Polystyrene-Polyisoprene: 130 layers

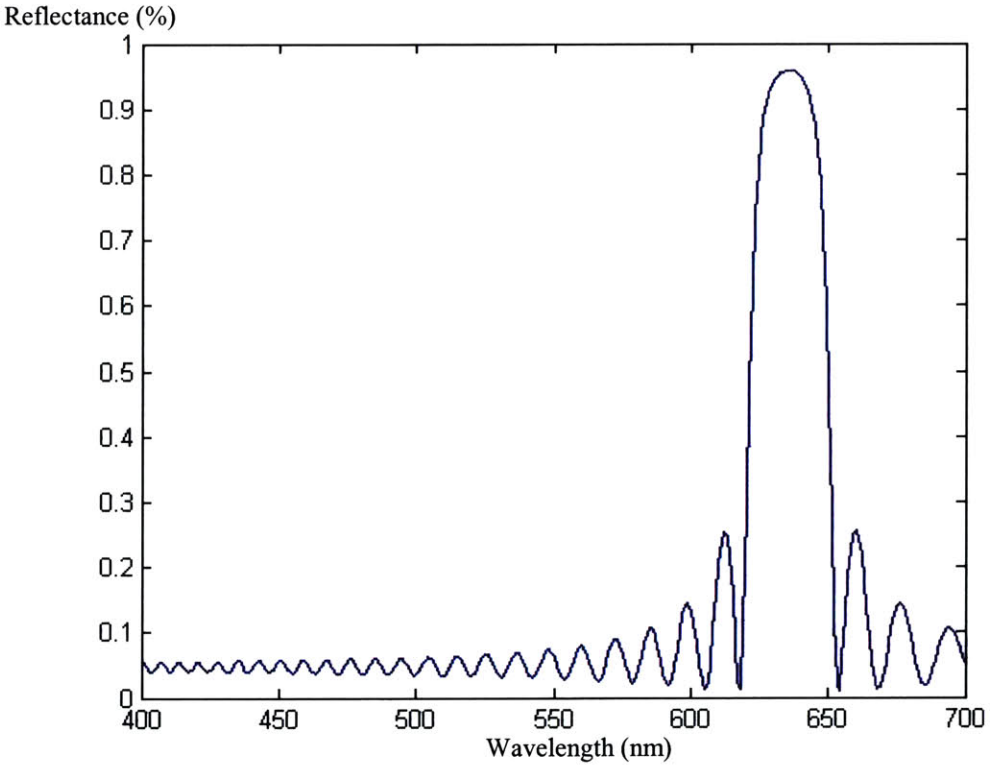

Figure 44 Predicted Reflectance Spectrum for Polybutadiene-Polyisoprene: 130 layers

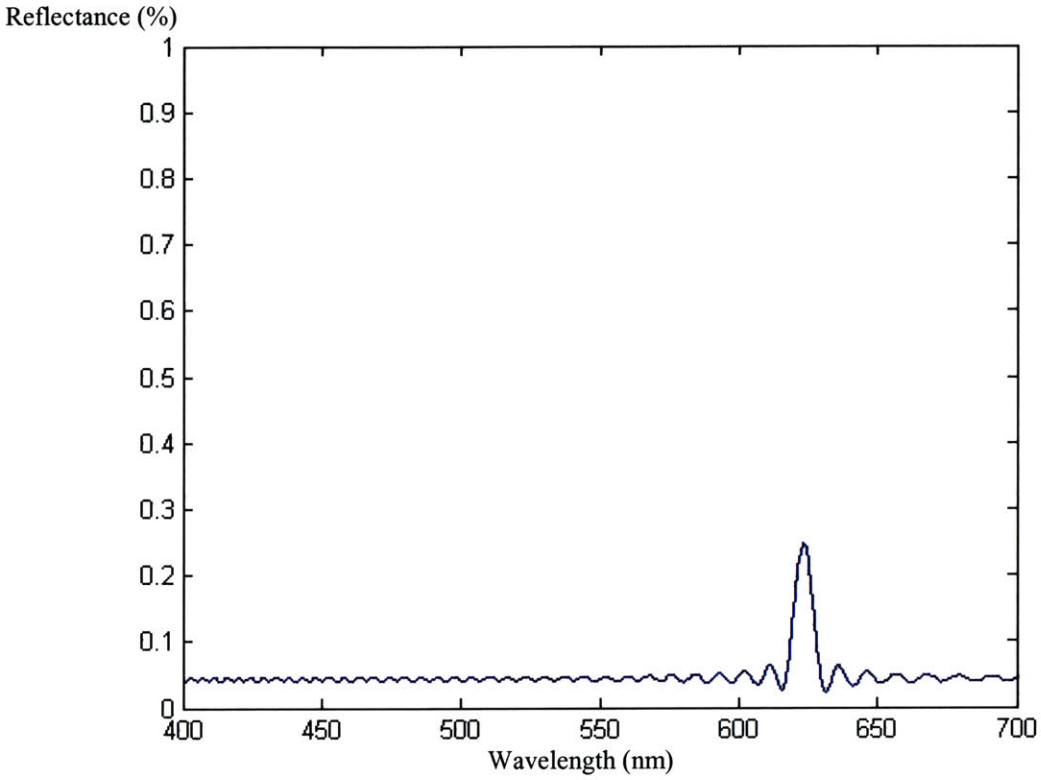

Figure 45 Predicted Reflectance Spectrum for Polybutadiene-Polyisoprene: 450 layers

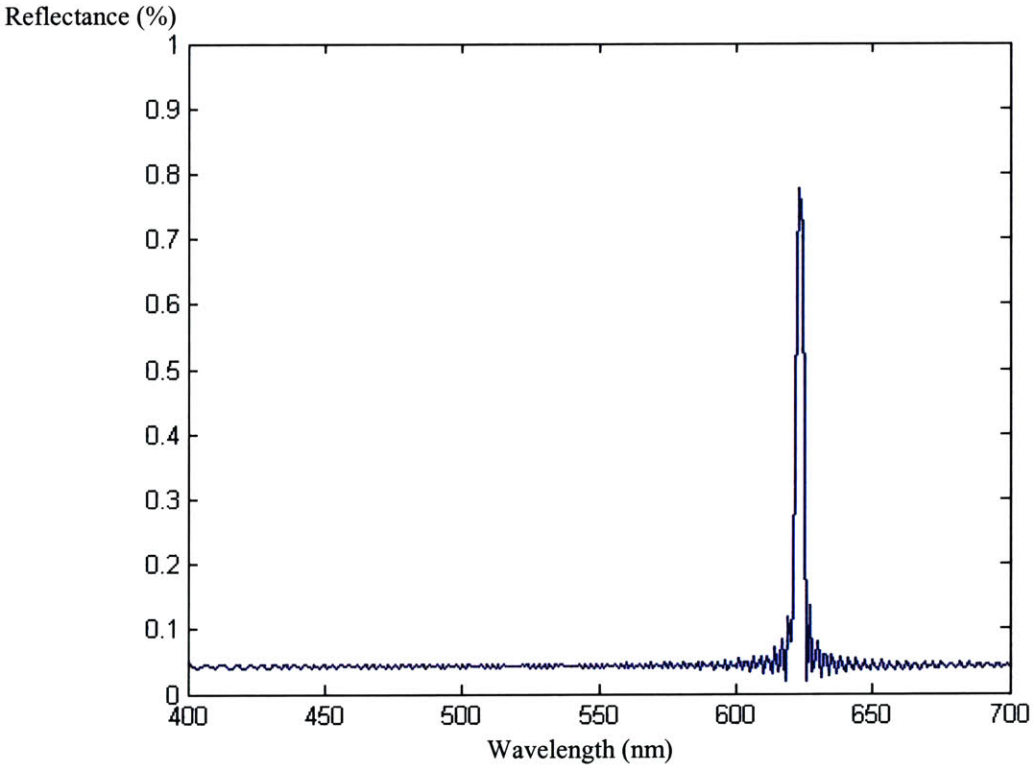

Figure 46 Predicted Reflectance Spectrum for Polybutadiene-Polyisoprene: 550 layers

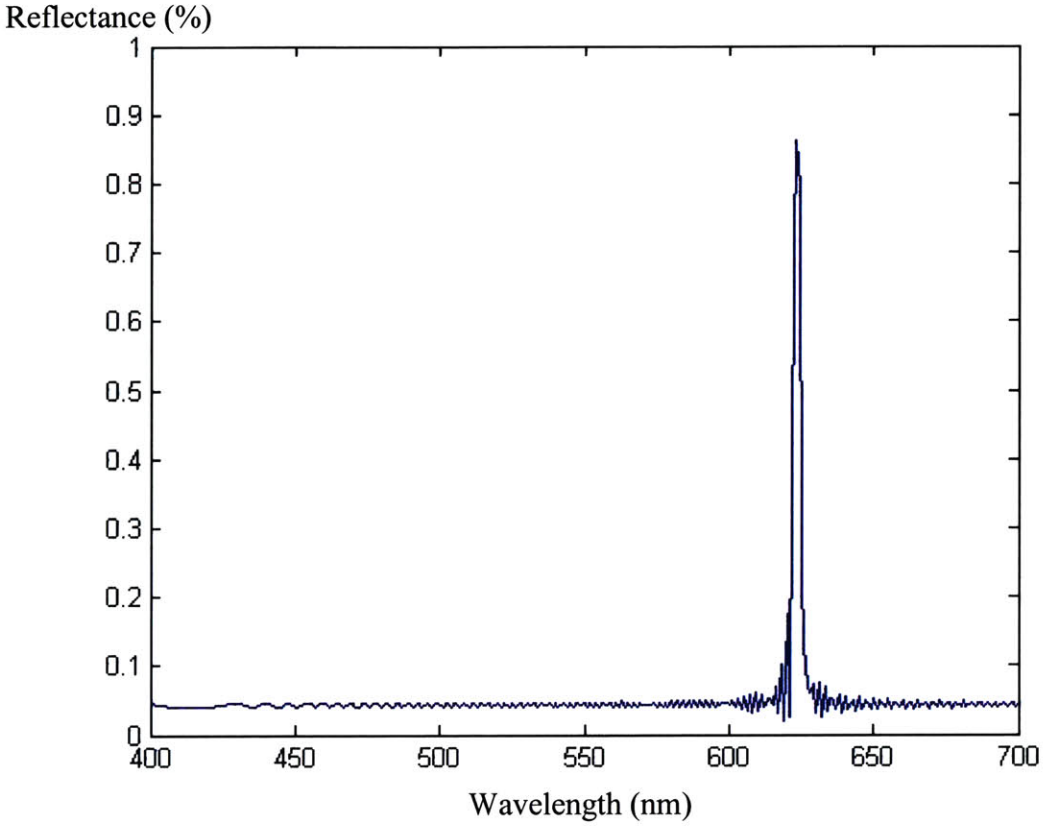

To realize the design of a pixel capable of repeatable color change, the time dependence of these effects must be studied. The current apparatus is insufficient for these studies. The additional characterization will require a time-resolved measurement under applied stresses, rather than the static measurements of the present work which compress the sample to a known deformation.

3.4. Integration Issues

The design tradeoffs discussed above are relevant to each component, the polypyrrole and the mechanochromic gel. The design of an integrated system of the mechanochromic BCP with the polypyrrole introduces several compatibility issues that must be overcome in the design.

3.4.1. Forces

The mechanical forces generated and required are a specific concern for this device. The mechanochromic BCP gel does not require large forces to strain it. In order to achieve reversible color change, the BCP must have some restoring force. This could be achieved with an elastomeric substrate, by selecting a more rubbery mechanochromic material, or by lightly crosslinking the BCP. The active polypyrrole must supply sufficient force to overcome the restoring force.

3.4.2. Strain Amplification

A 30 nm shift in wavelength requires 10% strain parallel to the lamellae in the BCP. However polypyrrole linear actuators can only produce 1%-3% strain over many cycles without degradation of the polymer. Some mechanical amplification device must be constructed to provide enough strain to demonstrate color change while maintaining sufficient force. Alternate designs will be considered for future work which exploit anisotropic actuation in polypyrrole (expansion in film thickness).

3.4.3. Chemical Compatibility

In addition to the mechanical considerations above, material and chemical interactions affect integration. The polypyrrole actuator must have an ion reservoir with which it can exchange ions during oxidation and reduction so that the shape changes will occur. In the literature, this has been achieved by either submergence in an electrolyte solution (acetonitrile, propylene carbonate, and water are common solvents) or by the use of an electrolyte gel layer. The casting solvent for the mechanochromic BCP is toluene, and the plasticizer is DOP. The polypyrrole and the BCP systems must be integrated such that the chemicals will not interfere with pixel function.

3.5. Design

In light of these primary integration concerns, chemical isolation and strain amplification, 2 design concepts were investigated. One concept used a bending polypyrrole actuator layered with an electrolyte gel actuated in air, the other used the polypyrrole actuator immersed in electrolyte solution, connected to the mechanochromic gel with levers.

3.5.1. Layered Bending Actuator

The advantage of the electrolyte gel layer in the bending actuator is that it eliminates the need for liquid in the system. A layered arrangement can be envisioned with the polypyrrole bending bilayer providing the actuation to a layer of BCP.

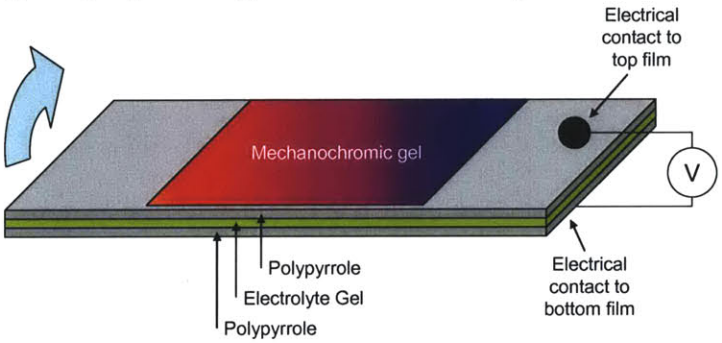

Figure 47 Proposed bending bilyer mechanochromic design concept

Some advantages and problems with this design are considered. The problem of forces is solved, since all the extensive forces from the polypyrrole are transferred directly to the BCP. Since the polypyrrole itself extends and contracts, an elastomeric restoring spring is not needed. One problem with this design is the chemical compatibility. The polypyrrole bilayer with electrolyte gel dries out after a few hours of operation and must be immersed in electrolyte solution (P. Madden, 2003). The BCP lifetime and adhesion

to the polypyrrole may be compromised by this repeated submersion in solvents. The strain amplification may also be insufficient. Though the bending bilayer shows increased deflection of the end of the strip, the surface strain along one face of the polypyrrole strip is still only 1-2%. This would only cause a color change of 3 nm in wavelength which is nearly imperceptible. The addition of a few millimeters of elastomeric buffer layer between the polypyrrole and the BCP could also be considered. This would achieve both chemical isolation to protect the BCP during the dipping process and mechanical strain amplification. However, the tradeoff is the additional force required to change shape against this thick elastomer. A thick layer of the BCP alone may allow for the increased color change without requiring large forces, but may still encounter the chemical compatibility and adhesion problems.

3.5.2. Lever Aided Linear Actuation

In another design, levers would achieve the needed strain amplification and connect the BCP to the polypyrrole while keeping the two chemically isolated. The polypyrrole in an electrolyte bath would connect to the short side of a lever, and an elastomer substrate for the mechanochromic BCP would connect to the long side. The BCP would not be exposed to the electrolyte solution environment at all. By using chemically compatible, electrically insulating material for levers and interconnects, the BCP and polypyrrole systems can be completely isolated and the levers can be tuned for the needed force and strain. The lever actuator was selected for the first design experiments based on the advantages of the chemical isolation and strain amplification.

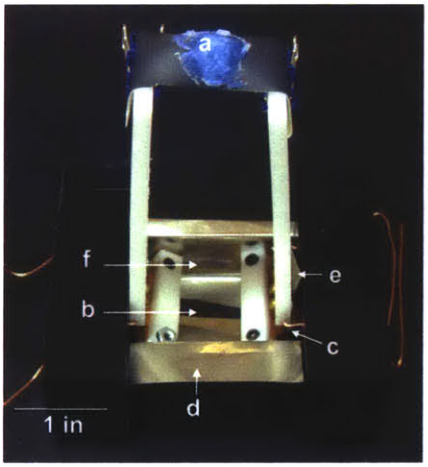

a. *Mechanochromic polystyrene-polyisoprene gel*
b. *Polypyrrole actuator*
c. *Fulcrum point*
d. *Stainless steel counter electrode*
e. *Working electrode (to actuator)*
f. *Electrolyte bath*

Figure 48 Lever-aided actuation mechanisms for mechanochromic pixel

The levers were milled from Delrin. Delrin was selected for chemical resistance to propylene carbonate, electrical insulation, easy machinability, and light weight. The fulcrum points were wires inserted through holes in the brackets. One lever was free to rotate, the other constrained in the vertical position. The brackets were held in place by set screws. Hinges were made from 2 layers of Kapton. They joined the levers with the clamps to hold a strip of polypyrrole. Stainless steel sheet electrodes made contact with the polypyrrole actuator for the working electrode, and another stainless steel sheet was the counter electrode. The bath was filled with the electrolyte solution, 0.05M tetraethylammonium hexafluorophosphate in propylene carbonate. The reference

electrode was held in place near the polypyrrole. The reference system used was silver/silver perchlorate in propylene carbonate.

3.5.3. Forces and Motion

Care must be taken in the design of a test stand to harvest the small force and small strain generated by electroactive polymers. Polypyrrole can produce 1%-3% strain without degradation and typically generate a stress of 5 MPa (J. Madden, 2003). With a thin film of typical cross section 50μm x 1cm, this results in total force on the order of 2 N. To capture and transfer such a small strain, the system must have minimal compliance. That is, components must be rigid and the connections between them closely mated. Otherwise, the small strains will be lost in the system components and interfaces and no useful work will be transferred. To harvest a small force, the moving parts must have minimal friction and inertia for maximum force to be transferred.

Use of a lever for strain amplification also results in force reduction according to the age old relation in which the product of force and distance is equal for both sides of the fulcrum. The distance ratio of the constructed levers will amplify strain 10 times, and consequently decrease force by the same ratio. Assuming a nominal value for active actuator length of 20 mm, 1% strain, and 10x amplification, the repeatable motion of the movable lever could be 2 mm. Based on the force quantities in the previous paragraph, the resulting force transferred may be as low as 0.2 N. This force must be used to deform the block copolymer and its elastomer substrate. The choice of elastomer substrate is critical since most of the resistive force comes from the substrate and not the polymer gel. A thin narrow strip must be selected so that the spring force may be overcome by the 0.2 N force. For example, a strip of the copolyetherester elastomer with cross section 0.2 mm x 5 mm with Young's modulus 2 MPa (DuPont) would deform 10% under the 0.2 N load.

The tradeoff space between low system compliance and low friction was explored with the design and fabrication of the lever test stand. Initial design was intended to minimize friction between moving parts to maximize the amount of force transferred from polypyrrole to mechanochromic polymer. However, the system compliance was too great and consequently no strain could be transferred. The fulcrum points and the hinge joints were the largest contributors to system compliance. Design iterations to improve the fulcrum points in the lever system resulted in further friction being added, which made the amount of force that could be transferred negligible. The hinge material was replaced with more rigid Kapton (originally elastomeric copolyesterether), but the design of the hinge still left compliance in the system. Applying tension to the tops of the levers with the elastomeric substrate of the block copolymer was not enough to pull the hinge-polypyrrole mechanism taut against its own weight, so actuation of the polypyrrole was lost in the slack of the hinges. The polypyrrole can be clamped directly onto the levers with small clips. This eliminates compliance in the hinge mechanism, but adds a point of high stress which could tear the fragile polypyrrole film. A piece of stainless steel foil could protect the film and also provide electrical contact. However, the compliance in the rest of the system would still be too large.

3.5.4. Alternate Design Considerations

Variations were considered for the portion of the lever system that transferred force and strain to the mechanochromic polymer gel. Designs were considered in which strain was applied in compression normal to the lamellae, instead of uniaxial tension parallel to them. When uniaxial tension is applied parallel to the layers, the normal strain (decrease in thickness) is only half of the applied strain, according to Poisson's ratio for incompressible materials. Since it is only the thickness of the layers that determines the reflectance, it could be advantageous to use the small strains to compress the gel directly. Two conceived designs were analyzed. In the first, discussed here, the additional mechanisms would only contribute to the existing problems of additional forces required and additional compliance in the overall system. The second is described in Future Work.

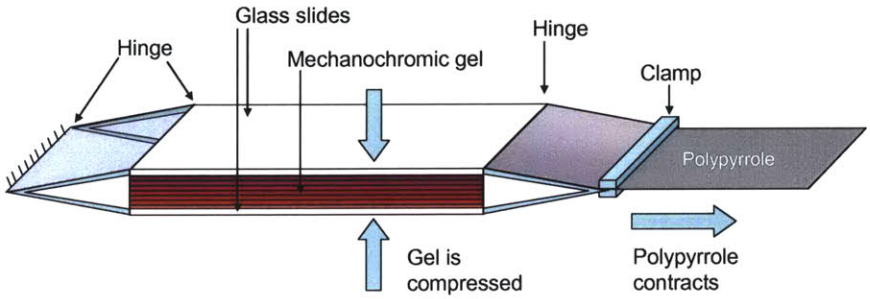

Figure 49 Compression envelope mechanism

A plausible design to transmit strain and force from a linear polymer actuator film into compression of the mechanochromic gel is shown below. Geometric strain analysis shows that for L = 5 mm and neutral design position x = 9.95, deformation in polypyrrole of 0.040 mm will compress gel thickness from 1 mm to 0.5 mm. This could be achieved by 1% strain in a 4 mm long film.

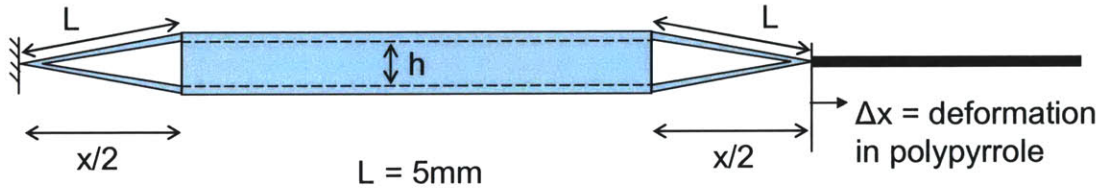

Figure 50 Strain analysis of compression envelope mechanism

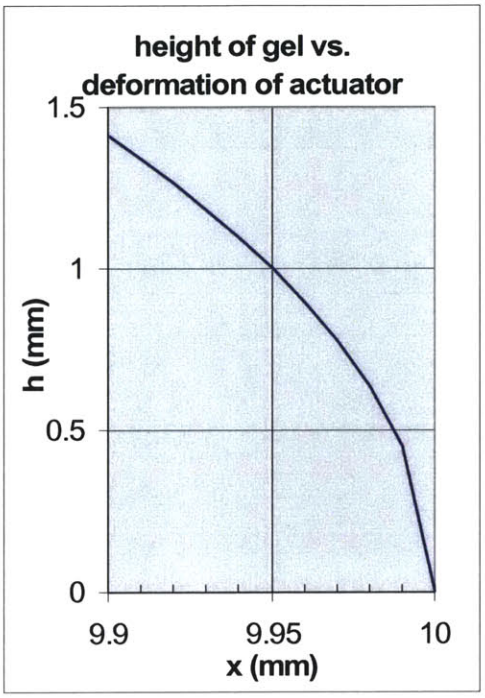

For L=5 mm and neutral design position x=9.95, deformation in polypyrrole of 0.040 mm will compress gel thickness from 1 mm to 0.5 mm. This could be achieved by 1% strain in a 4 mm long film.

Figure 51 Height of mechanochromic gel vs. deformation of actuator

Analysis of the forces shows that this region of high strain amplification is also the region of lowest force transmission. By considering the torques about the hinge joint, one can see that the compressive force transmitted to the gel is related to the torque produced by the polypyrrole about the hinge joint. The torque is minimized at the greatest extension of the hinge (largest x) because the lever arm of the actuator is minimized. Specifically, the product of the actuator force and its lever arm (half the internal height h) is at all times equal to the integral of the product of the force and lever arm distributions transmitted to the gel. In addition, this region of weakest force transmission will be the same configuration in which the gel is most compressed. As with any spring, this is the region of high force to strain ratio.

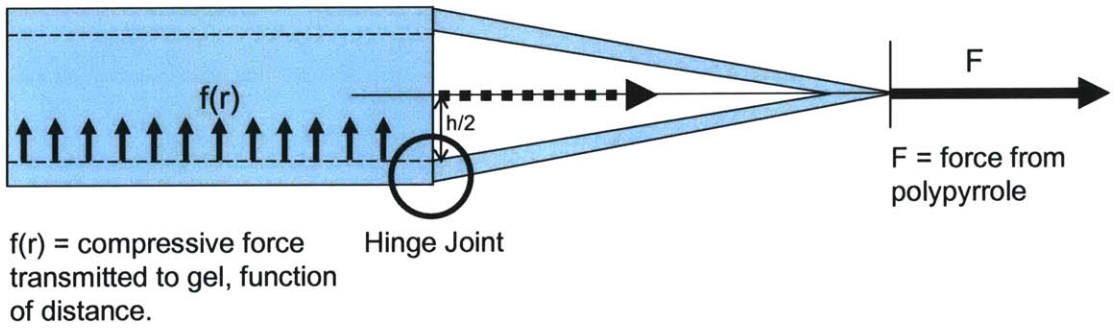

Figure 52 Schematic of one end of compression mechanism showing forces

3.5.5. Polypyrrole Interface

Additional design challenges were in making the contact with the polypyrrole. The contacts to the polypyrrole must provide sufficient electrical contact and prevent slippage. The clamp devices must be extremely smooth and screwed in tightly, while not creating sharp corners which could tear the fragile polypyrrole film.

3.6. Future Work: Design Concept for Mechanochromic Pixel

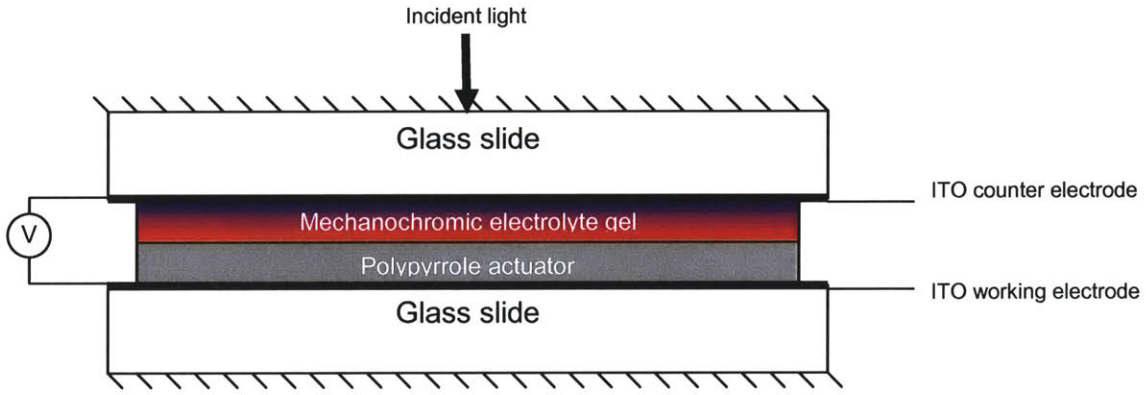

Figure 53 Proposed pixel design based on mechanochromic electrolyte gel.

The above schematic describes another design concept for a uniaxial compression mechanochromic pixel. The mechanochromic electrolyte gel is the key innovation of this design. The gel is both the color changing element and the electrolyte for the electrochemical cell that supplies the ions needed for polypyrrole actuation. The polymer needed for this design is a high index mismatched block copolymer with high molecular weight and lamellar microstructure, which also has good mobility for an electrolyte system for polypyrrole actuation. The ions will be mobile in the mechanochromic gel and easily transfer to the polypyrrole layer. The ion mobilization will alternately swell and relax the polypyrrole when redox switching occurs in the polypyrrole. The movement of ions out of the BCP will shrink the BCP, augmenting the mechanochromic effect.

The mechanochromic polymer electrolyte gel is compressed by the swelling of the polypyrrole film. The electrical contact will occur through the indium tin oxide (ITO) layer on the glass. The ion source will be in the polymer gel. The ITO layer on the opposite side will be the counter electrode. This will give all the proper elements and proper field alignments for polypyrrole actuation. The ITO coating on the glass slides will allow for the electric circuit and for the necessary clear window to observe the mechanochromism. The black polypyrrole will enable better observation of the reflectivity of the mechanochromic gel.

3.6.1. Design Calculations

Using the transfer matrix method, it was calculated that a highly ordered 13 μm thick PS-PI film would achieve over 90% reflectance, and that a 5 μm thick film would achieve 70%-80% reflectance. To induce significant mechanochromic effects, the sample must be compressed with 5%-10% strain. For the films mentioned, this requires deformations

of 1.3 μm and 0.5 μm, respectively. A polypyrrole film of thickness 1 μm can expand in thickness by 20%-30% (Smela, 1999). A 6.5 μm thick actuator with 20% strain would yield displacements sufficient to compress the thicker film, while an actuator only 2.5 μm thick with 20% strain would compress the thinner film. Thicker polypyrrole may produce larger deformations, though it is unclear whether the high anisotropic strain will occur in thicker films.

The rigidity of the clamping mechanism is of critical importance. If the compliance allows even microns it could negate the mechanochromic effects. This should be simple to achieve. If the clamping mechanism is significantly stiffer than the BCP (>>1 MPa), the polypyrrole will deform the BCP without moving the glass slides.

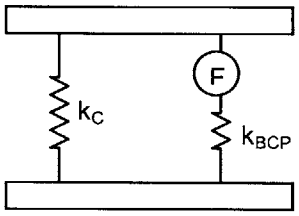

Figure 54 F=force generated by polymer actuator. k= stiffness in clamp (C), block copolymer (BCP). The clamping mechanism must be significantly stiffer than the block polymer gel.

Another advantage of this design is that it can easily enable small pixel sizes. The design may even be improved by small pixel sizes. Some key factors will contribute to this.

- Film resistance. Resistance in polypyrrole film causes voltage drop and therefore decreased and nonuniform actuation. Smaller films will experience a smaller voltage drop and therefore will have more uniform actuation. The ITO layer will also mitigate the voltage drop.
- In-plane strain. There will be some strain in the plane of the film. This could cause buckling or delamination problems in large pixels.

3.6.2. Mechanochromic Electrolyte Gel

Some significant systematic studies will be needed to develop the electrolyte gel. The tradeoffs between good properties for mechanochromism and good properties for an electrolyte gel need to be understood. A systematic study of ion mobility properties in the BCP with different ion systems would be necessary. Several physical processes would need to be investigated.

- Solvent-salt-polymer solubility. The salt needs to be soluble in a solvent that will carry it into the gel matrix by swelling both domains of the block polymer.

- Ion mobility. Lamellar interfaces cannot impede ion mobility (the electrolyte must have high mobility in both domains).

- Electrolyte effect on optical properties of both domains. Scattering and absorption would likely increase, making the gel less transparent, which would

detract from mechanochromic effects. A change in refractive index is also likely. But this effect could be exploited to *enhance* mechanochromism. The change in optical thickness (n·d) could be altered more dramatically with the ability to simultaneously change both refractive index (n) *and* layer thickness (d). The index mismatch between domains could thus be actively changed.

- Actuation effects of electrolyte system. The relative sizes and charges of the ions will be important to actuation and by extension to mechanochromic effects. Since size change is important in both the polypyrrole and the gel, the selection of an ion system will be a dominant factor in this design. Several electrolyte systems in use for polypyrrole actuation involve small counter ions (-) with large co-ions (+). In these systems, the small anions are mobile and enter the polymer when it is oxidized. Smaller ions result in faster response and smaller strain. Other systems to investigate would be of a class of salts characterized by $AB_2 \rightarrow A^{2+} + 2B^-$. Large cations would be immobile, and smaller anions would be the mobile species. But, having twice as many anions for the same molarity of salt may increase the shrinking/swelling effect in the BCP. Ionic liquids should also be investigated. They have been used to actuate polypyrrole and have low vapor pressures.

3.6.3. Alternate Design

A simpler version of this design concept is shown below. The ion source for the polypyrrole is the electrolyte gel, similar to that used for the polypyrrole trimorphs discussed previously. A lens paper is wetted with a solution of acetonitrile, propylene carbonate, polymethylmethacrylate (PMMA), and lithium perchlorate, clamped together with the polypyrrole film and allowed to dry. In this design, the gel would be clamped between the polypyrrole actuator film and an ITO coated glass slide to complete the circuit as the counter electrode. A strip of stainless steel foil would aid in making electrical contact to the polypyrrole layer. The mechanochromic gel would be placed on this construct and topped with another glass slide. The whole mechanism would be clamped in place with a fixed width between slides. The gel would presumably have a lower modulus than the lens paper electrolyte layer, so the change in thickness of the polypyrrole layer with oxidation and reduction would reversibly compress the mechanochromic gel, inducing color change. The black polypyrrole actuator would aid in the observation of the reflective properties of the mechanochromic gel.

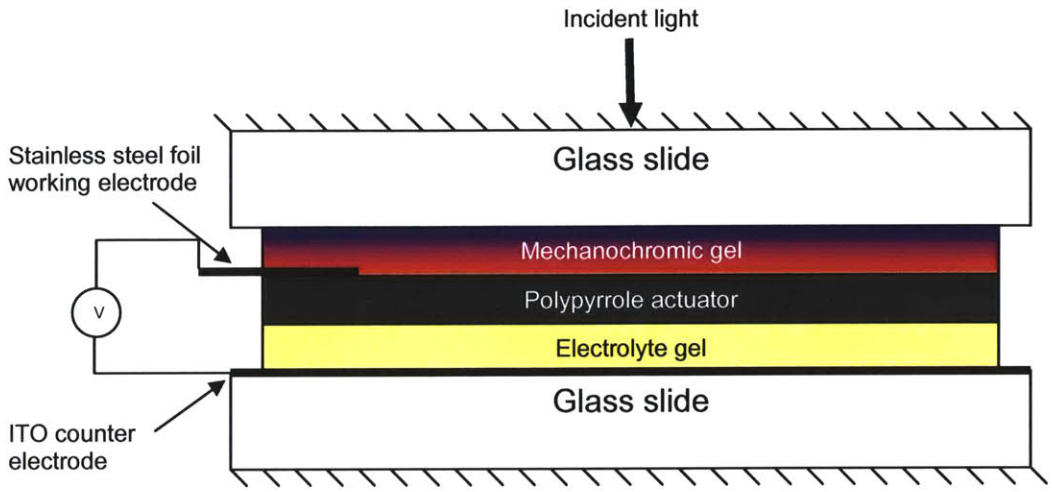

Figure 55 Alternate pixel design based on separate mechanochomic and electrolyte gels

3.7. Summary and Conclusions

Mechanochromic polymers can be combined with actuating polymers to achieve active multifunctionality. To enable design calculations, mechanochromic materials were characterized. Several designs were analyzed and tested in which polypyrrole actuation induces deformation of the mechanochromic block copolymer to create a color changing pixel. The development of the mechanochromic pixel involves core issues of mechanical design, polymer physics, and actuation science.

The pixel is based on two mechanochromic block copolymers with lamellar microstructures: polystyrene-polyisoprene and polybutadiene-polyisoprene.
From the quarter wave stack model it was predicted that the reflected wavelength will shorten by 30 nm for 10% uniaxial strain (extension) parallel to the layers, or with only 5% strain (compression) normal to the lamellae. The reflectance spectrum of PS-PI was measured as a function of uniaxial compressive strain by compressing the sample to a series of discreet thicknesses and measuring the spectrum at each.

Two important aspects of polymer physics can account for the differences between the PS-PI spectral measurements and the prediction of the models: mechanical deformations and microdomain orientation. The mechanochromic effect depends on the change in optical thickness ($n \cdot d$). The stiffer layer will deform less and will also constrain the softer material. Compression of the sample tends to align the lamellae horizontally. As the microdomains rotate from grazing incidence to normal incidence, there is a resulting redshift which counteracts the overall blueshift that results from compression of the layers.

The intensity of light reflected in a stack of dielectric layers was calculated using the transfer matrix method. The refractive indices were measured by ellipsometry. The PB-PI system has on order-of-magnitude smaller gap between the refractive indices (Δn=0.008 for PB-PI, Δn=0.08 for PS-PI). The physical result is that the bandgap (range of wavelengths of light which cannot pass through) is narrower, and at each layer less

light is reflected. Thus for the same number of layers, the smaller bandgap material (PB-PI) has a much lower reflectance. The number of layers of PS-PI needed to achieve sufficient reflectance was found by the Transfer Matrix Method. With 130 total layers (65 periods), over 90% reflectance can be achieved if the layers are well-ordered. This would correspond to a film 13 μm thick. Thus pixel design will involve a tradeoff between film thickness (and corresponding deformations required) and total reflectance.

Several pixel design concepts were investigated. One pixel concept used a bending polypyrrole actuator layered with an electrolyte gel actuated in air. Though the bending bilayer with a layer of mechanochromic gel shows mm to cm scale deflection of the end of the strip, the surface strain along one face of the polypyrrole strip is still only 1%. This would only cause a color change of 3 nm in wavelength which is nearly imperceptible.

Another used the polypyrrole actuator immersed in electrolyte solution, connected to the mechanochromic gel with levers. The levers were to supply the needed strain amplification and connect the BCP to the polypyrrole while keeping the two chemically isolated. Forces and deformations generated and transferred were calculated. To capture and transfer the small strain, the system must have minimal compliance. To harvest a small force, the moving parts must have minimal friction and inertia for maximum force to be transferred. The contacts to the polypyrrole must provide sufficient electrical contact and prevent slippage, without creating sharp corners which tear the polypyrrole film.

The tradeoff space between low system compliance and low friction was explored with the design and fabrication of the lever test stand. However, the system compliance was too great and consequently no strain could be transferred. Design iterations to lessen compliance in the fulcrum points resulted in additional friction, which made the amount of force that could be transferred negligible.

Alternate designs were considered in which strain was applied in compression normal to the lamellae, to use the small strains to compress the gel directly. In the compression envelope mechanism analyzed, the additional mechanisms would only contribute to the existing problems of additional forces required and additional compliance in the overall system. Analysis of the deformations and forces showed that the region of highest strain amplification was also the region of lowest force transmission. Another drawback of this design is that the gel is most compressed in the configuration which transmits the lowest force. As with any spring, this is a region of high force to strain ratio.

The uniaxial compression mechanochromic pixel design proposed as future work will address these design issues. The deformations in the polypyrrole will be applied directly to compress the gel. Based on the transfer matrix calculations for reflectance and film thickness, the mechanochromic effect can be achieved without levers and moving parts which introduce friction and compliance to the system.

The mechanochromic electrolyte gel is the key innovation of the design. Movement of ions out of the BCP will shrink the BCP, augmenting the mechanochromic effect. The gel is both the color changing element and the electrolyte for the electrochemical cell that supplies the ions needed for polypyrrole actuation. The polymer needed for this design is a high index mismatched block copolymer with high molecular weight and lamellar microstructure, which also has good mobility for an electrolyte system for polypyrrole actuation. The success of the proposed design will depend on anisotropic actuation in polypyrrole and the development of the mechanochromic electrolyte gel. The gel will function as an electrolyte system, donating and accepting ions with high mobility.

4. Systems Architectures: Informing The Systems Design Of The Far-Future Battlesuit

4.1. Introduction

The far future battlesuit will be a complex system in a complex multiscale system-of-systems. It will be the primary enabler of the integration of the individual soldier and the larger US Army. Thus rigorous study of the human body and the US Army are important. But in addition to dictating operating requirements of the deployable battlesuit, both systems teach important multifunctional, multiscale systems design paradigms. Lessons learned from the human skin, vasculature, and neural control systems, as well as from the US Army Battle Command Construct are described. To realize these paradigms in an eventual battlesuit system, the integration paradigms learned from the human body and the US Army must influence basic research and early technology development. The Resonance Hypothesis is introduced: a method to identify potentially nonintuitive areas for innovative research which can lead to born-integrated technologies. The Dynamic Systems Integration Map (DSIM) is proposed. DSIM is a tool to inform the systems integration aspects of basic research. The dynamic node-based taxonomy is inspired by the Resonance Hypothesis. DSIM also highlights system interactions between components that contribute to a particular soldier survivability capability, identifies components with similar features and functionalities, and informs innovative teaming of R&D assets, with a graphical interface that can be dynamically explored and tailored to a stakeholder's needs. DSIM maps out an open system architecture that will be user-friendly, yet competent for the high complexity of nano components integration and the early stage of research.

4.2. The Human Body

The human body is a natural, massive functionality protection and survivability system. Multiscale systems design solutions employed in the human body can be used to inform the design and development of the battlesuit.

4.2.1. Multiscale, Multifunctional System

The human body uses a hierarchy based on nano-scale building blocks resulting in a multifunctional macro-scale system. Different functionalities are enabled at each level of the hierarchy. Likewise, the battle suit will be a macro-scale system with a nano-rich hierarchic structure, with additional functionalities enabled at each level of the hierarchy. In the body, small molecules (amino acids) are assembled into polymers (proteins). Proteins have a myriad of functions, including breakdown of food, transmission of nervous and endocrine control signals, mechanical structure, and maintenance of chemical processes in the body. To enable unprecedented functionalities, the battle suit will likewise exploit nano-enabled functionalities, and also the integration of nanotechnologies and nanocomposite materials. Like biological systems, many ISN research projects work to exploit unique behaviors of polymers. Some proteins are formed into nanoscale organelles which carry out specific functions inside a cell; others are formed into extracellular matrix to give the tissues structure and various other functions. Cells are grouped together into distinct tissues and organs, each with their own

function, and these organs combine to make the dynamic, multifunctional human body, capable of sensing, responding to, and acting on the environment. Similarly the battle suit will be dynamic and multifunctional, capable of sensing and responding to the threats and situations of the environment and closely interfacing with the human. It too will depend on functionalities enabled at scales from atoms through macroscopic materials. In particular, the dermal, nervous, and circulatory systems in the human body are multiscale, multifunctional, integrated systems which can inform battlesuit design.

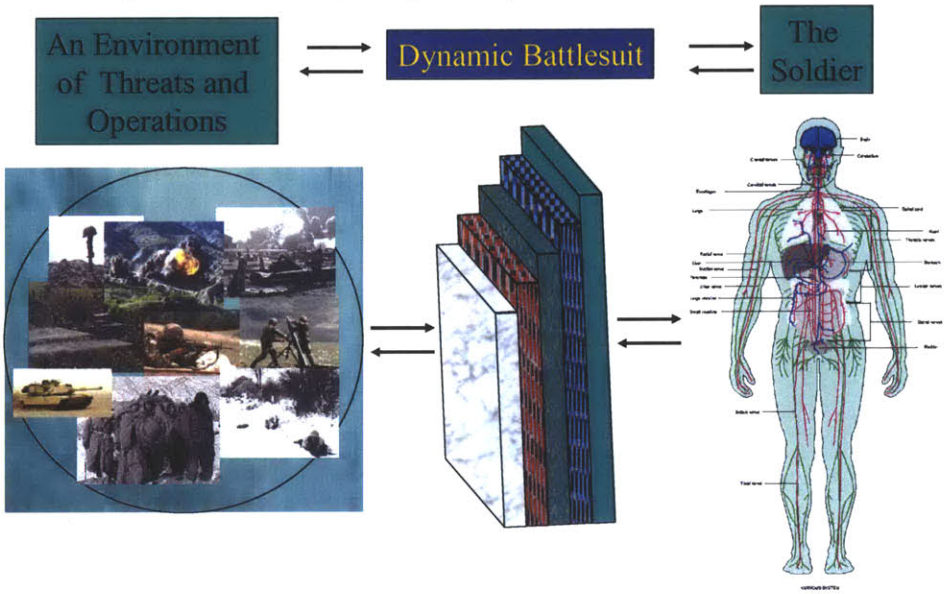

Figure 56 The battlesuit will define the interactions of the soldier and the environment.

4.2.2. Lessons from the Dermal System

The battle suit can be thought of as a second skin, highly analogous to natural human skin. The skin is a protective layer that also senses, all without hindering the motion of the body. Likewise, the battle suit will provide improved situational awareness through a myriad of sensors and information processing and will provide improved protection from a variety of threats without significantly hindering motion and soldier performance. The skin has nanometer-scale and micron-scale protective and sensory elements (cells, proteins, structures) arranged in interacting layers. Such elements include the hairs on mammalian skin that provide both additional protection and additional sensing capabilities. This sort of multifunctionality combined with spatial integration is the design paradigm that will characterize the battle suit. It will also inform the direction of the ISN basic research to develop nanotechnology to enable multifunctional materials and integration.

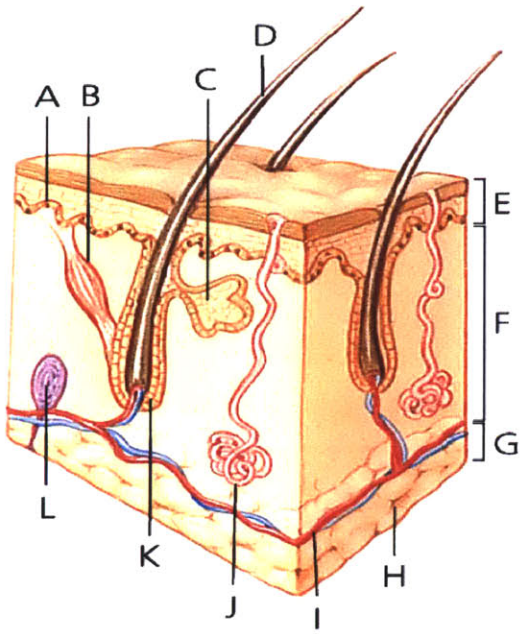

Thermal Management
Immediate Response to Injury
Wound Healing
Environmental Protection
Liquid/Gas Impermeable

Figure 57 The skin has nanometer-scale and micron-scale protective and sensory elements (cells, proteins, structures) arranged in interacting layers.

4.2.3. Lessons from the Circulation System

Blood circulation is also an informative multifunctional system, with mechanisms that span a large range of size scales. The circulatory system provides nutrient delivery and waste removal for the organs and cells of the body, maintains body temperature, and detects and fights bacteria-scale invaders. The main pump is macroscopic, but the smallest capillaries are smaller than one red blood cell (3 μm). The heart pumps large volumes of blood (5 liters/minute)(Vogel, 1981) and yet the mechanisms for each of the above described functionalities are on the scale of single cells and proteins. The delivery of the appropriate nutrients to the body happens molecule by molecule through membranes with pores and gates. Contraction of the heart depends on both molecular interactions of actin and myosin to generate force, and intercellular communication to coordinate pulses. Heart cells respond to local fluid stresses and adjust the configuration of the cytoskeleton through mechanotransduction. Similarly, in the battlesuit, sensors at the nanometer and micron scales will result in multi-scale feedback and response. The circulatory system has ~100,000 km of blood vessels of varying diameters. The heart does not directly supply pumping force to the entire vasculature. Other mechanisms are at work, particularly in the veins returning blood from the extremities. The body parasitically uses motions from the muscles surrounding the blood vessels to compress sections of the veins. One-way valves keep the blood moving in the right direction. The complementary circulation system is the lymphatic system, which parallels the vascular system throughout the body. The lymphatic system collects interstitial fluid which diffuses out of the blood, filters it of bacteria, restores lymphocytes which aid the immune system, and returns it to the bloodstream.

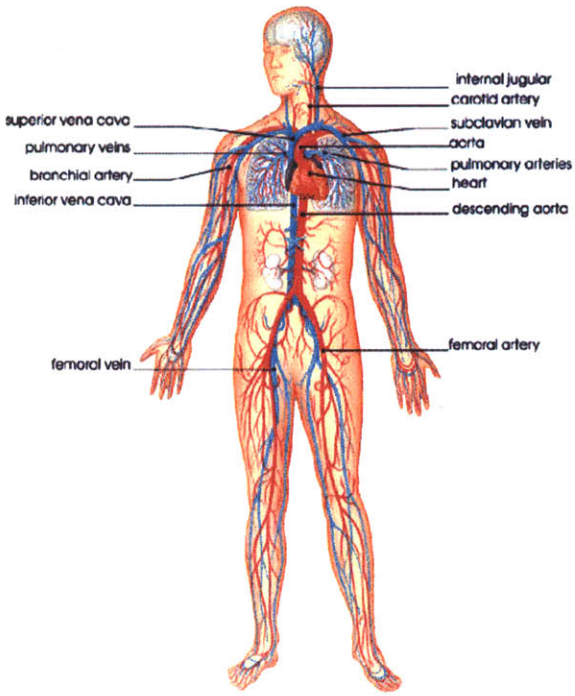

Figure 58 The circulatory system provides nutrient delivery and waste removal for the organs and cells of the body, maintains body temperature, and detects and fights bacteria-scale invaders.

The teachings from the circulatory system inspire a battlesuit subsystem enabled by the integration of ISN nanotechnologies. The envisioned subsystem is an artificial vasculature that can transport protective fluids within the flexible battlesuit. Tiny 'capillaries' could be made from hollow polymer microfibers (product of ISN partner DuPont) and functionalized for drug delivery, local thermal control, stiffness on demand, and chemical control systems. The vision of this future system informs the present research at its early stage. Like in the body, pumping only with a single central pump would not be the optimal design, since such a pump would necessarily be large and have to be worn externally. Instead, distributed pumping power would be needed. A key enabling technology will be the development of pumping microfibers. Sections of an elastomer microfiber could be compressed in succession by separate bands of a polymer actuator such as polypyrrole (another material studied at the ISN), creating a peristaltic pump that mimics pumping of blood in the body. This pumping paradigm also would depend on multiscale interactions. It involves the molecular actuation mechanism of the polymer actuator, synchronization of the pumping sequence, and feedback control. Discussion and experimental investigation into the feasibility of such an artificial vasculature are discussed further in chapter 2. Interactions with parallel systems to clean and maintain fluid levels (analogous to the lymphatic system) is also a likely design solution.

Such complex functionalities require control over a huge range of length scales and time scales. The human nervous system has hierarchical levels of planning and implementation of multi-scale responses both conscious and subconscious. Higher levels of the central nervous system are involved in planning, but much of the implementation

and control goes through feedback loops at lower, local levels. This increases the speed of the response and decreases the computational load on the central nervous system. Similarly, in the battle suit the nano-rich design will call for a huge control requirements. A key design paradigm is that the individual nano-enabled functionalities must be self-controlling or controlled at decentralized localized hubs throughout the suit. To centrally control a suit full of one layer of square-micron devices would require a computer 5000 times faster than laptops available on the market today. See Discussion of Control Requirements.

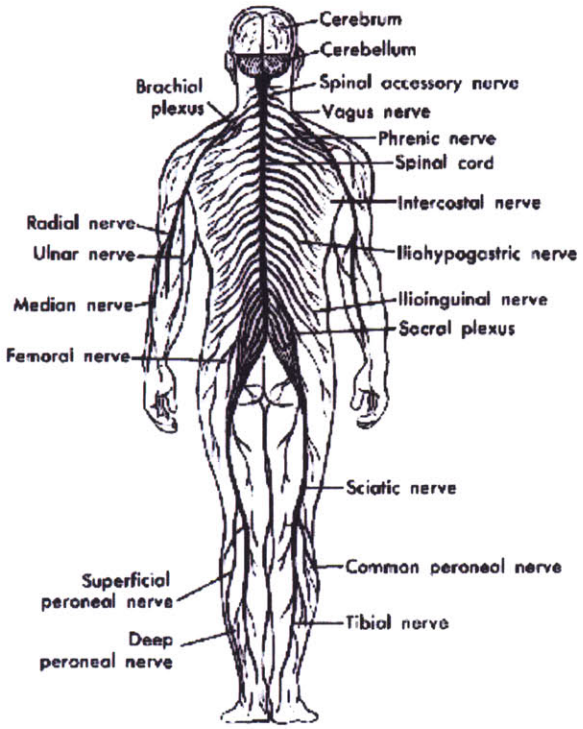

Figure 59 The human nervous system has hierarchical levels of planning and implementation of multi-scale responses both conscious and subconscious.

4.3. The US Army Battle Command Construct

The Army itself is an informative system for battlesuit systems design, as both are complex systems of dynamically coordinated discrete elements. The design of a nano-rich battlesuit involves challenges similar to coordinating an Army with many individual members. The US Army Training and Doctrine Command's (TRADOC) 'Ten Big Ideas' of Battle Command Construct provide direct teaching to the Battlesuit Design Construct. (TRADOC Pam 525 pp 13-14).

"(1) Commander-Driven, Purpose-Oriented, Knowledge-Based Mission Orders
Very high tempo, widely distributed land operations, in a complex environment, will overwhelm any leader or system that attempts to centrally control execution. Decentralized execution by all arms becomes mandatory. Maximum initiative, within commanders' intent, will allow application of combined arms, at the tempo envisioned."

Similarly, to directly control the function of each nano-enabled device in the suit would require a computer more than 5000 times faster than a current laptop computer! Decentralized computing and local analog responses will allow application of the desired effects within the time and computing restraints.

"(2) Echelonment of Command is not the same as Echelonment of Unit Formation
The completely flexible tailoring of forces is central to combined arms warfare and dominant maneuver. The appropriate mix of Battle Command, maneuver, maneuver sustainment, and maneuver support is mission dependent, not tied to organizational convenience."

The battlesuit will have the ability to dynamically recruit and control the appropriate set of subsystems. For example, the subsystems will provide on-demand ballistic protection, burst power to enhance physical performance, or antidote delivery at the appropriate times in the relevant quantities. It will optimize protection, response time, situational awareness, and power conservation in a variety of situations. From research through product development through deployment, the science and engineering behind the battlesuit must likewise be centered around the mission and not limited to organizational convenience. In the ISN, research projects are not bound by traditional academic discipline. Instead of conforming the science to fit the organizational pattern, the ISN has structured the organization around the mission relevance of the science. Research projects are interdisciplinary to better focus on the mission of developing protective nanotechnologies for the soldier.

"(3) Battle Command Resourced for Sustained Operations
The Battle Command System must be structured and resourced for the long haul, in terms of distance and duration."

The battlesuit must likewise maintain all critical functions over long times and distances. System integrity must be maintained throughout the suit while interfacing with subsystems over a huge range of time and length scales which span several orders of magnitude. The battlesuit must maintain its short response time to threats over a long lifetime. For example, dynamic armor or blast protection countermeasures must respond quickly to an adverse event (of order μs or ms), exomuscle must supply short periods of increased physical strength (of order min), and the battlesuit must maintain these capabilities over its service lifetime (months to years). Similarly the battlesuit must correctly coordinate with length scales within the suit and with the systems into which it must integrate, from molecular scale sensing of explosive residue in the air (of order Angstroms) to macroscale force generation (cm-m), over the entire geographic range of service (km).

"(4) Battle Command—Anytime, Anywhere
High tempo, fluid maneuver, from strategic distance, will require the commander to exert personal presence, at the points of decision, across vast areas. The BCS must allow

commanders to move and command effectively, from alert, through redeployment, from whatever location the circumstances require."

This informs the battlesuit design requirements directly and by analogy. The battlesuit must allow tailorable exogenous communications within various echelons so that actionable information can reach the right people to be properly addressed.

By analogy, there must be mechanisms by which the soldier can determine when central override of battlesuit subsystems is needed, and mechanisms by which the soldier can exert that override. From the scale of a nano-enabled device, the topography of the human body is also a vast area! One square micron in relation to 2 square meters (average human skin surface area) is the same area ratio as one human standing in 193,000 sq miles! (larger than California; half the size of Iraq). So an individual person or central processing unit commanding a single battlesuit has similar danger for information overload that a single commander would face in a large scale military operation. Again, as in (1), this further supports the need for decentralized control, which TRADOC states as "maximum initiative [by subordinates nearer the point of action] within commanders' intent."

"(5) Teaming Commanders and Leaders—On Demand Collaboration
Distributed operations and high tempo maneuver will demand rapid synchronization, swift adaptation of plans and control measures, flexible groupings of distributed staff elements, and direct exchanges between commanders across hierarchies."

The battlesuit will not only have to dynamically recruit the correct set of subsystems, it must also control those subsystems and their interactions, adapting to every situation. The Dynamic System Integration Map discussed later in this chapter serves to identify nonintuitive interactions between subsystems at as early stage of research, which will inform the rules for development of subsystems and the dynamic recruitment of subsystems within the battlesuit.

"(6) Fully Integrated: Space to Mud, Factory to Foxhole
Joint interdependence demands that Army Forces (ARFOR) dominate maneuver, execute precision fires, efficiently support Army and joint elements, and provide full dimensional protection. Army combined arms will complement and reinforce each other, and other joint elements, throughout the campaign. The BCS will become the catalyst for effective multinational operations."

The battlesuit subsystems must be fully integrated with each other. The battlesuit will serve as a catalyst to supply multidimensional protection to the soldier, efficiently enabling the maneuver by supplying burst power, medical intervention on demand, etc.

"(7) One Battle Command System
A unitary BCS empowers tactical commanders to execute combined arms maneuver more effectively than any in history. The same system that controls wartime operations

will regulate activities in garrison, and in training. Because the BCS is part of the joint system, ARFOR will support, and be supported by, joint elements."

The same battlesuit control systems must meet the distinct needs of soldiers in wartime and in training. Embedded training modules will increase effectiveness and relevance of training and enable smooth transition to deployment. The battlesuit must likewise be an enabler of joint operations. Symbiotic interconnections and automatic coordination between 2 or more battlesuits could enable powerful teaming between individual soldiers.

"(8) Unprecedented Information Network Dependability
A multitiered network will allow commanders to reach across tactical boundaries, and across theater and intercontinental distances, to access and share actionable information. The system will allow humans to apply judgment and experience, exploiting vast amounts of information, managed more effectively. The network will tie global maneuver, maneuver support, and maneuver sustainment, and provide redundancy and security to protect it."

The battlesuit must efficiently manage large amounts of information from many internal sensors and external networks. The network must allow for soldier communication integrated into the battlesuit. In addition, the battlesuit has its own internal networks. It must deliver the proper amount and type of information to the soldier and to the automatic systems. This multitiered dynamic system must include redundancy and protective measures.

"(9) Modular, Scaleable, Tailored Battle Command
Highly tailored and responsive ARFOR will require Battle Command, matched and positioned precisely, for theater needs. Just as ARFOR are task organized, the BCS will constantly adapt, move, expand, and contract in size, and adjust capability, as the situation demands."

The dynamic precision capabilities of the battlesuit will require a highly adaptive control system with similar abilities to expand, contract, and adjust capability as the situation demands. The product design phases of the battlesuit will build on the information learned in research and development to establish the proper design tradeoffs. Key design paradigm tradeoffs are between central and distributed control. Dynamic recruitment of subsystems provides a balance between timely response and power consumption.

"(10) Dramatically Smaller Deployed Footprint
The pace and scope of maneuver, in and outside the theater, mandates a BCS that is equally maneuverable. A stretch goal to make the BCS much more tactically, operationally, and strategically responsive is to reduce the footprint of command posts (CP's) at UA level, as well as higher echelon levels, by a factor of ten."

The unprecedented capabilities of the battlesuit will require increased number and complexity of components, but must result in a small logistical footprint (long duration

power supply, increased on-board capabilities, etc.) for smooth operation, deployment, and integration into the force.

4.4. Discussion of Control Requirements

An emerging paradigm for nanotechnology integration is that we central micromanagement of every nano-component in the suit is not a plausible design. With current computing technology, it would be impossible for every operation of every suit component to be controlled through a single central processor. The following estimations agree with the teachings on control paradigms of the inspirational systems, the Army and the human body. Distributed, redundant systems must pervade the suit. Rigorous research will determine the appropriate type and amount of information needed at each level, and the optimal level at which to make certain decisions to improve time and accuracy of response.

The surface area of the human skin divided by an estimated nano-enabled device size, multiplied by a modest control requirement yields the estimate that a centrally controlled battlesuit would require a digital computer 5000 times faster than high end laptops on the market today.

$$\frac{A_h}{A_d} = n = 1.6 \cdot 10^{12} \, devices$$

$$n \cdot f_d = f = 16 \cdot 10^{12} \, flops/s$$

Assume no layering of devices
A_h = Human skin surface area = 1.6 m^2 (up to 2 m^2)
A_d = Estimated nano-enabled device size = 1 μm^2
n = number of devices = $1.6 \cdot 10^{12}$
f_d = estimated computation requirements per device = 10 flops/s·dev.
f = estimated computation requirements = $16 \cdot 10^{12}$ flops/s·dev.

Equation 19 Computing requirements for battlesuit control systems

By comparison to a 3200 MHz computer, this requirement is 5000 times faster. This number gets worse for layering of devices, smaller device size, higher control requirements, smaller computers, and more surface area.

4.5. Inspirational Design Solutions From Complex Systems

Some proposed design solutions are inspired by the human body and the Army. TRADOC states that "maximum initiative, within commanders' intent, will allow application of combined arms, at the tempo envisioned." The quick response times of protective elements within the battlesuit will be enabled by the majority of threats being addressed directly and locally, with mechanisms that do not pass through a single central processor. The human body also uses such distributed control, for example the knee-jerk reflex mechanism is contained within a circuit that does not travel to the brain before firing. The body uses different methods of control on different scales as another design solution. Cells can react directly to changes in their environment by way of complex processes which involve mechanical, chemical, and electrical signals and responses. The time scales of responses cover many scales: cell motility in response to external environment can occur in seconds, cell restructuring in response to loading can occur in days or weeks, complex coordination of organ function and endocrine signaling can happen over scales of hours, days, and months. In a sense, many of these (especially chemical and mechanical) are analog systems. The battlesuit must likewise depend on the interactions between mechanical, chemical, and electrical subsystems in a mixture of

analog and digital systems to implement local control paradigms with the best response for survivability. For example, an analog local feedback response system might be triggered by a chemical hazard detection with a fluoropolymer. Another florescent sensitive molecule acts as a gate to change conformation and release a proportional amount of antidote based on the change in fluorescence the detector molecule. Additional design solutions are discussed later in this chapter.

4.6. Systems Architecture Design: Dynamic System Integration Map

A mechanism by which these emerging multiscale, multifunctional systems design solutions can improve basic research is required. The instructions for systems integration are systems architectures. Project 7.3 seeks fundamental understanding to integrate nano-scale and nano-enabled components to produce soldier survivability systems, including, in the longer run, a massive functionality battle suit. In addition to basic research to design, build and test simple, nano-enabled prototype systems, project 7.3 formulates systems architectures to exploit nanotechnology in the battle suit. Revolutionary survivability capabilities for the soldier will depend on new nanotechnologies and the integration of those technologies. Invariably in such a complex system, interface problems will arise. This often occurs far downstream in the product design phase.

4.6.1. The Resonance Hypothesis

A hypothesis of ISN Team 7 is that by considering systems design issues from an early stage, the R&D assets can be informed and leveraged to identify symbiotic as well as destructive interactions among system components. How can the science be informed to mitigate or capitalize on these interactions at the basic research stage? First these interactions must be found. One way proposed here is by comparing characteristic time scales, length scales, and energy scales of emerging technologies and anticipated threats.

The Resonance Hypothesis states that mechanisms on the same scales, or same ratios of scales, are at higher probability to interact. These potentially non-intuitive interactions are in addition to mechanical, chemical, material, and electrical interactions.

Resonance phenomena are widely observed and well documented in many areas of science. In mechanical systems, coupled systems with similar natural frequencies will begin to oscillate at the same frequency. The classic example of this is observed by hanging 2 pendulums with different natural frequencies on the same rigid wall. The pendulums will eventually swing together at the same frequency. For further explanation, see McMahon, 1984. A child can swing higher by 'pumping', taking advantage of the same resonance phenomenon. A catastrophic example was the collapse of the Tacoma Narrows Bridge which occurred when wind perturbed the bridge at its natural frequency for torsional deformations.
(http://www.vibrationdata.com/Tacoma.htm) In electrical systems, resonances occur in circuits that include a capacitor, inductor, and resistor ('RLC' circuits) as the electrical energy is alternately stored in and released from the capacitor. Exploitation of this phenomenon is widely used in telecommunications to selectively communicate between

transmitter and receiver tuned to the same frequencies. In optical systems, the manipulation of constructive and destructive interference in electromagnetic waves has a myriad of applications, including materials characterization and using lasers for interference lithography. In chemistry, different bond types can be excited at different frequencies. All of these interaction types can be harnessed for beneficial or detrimental results. Each acts over various characteristic time scales, such as the period of the natural frequency, time to reach steady state, or time to failure. The phenomena will occur over a range of characteristic lengths: bond vibration lengths in Angstroms, interference lithography features in nanometers, torsional bridge oscillations in meters. Another important characteristic scale is energy; the energy being stored and released associated with a bridge deforming ($\frac{1}{2}mv^2$) is much different than that associated with the oscillations of molecular bonds (kT).

On the simplest level, mechanisms with the same time scales may be candidates for integrated control systems. Or they may be the building blocks of an innovative analog feedback response system, in keeping with the emerging distributed control paradigms. Analysis of ratios of scales is also important. For example, ratios of time and length scales can be observed as velocities or frequencies. Resonance on the same frequencies have been discussed above. Characteristic power is energy per time. Elements with the tendency to exchange similar amounts of energy over the same time scales would be candidates for power interactions. A proxy for relative power density can be obtained by considering characteristic power divided by characteristic length cubed. Thus the characteristic scales of each emerging technology can quantify the storage, inertial and resistive responses to the types of energy present. Then, by comparing these values researchers can identify elements that have resonance potential and exploit the nature of these interactions.

Figure 60 Characteristic time, length, and energy scales

Threat	Time scale	Length scale	Energy scale	ISN Research Response
5.56 & 7.62 mm Rounds	μsec	mm	Many MJ/ms	Ballistic protection materials
Chemical & Biological Agents	sec Min	nm to μm	kT~ 4pN/nm	Sensors, antidote delivery
Fatigue	hrs Days	cm to m		Systems integration, exomuscle,
Heat	mins hrs	mm to m	kJ/hr to MJ/hr	HVAC
Many additional threats and responses to add…				

Needs in the research portfolio can be identified by comparing the characteristic scales of threats and the technologies that address them. Potentially nonintuitive interactions can

be identified between emerging technologies that occur over the same characteristic scales or ratios of scales (i.e. characteristic power, frequency, etc.).

4.6.2. Multidomain Resonance

Oscillations and resonance can occur where energy can be alternately stored and released within a system. The described resonances are important for design considerations. However, there is an additional level of design complexity that arises when resonances occur between different domains. Energy can transfer between electrical, mechanical, and chemical domains. A common way to derive equations with which to analyze the dynamics of a given system is to account for all the energy in the system in its different forms through each system component. A formalism for this analysis known as bond graphs has a unified treatment of energy throughout the various domains of a system. The bond graph system treats each component as a lumped parameter element: storage element (spring, capacitor, etc.), inertial element (mass, inductor, etc.), or resistive element. Other elements are used to describe the energy relationships ('bonds') between domains and between specific elements. The representation can quickly illuminate potential oscillatory responses, even across domains. For full description, see Karnopp, 1990. Bond graphs can aid the dynamic analysis of a multidomain system, and also give insight into multidomain resonance. In further developments, effects of noise/perturbations on the system must be understood.

The battlesuit will also be a multidomain system. A full lumped parameter model of a battlesuit with all its functionalities would be prohibitively complex and premature for the early stage of ISN research. However, a quantitative analysis of the storage, inertial, or resistive effects of an emerging technology could be extremely informative towards identifying and exploiting potentially nonintuitive crossdomain resonances.

4.6.3. Distributed Control Enabled By Multidomain Resonances in Biological Systems

Powerful coordination and resonance effects can be achieved with multidomain resonances. The heartbeat is one such phenomenon. A mammalian cardiac myocyte (heart smooth muscle cell) contracts independently with a certain pulse rate when isolated from surrounding tissue. Multiple isolated cells in a culture dish will contract independently at a distribution of frequencies out of phase with one another. When cells are brought in contact with neighboring cells, they almost immediately begin to contract in unison. This is enabled by a complex resonance involving chemical, mechanical, and electrical subsystems of the cell. The electrochemical responses of cells to mechanical stimuli are collectively called mechanotransduction. Chemical signaling transfers the mechanical deformations sensed in neighboring cells and coordinates the electrical signals within the cell to control actin/myosin molecular motors to generate force at a coordinated frequency and phase. Note that this is another local feedback control loop that enables a powerful function, the heartbeat, without the control of a central processor.

The human brain uses another version of resonance to manage the interactions between simultaneous subconscious elements of complex serial and parallel search tasks (Bichot,

2005; Wolfe, 2005). Millions of neurons are constantly sending and receiving signals about the surrounding environment. Most of this information is processed subconsciously. Some neurons are tuned to specific elements, such as specific aspects of shape, a certain color, or a particular scent. When neurons tuned for different aspects of a search target are triggered, they raise their signal level. The power of resonance coordination is that when many of these specialized neurons, tuned to different aspects of a specific search target, are triggered, they synchronize their firing patterns. The elevated and synchronized firing patterns attract the conscious attention of the individual.

The authors compare the constant level of neuron firing to the general din in a noisy room. If a few individuals randomly raise their voices, the room just gets louder. But, if a group starts chanting in unison, they are heard above the level of background noise in the room.

The battlesuit could adopt similar control patterns to capitalize on multidomain resonance to address the control challenges discussed previously. The battlesuit will have a myriad of sensors taking a constant survey of the environment, similar to the constant signaling of neurons in the brain. In order to identify a particular threat, suites of sensors could be designed to resonate with one another when the multidimensional signal of a threat is perceived. This could alert the soldier and attract the virtual "attention" of the proper countermeasures, in a method that would be resistant to false positives and general signal noise.

4.6.4. Conclusions

Multidomain resonance can enable critical complex capabilities with local feedback control. It can also help to achieve what TRADOC calls "Actionable Information": the balance of the right amount and type of information with which to make a decision (pam. 525). Analysis of the characteristic scales of resonance of battlesuit technologies can identify target technologies to be enabling components of multidomain resonance. The scale data comparison, along with other types of data can be managed with a proposed graphical interface tool, the Dynamic System Integration Map (DSIM).

4.7. Dynamic Systems Integration Map

The Dynamic Systems Integration Map (DSIM) is a visualization tool to guide the current research and development stages of the far-future battlesuit. A core strength of the ISN is innovative teaming of cutting edge science. This tool is a way to inform teaming based on multiple ways of looking at the emerging technologies. The DSIM maps out an open system architecture that will be user-friendly, yet competent for the high complexity of nano components integration and the early stage of research. The DSIM is a mapping system of nodes which represent projects, capabilities, functionalities, and characteristic scales. The map provides an active taxonomy, allowing the designer to focus on any suit component and see its relevant relations to other aspects of the system. A user can 'click' on any node and the map will recenter around that node, and bring to view additional relations to the new center node. Nodes can easily be changed, added, or linked as research progresses and changes. A Dynamic System

Integration Map is proposed that provides a visual representation of several types of interactions between components. The proposed DSIM:

- Highlights system interactions between components that contribute to a particular soldier survivability capability
- Identifies components with similar features and functionalities
- Elucidates characteristic time, length, and energy scales revealing potentially unexploited interactions and synergisms
- Informs innovative teaming of R&D assets, as well as born-integrated technology

The DSIM is not a scheme for categorization or classification, nor is it a business plan or an organizational framework. It cannot "think" on its own, but it can stimulate creative thought. It is intended as a tool to organize information in such a way that a researcher can identify trends and potentially fruitful areas to continue research.

In the configuration shown, the DSIM highlights system interactions between components that contribute to a particular soldier survivability capability. Here, the selected central node is the capability Ballistic Protection. By 'clicking' on the Ballistic Protection node, one can look at a single capability and see the projects working synergistically towards that capability.

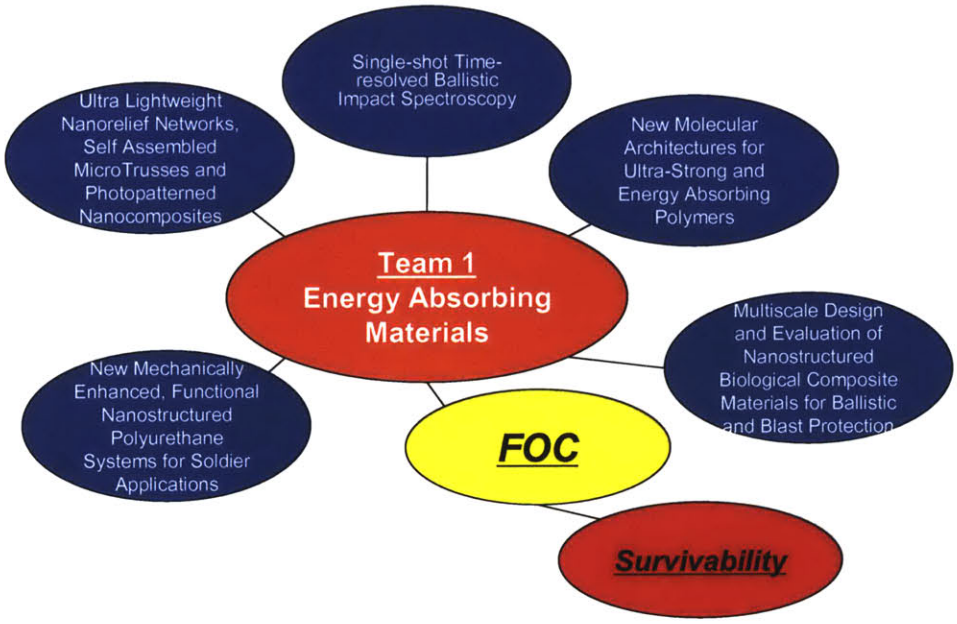

Figure 61 DSIM centered on Energy Absorbing Materials

Note that this orientation of the DSIM matches the organizational arrangement of the ISN into capability-based teams. For this example, the energy absorbing materials effort

(including ballistic protection) is shown, which includes projects in ISN Team #1. This mirrors the capabilities-based collaboration established at the ISN.

The DSIM can also identify components with similar features and functionalities. By selecting 'sensor' as the central node, one can look at a single feature and see projects that share a certain functionality. For example, various sensor types might operate on similar mechanisms and be combined into a single multifunctional sensor. Or there might be alternate approaches to sense a certain event that could be used synergistically. Perhaps a certain type of threat has a multidimensional signature that requires different sensors working together to properly identify it and to trigger a suite of countermeasures. (Note that these would also show up on a threat-centered arrangement of the DSIM. Nodes that appear connected in many views are likely ripe for investigation of their potential interactions.)

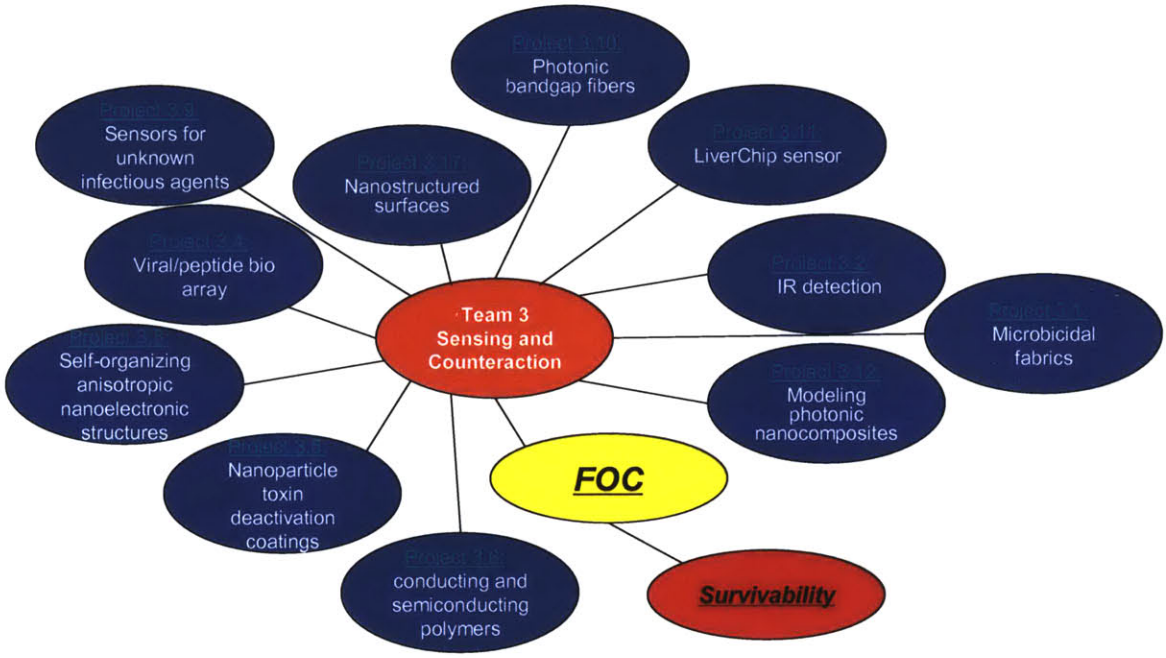

Figure 62 DSIM centered on sensing technologies

Alternatively, a certain feature or component type may be selected, such as a gel. Every project using any type of gel would appear (i.e. polymer actuators using electrolyte gels, mechanochromic gels, materials with varying rigidity, nanocomposites, or gel-based sensors.) This could lead to research into multifunctional gels, such as a mechanochromic electrolyte gel discussed in chapter 3.

Analysis of characteristic time, length, and energy scales can reveal potentially unexploited interactions and synergisms. The DSIM includes the characteristic scale information contained in the table shown previously. For example, one can look at a single time scale and see all projects that may have critical functions operating on that

time scale. Ratios of characteristic scales can also be seen, such as characteristic power. This could lead to integration strategies to optimize response times and power consumption, or identify possibly non-intuitive interactions between varied phenomena that occur over the same characteristic scales.

Example: click on "time scales" node to recenter the D-SIM, highlighting projects that operate on similar time scales.

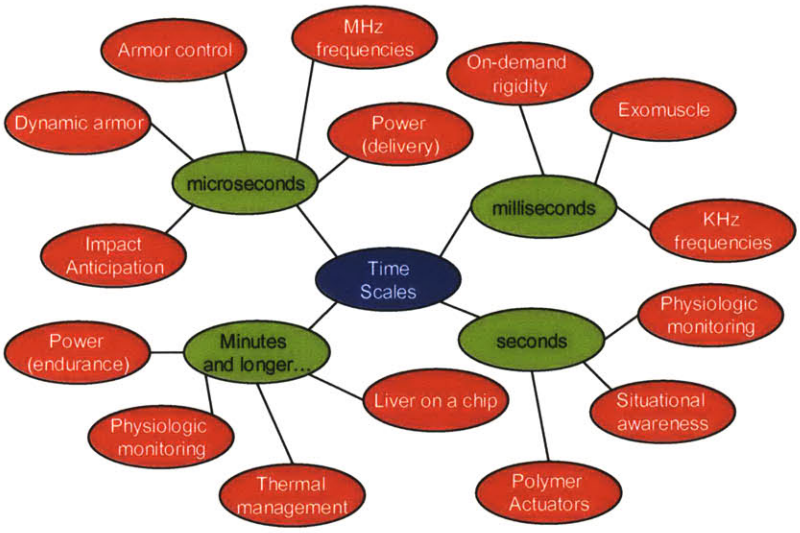

Figure 63 DSIM centered on characteristic time scales of threats and technologies

The DSIM informs innovative teaming of research and development assets, which leads to born-integrated technology. 'Born-integrated' means that in the basic research phase ('gestation period') relationships with other technologies are already identified, allowing them to be accounted for in design, building, and testing. In maintaining a large basic research portfolio, projects are phased in and out. The nodal arrangement allows for simple spiral insertion to track this. Documentation of past work remains to avoid repeating unproductive investigations and to allow for old data to be revisited in light of new findings.

4.7.1. Adaptable Views Relevant to Different Stakeholders

The DSIM is a potentially powerful tool to inform the science, and also a tool to communicate the science to different stakeholders. The tool is flexible; one can look at the same interactions from many perspectives. By adapting to these different perspectives, the DSIM can present the research in a way that is relevant to each observer. Several stakeholders are involved, including subgroups within industry, academia, and military. University structures are traditionally centered around individual research projects. Military and industry tend towards top-down, requirements-based approaches, and fit individual technologies around that framework. Different stakeholders view the same science from different perspectives, and the DSIM can be a valuable tool to bridge the gap.

For example, a graduate student might begin looking at the DSIM with his project (microtrusses) as the central node. The peripheral nodes would be the supported

capabilities, the functionalities/components, and characteristic scales. From there, he recenters the map around the other nodes in turn, where he sees connections to other projects and can identify fruitful ways to interact with other researchers. The critical time scales associated with the microtrusses are the time scales of ballistic events, other impacts (such as blunt trauma), and diffusion. Investigation of the diffusion time scale node would show links to other diffusion events, such as chemical delivery through various media and evaporative cooling. Studies into the limits of evaporative cooling through the microtrusses would follow, investigating the feasibility of breathable body armor.

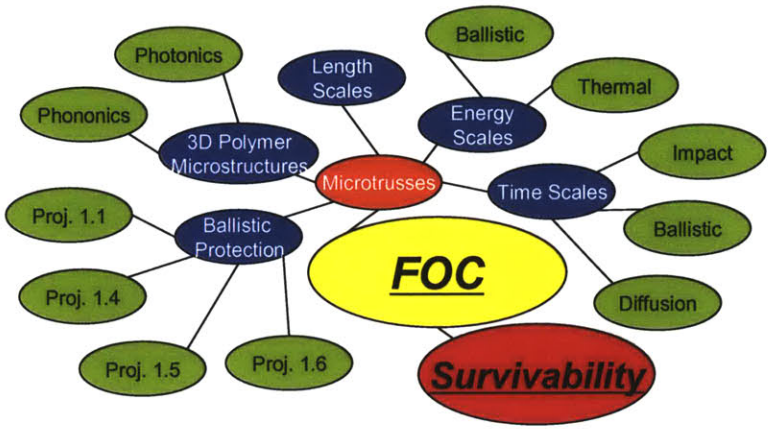

Example: click on "microtrusses" node to center the D-SIM, highlighting relevant relationships of a single project

Figure 64 DSIM centered on an individual research project

Or, a military advisor to the ISN may start with a central node of a certain capability or threat that needs to be addressed for the soldier. She can quickly see which projects are supporting that effort and identify areas for more research. For example, centering on FOC Human Engineering would reveal projects contributing to reducing soldier load and enhancing soldier endurance. She would view the microtruss project as part of a suite of technologies emerging to provide enhanced protection with lower bulk and weight.

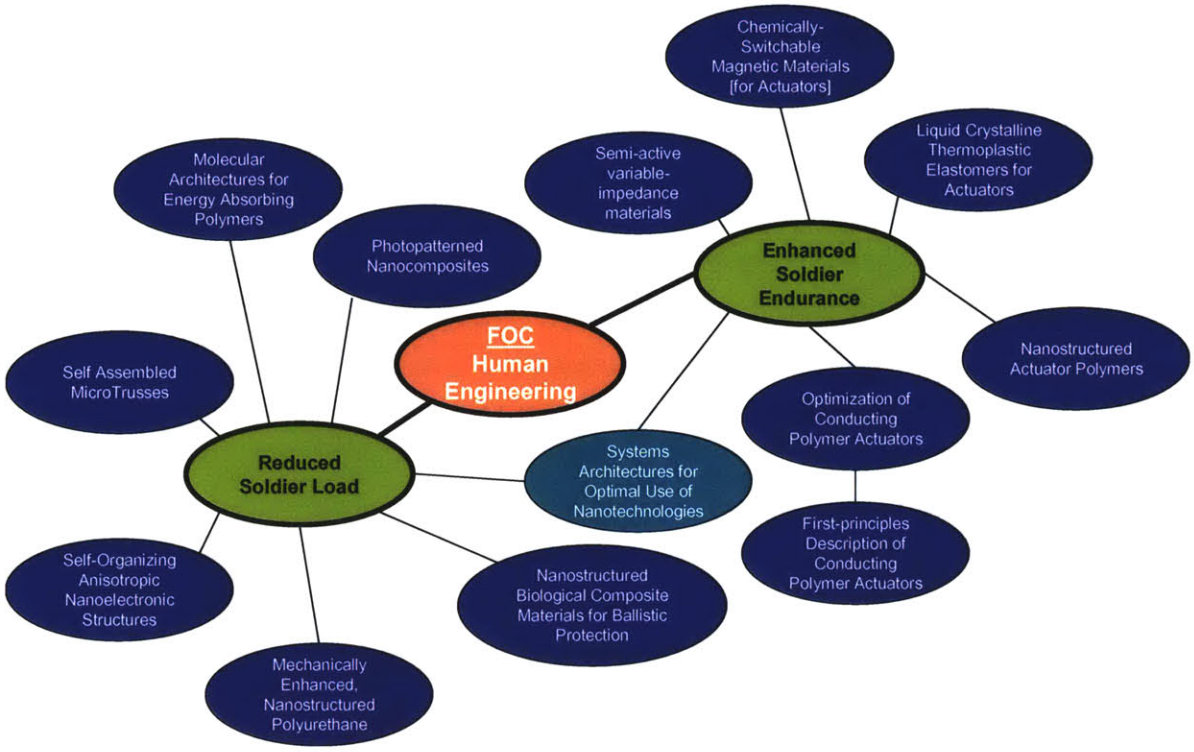

Figure 65 DSIM centered on Force Operating Capability: Human Engineering

An industry sponsor may represent a company with a particular expertise, for example photopatterning or photolithography. Centering the DSIM on photonic based technologies would reveal projects involving photonic crystals, interference lithography, photopatterning, and photochemistry. The DSIM would help him identify projects his company may be interested in supporting as a research partner or transitioning to product development. In this case, he would see the microtrusses project as one of several potential products which interference lithography can produce. Each case helps the user to understand and direct the science in different ways.

4.7.2. System architecture relevant to the stage and complexity of the system

The dynamic map can grow in structure with the battlesuit. In its current form, the taxonomy is very loose, reflecting the basic research stage. As more interactions are found and investigated, their relative importance will emerge and that will naturally lead to an informed arrangement of a more traditional hierarchy for product development. Thus, at the research stage, the DSIM informs innovative research. As the research progresses, it determines which branches of the web will dominate the eventual design process. Finally, when a traditional hierarchy is needed for manufacture and assembly, it will have evolved in a process that reflects the best leverage of the science, not from an arbitrarily enforced structure.

The purpose of a system hierarchy is different at different stages of a project. The systems integration at the development stage is to inform the R&D so that the eventual

product will have a smoother transition, higher functionality, and faster commercialization. Specifically, what the DSIM (and the general study of systems integration) informs is where to do more research in areas that might interact, especially to solve newly identified problems. Then researchers are more likely to harness the synergy than to have to mitigate damages. The definition and design of these interactions will evolve at varied rates throughout the system as technologies mature.

As the specific goals of systems integration change with the phase of a project, so too the form must necessarily change. There is a balance of enough structure to mobilize but not so much structure that it inhibits progress. The proper balance point constantly shifts. A key strength of the DSIM is that is that it aids structure in seeing the above described connections, but does not define what they are. This allows freedom in the research. The DSIM is the right amount of structure for the early stage of development, and does not oversimplify the complex nature of the multiscale, multifunctionality battlesuit enabled by nanotechnologies.

4.7.3. Illustration: Department of Defense Architecture Framework (DoDAF) and DSIM

To illustrate the important differences and interrelationships between an open system architecture useful for informing basic research and a rigorously structured system architecture for managing far downstream systems, the DSIM is compared and contrasted with the Department of Defense Architecture Framework (DoDAF). There are distinct synergistic principles in the two systems representation tools, such as customizable nodes and different organization of the same information to make it relevant to different stakeholders. The primary differences in form and function arise from differences in purpose (see previous discussion). The DSIM is intended to identify areas ripe for innovative research that will lead to the eventual development of multifunctional systems, whereas DoDAF is geared toward a multifunctional system in or near to operation.

DoDAF was released by the Department of Defense in 2003 and adopted in 2004 as a unified systems architecture representation to enable communication and interoperability in joint and multinational operations. It is a successor to the previous versions for system architecture descriptions: Command, Control, Communications, Computers, Intelligence, Surveillance, and Reconnaissance (C4ISR). (Telelogic 2005)

Both DoDAF and DSIM are highly customizable and based on nodes and interconnections representing components, functionalities, and interrelationships. Both systems recognize the need for different stakeholders to view the same information in different ways. The arrangement of the data strongly influences the clarity and perceived relevance to the stakeholder. DoDAF has several predefined views that call out a specific set of information, geared to answer specific questions relevant to the operation of the system. To address a specific and well defined question, the DoDAF can call out the proper set of predefined data.

Table 2: DoDAF Architecture Products

APPLICABLE VIEW	FRAME-WORK PRODUCT	FRAMEWORK PRODUCT NAME	GENERAL DESCRIPTION	UML DIAGRAMS
All Views	AV-1	Overview and Summary Information	Scope, purpose, intended users, environment depicted, analytical findings	Text (or DOORS) documents
All Views	AV-2	Integrated Dictionary	Data repository with definitions	UML model queries
Operational	OV-1	High-Level Operational Concept Graphic		
Operational	OV-2	Operational Node Connectivity Description		
Operational	OV-3	Operational Information Exchange Matrix		
Operational	OV-4	Organizational Relationships Chart		
Operational	OV-5	Operational Activity Model		
Operational	OV-6a	Operational Rules Model		
Operational	OV-6b	Operational State Transition Description	One of three products used to describe operational activity sequence and timing - identifies business process responses to events	State Machine Diagram
Operational	OV-6c	Operational Event-Trace Description	One of three products used to describe operational activity sequence and timing - traces actions in a scenario or sequence of events and specifies timing of events	Sequence Diagram
Operational	OV-7	Logical Data Model	Documentation of the data requirements and structural business process rules of the Operational View.	Class diagram
Systems	SV-1	Systems Interface Description	Identification of systems and system components and their interconnections, within and between nodes	Composite Structure diagram
Systems	SV-2	Systems Communications Description	Systems nodes and their related communications lay-downs	Composite Structure diagram
Systems	SV-3	Systems-Systems Matrix	Relationships among systems in a given architecture; can be designed to show relationships of interest, e.g., system-type interfaces, planned vs. existing interfaces, etc.	DOORS Traceability View automatically populated as interfaces are defined in model.
Systems	SV-4	Systems Functionality Description	Functions performed by systems and the information flow among system functions	Activity diagram with Object Flows
Systems	SV-5	Operational Activity to Systems Function Traceability Matrix		
Systems	SV-6	Systems Data Exchange Matrix		
Systems	SV-7	Systems Performance Parameters Matrix		
Systems	SV-8	Systems Evolution Description		
Systems	SV-9	Systems Technology Forecast		
Systems	SV-10a	Systems Rules Model	One of three products used to describe systems activity sequence and timing—Constraints that are imposed on systems functionality due to some aspect of systems design or implementation	Text (or DOORS) document linked to System Functions
Systems	SV-10b	Systems State Transition Description	One of three products used to describe systems activity sequence and timing—Responses of a system to events	State Machine diagram
Systems	SV-10c	Systems Event-Trace Description	One of three products used to describe systems activity sequence and timing – System-specific refinements of critical sequences of events and the timing of these events	Sequence diagram
Systems	SV-11	Physical Schema	Physical implementation of the information of the Logical Data Model, e.g., message formats, file structures, physical schema	Class diagram
Technical	TV-1	Technical Standards Profile	Extraction of standards that apply to the given architecture	Text (or DOORS) document linked to Systems
Technical	TV-2	Technical Standards Forecast	Description of emerging standards that are expected to apply to the given architecture, within an appropriate set of timeframes	Text (or DOORS) document linked to Systems

Figure 66 Sample of views generated by DoDAF

Good research answers a good question, but part of the challenge of research is often discovering the right question. To this end, the DSIM by its exploratory nature can lead one to creatively formulate "a good question" based on interactions mapped out between emerging technologies. A large number of predefined answers does not aid the person looking for a good question.

Differences between the two systems arise from the development stage of the system they represent and the resulting purpose of the system architecture. The biggest difference is in the balance point of open mapping to explore complex interrelationships versus rigorous definitions to structure and manage complex interrelationships. Some representative diagrams give an indication of the relative structure level.

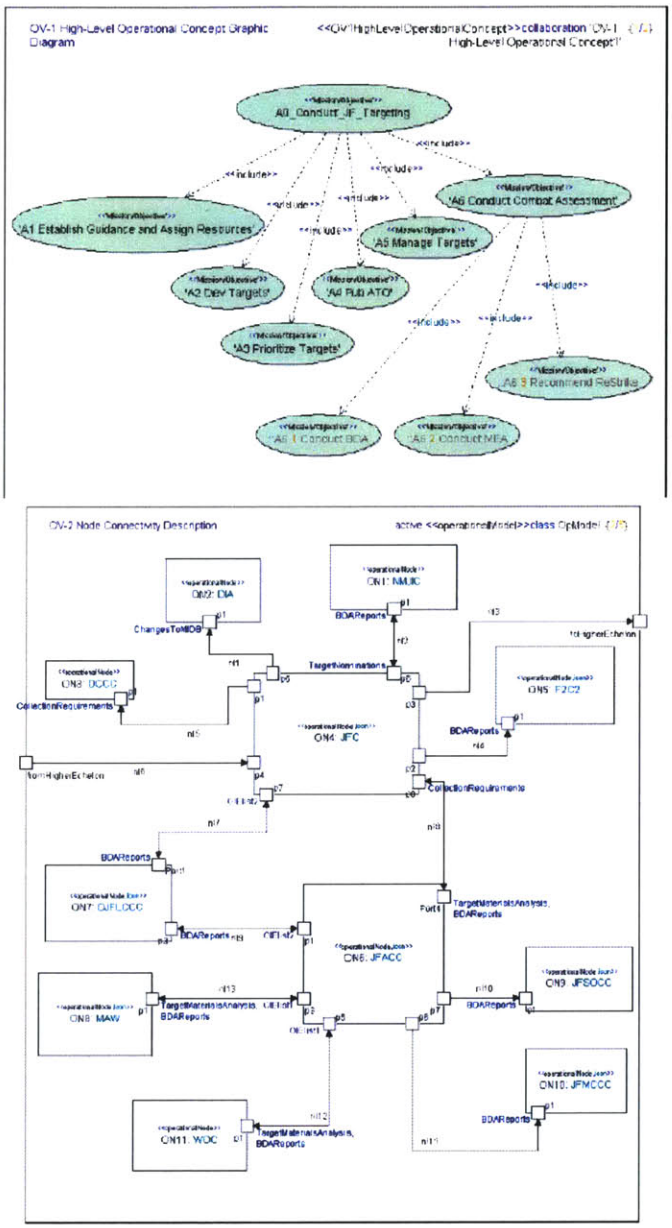

Figure 67 Examples of DoDAF representations of system interactions

There are also differences in what type of information the two systems represent. The DoDAF emphasizes establishing systems for reuse based on established best practices (DoDAF, 2004). Basic research does not have the same luxury of having established "best practices" for discovery and early development of new technologies. Instead, it emphasizes finding research areas ripe for innovation. DoDAF divides architectures between multiple layers, decoupling business logic and technical requirements/processes into separate layers. In the form proposed here, the DSIM does not address business practices associated with higher technology readiness levels and ultimate commercialization.

4.7.4. Conclusions

The DSIM would be a powerful tool that fills the need of the basic research community in a way that will naturally feed into a DoDAF compliant architecture necessary for the deployment of a far-future battlesuit. To conform emerging ISN technologies at the basic research stage into a fully DoDAF compliant format would be counterproductive. Many of the informational categories in the DoDAF views listed above do not yet have meaning or relevance for the battlesuit. But, the DSIM sets a strong foundation for eventual smooth transition to DoDAF. DSIM is a mapping of relationships. It seeks NOT to classify and compartmentalize, but instead to identify potential relationships and interactions. As these potential interactions are explored, they will lead to the development of functional interactions between technologies, and eventually to operational interactions between components. These operational connections are the prime information that the DoDAF is equipped to manage. Thus, as discussed previously, the eventual downstream system architecture will have evolved naturally from the best leverage of the science, not from an arbitrarily enforced set of definitions.

4.7.5. Future Work

Significant future work is required to realize full development and implementation of the DSIM. To inform future research, the tool must accurately reflect the current state of the science. It requires time and effort to obtain this information from researchers; it is not a trivial task in an organization the size of the ISN. It would be a whole masters project to acquire the necessary data and develop a cohesive database so that a software program could identify the interrelationships discussed in this chapter. The commercially available Th!nkmap® line of visualization tools (www.thinkmap.com) is a potential software platform to support the DSIM. To realize the full effectiveness of such a tool requires researchers to explore the map and use scientific judgement and scientific curiosity to undertake research into exploiting these interactions. The DSIM is not expected to predict the exact nature of the interactions. A tool can organize data in such a way that a trend can be recognized. Like any tool, the DSIM cannot think, it is an aid for the creative research mind. Until future work produces the necessary support software and databases, the DSIM serves as a graphical representation of an intangible integration paradigm that informs innovation and teaming by analysis of capabilities, component types, and characteristic time, length, and energy scales.

5. Conclusions and Suggestions for Future Work

The mission of the ISN is to explore the long-range vision of the role of nanotechnology in the future of soldier protection. Such a survivability system is highly complex with manifold opportunities for interactions between battlesuit technologies. The unprecedented capabilities will arise from the ability to cohesively and comprehensively coordinate and capitalize on the functions and interactions of each technology. The present work approaches these objectives with basic research to support the development of two multifunctional soldier survivability systems, pumping microfibers and mechanochromic pixels.

Integrative studies inform the overall systems architecture of the far future battlesuit. Scoping calculations to investigate battlesuit functionality requirements were performed. The multiscale, multifunctional design solutions employed in the human body and the US Army and were studied, and systems architectures were developed to apply the lessons learned to coordinate and leverage the many emerging survivability technologies.

5.1. Pumping Microfibers

Progress was made along the two major paths of investigation towards the realization of a pumping microfiber. The two branches explored the chemical deposition of a smooth, conductive layer of polypyrrole onto copolyetherester which would adhere to the copolyetherester and serve as a working electrode for the electropolymerization of actuator quality polypyrrole. Investigations into the interface of the two materials (copolyetherester and chemically deposited polypyrrole) resulted in polypyrrole layers with conductivity or integration within the copolyetherester. Further development is needed to simultaneously achieve both conductivity and adhesion in this case where one material is deforming the other, and also to improve smoothness and mechanical integrity. Tubular polypyrrole actuators at the millimeter scale were fabricated and actuated. Radial actuation properties at this more manageable scale must be understood and then the micron scale can be investigated. The importance of a radial electric field was shown and a set of requirements was developed for a test setup to further characterize radial actuation.

Future work towards the development of a pumping microfiber should focus on the radial actuation of polypyrrole. If polypyrrole cannot be made to generate sufficient strain and stress to deform the hollow fibers, then the pump as conceived here will not work and the surface adhesion problem will not be important. Polypyrrole as an actuator is still the subject of much research. Radial actuation is all but omitted in the literature. As its structure-property relationships are better understood, the ability to harvest those properties in useful devices will grow. Anisotropic properties in polypyrrole can be manipulated by stretch alignment and electric field effects, and it is not obvious how these properties, studied primarily in films, will manifest themselves in a radial actuator of small diameter.

Another reason to focus future experimentation on radial polypyrrole actuators is that the problems of electrical contact and electrical circuit development can be addressed independently of the adhesion problem. Polypyrrole has been used as both an actuator and a sensor (Spinks, Madden thesis). Some polypyrrole tube segments could be actuators deforming the elastomeric fiber and functioning as pumping stations, while other tube segments would measure the pulses felt through the elastomeric tube. Thus the pumping microfiber has the potential for the future development of embedded sensing for feedback control. The feedback system could be applied locally over just a few segments, in keeping with the biomimetic distributed control paradigm discussed in chapter 4. Much more research would be needed to characterize the gage parameters and time responses of polypyrrole as a strain sensor, and to correlate those data to the internal flow.

Far future integration of pumping microfibers into functional circuits, including soldier protection systems for the battlesuit, will require efficient ways of connecting the pumping microfibers with macro, micro, and nanoscale components. This challenge will have a different design solution for each subsystem in which it is used. The economic and robust manufacture of the pumping microfibers would also be necessary to field large numbers of battlesuits with the ubiquitous artificial vasculature envisioned.

5.2. Mechanochromic Pixel

Mechanochromic polymers can be combined with actuating polymers to achieve active multifunctionality. To enable design calculations, mechanochromic materials were characterized. Several designs were analyzed and tested in which polypyrrole actuation induces deformation of the mechanochromic block copolymer to create a color changing pixel. The development of the mechanochromic pixel involves core issues of mechanical design, polymer physics, and actuation science.

The pixel is based on two mechanochromic block copolymers with lamellar microstructures: polystyrene-polyisoprene and polybutadiene-polyisoprene.
From the quarter wave stack model it was predicted that the reflected wavelength will shorten by 30 nm for 10% uniaxial strain (extension) parallel to the layers, or with only 5% strain (compression) normal to the lamellae. The reflectance spectrum of PS-PI was measured as a function of uniaxial compressive strain by compressing the sample to a series of discreet thicknesses and measuring the spectrum at each.

Two important aspects of polymer physics can account for the differences between the PS-PI spectral measurements and the prediction of the models: mechanical deformations and microdomain orientation. The mechanochromic effect depends on the change in optical thickness (n·d). The stiffer layer will deform less and will also constrain the softer material. Compression of the sample tends to align the lamellae horizontally. As the microdomains rotate from grazing incidence to normal incidence, there is a resulting redshift which counteracts the overall blueshift that results from compression of the layers.

The intensity of light reflected in a stack of dielectric layers was calculated using the transfer matrix method. The refractive indices were measured by ellipsometry. The PB-PI system has on order-of-magnitude smaller gap between the refractive indices (Δn=0.008 for PB-PI, Δn=0.08 for PS-PI). The physical result is that the bandgap (range of wavelengths of light which cannot pass through) is narrower, and at each layer less light is reflected. Thus for the same number of layers, the smaller bandgap material has a much lower reflectance. The number of layers of PS-PI needed to achieve sufficient reflectance was found by the Transfer Matrix Method. With 130 total layers (65 periods), over 90% reflectance can be achieved if the layers are well-ordered. This would correspond to a film 13 μm thick. Thus pixel design will involve a tradeoff between film thickness (and corresponding deformations required) and total reflectance.

Several pixel design concepts were investigated. One pixel concept used a bending polypyrrole actuator layered with an electrolyte gel actuated in air. Though the bending bilayer with a layer of mechanochromic gel shows mm to cm scale deflection of the end of the strip, the surface strain along one face of the polypyrrole strip is still only 1-2%. This would only cause a color change of 3 nm in wavelength which is nearly imperceptible.

Another used the polypyrrole actuator immersed in electrolyte solution, connected to the mechanochromic gel with levers. The levers were to supply the needed strain amplification and connect the BCP to the polypyrrole while keeping the two chemically isolated. Forces and deformations generated and transferred were calculated. To capture and transfer the small strain, the system must have minimal compliance. To harvest a small force, the moving parts must have minimal friction and inertia for maximum force to be transferred. The contacts to the polypyrrole must provide sufficient electrical contact and prevent slippage, without creating sharp corners which tear the polypyrrole film.

The tradeoff space between low system compliance and low friction was explored with the design and fabrication of the lever test stand. However, the system compliance was too great and consequently no strain could be transferred. Design iterations to lessen compliance in the fulcrum points resulted in additional friction, which made the amount of force that could be transferred negligible.

Alternate designs were considered in which strain was applied in compression normal to the lamellae, to use the small strains to compress the gel directly. In the compression envelope mechanism analyzed, the additional mechanisms would only contribute to the existing problems of additional forces required and additional compliance in the overall system. Analysis of the deformations and forces showed that the region of highest strain amplification was also the region of lowest force transmission. Another drawback of this design is that the gel is most compressed in the configuration which transmits the lowest force. As with any spring, this is a region of high force to strain ratio.

The uniaxial compression mechanochromic pixel design proposed as future work will address these design issues. The deformations in the polypyrrole will be applied directly to compress the gel. Based on the transfer matrix calculations for reflectance and film thickness, the mechanochromic effect can be achieved without levers and moving parts which introduce friction and compliance to the system.

The mechanochromic electrolyte gel is the key innovation of the design. Movement of ions out of the BCP will shrink the BCP, augmenting the mechanochromic effect. The gel is both the color changing element and the electrolyte for the electrochemical cell that supplies the ions needed for polypyrrole actuation. The polymer needed for this design is a high index mismatched block copolymer with high molecular weight and lamellar microstructure, which also has good mobility for an electrolyte system for polypyrrole actuation. The success of the proposed design will depend on anisotropic actuation in polypyrrole and the development of the mechanochromic electrolyte gel.

5.3. Multiscale Design Solutions

Lessons learned from the human skin, vasculature, and neural control systems, as well as from the US Army Battle Command Construct are described. To realize these paradigms in an eventual battlesuit system, the integration paradigms learned from the human body and the US Army must influence basic research and early technology development.

The human body uses a hierarchy based on nano-scale building blocks resulting in a multifunctional macro-scale system. Different functionalities are enabled at each level of the hierarchy. Likewise, the battle suit will be a macro-scale system with a nano-rich hierarchic structure, with additional functionalities enabled at each level of the hierarchy.

The circulatory system inspires the present work towards pumping microfibers to support an artificial vasculature that can transport protective fluids within the flexible battlesuit. Tiny 'capillaries' could be made from hollow polymer microfibers (product of ISN partner DuPont) and compressed in sequence by a polymer actuator to enable pumping. Flexible microfluidic systems could be functionalized for drug delivery, local thermal control, stiffness on demand, and chemical control systems.

A key design paradigm learned from the human nervous system is that the individual nano-enabled functionalities must be self-controlling or controlled at decentralized localized hubs throughout the suit. Higher levels of the central nervous system are involved in planning, but much of the implementation and control goes through feedback loops at lower, local levels. This increases the speed of the response and decreases the computational load on the central nervous system. Dynamic recruitment of subsystems provides a balance between timely response and power consumption.

> "Understanding how biological systems do so well at performing a range of search tasks should help us to improve the outcome of those artificial search tasks on which we, quite literally, stake our lives."
> -Wolfe (Science, 2005)

A nano-rich battlesuit and the US Army are complex systems of dynamically coordinated discrete elements. The US Army Training and Doctrine Command's (TRADOC) 'Ten Big Ideas' of Battle Command Construct (Pam 525) provide direct teaching to battlesuit design. Lessons learned from the Battle Command Construct include distributed control ("maximum initiative within commander's intent"), rapid synchronization and situation-relevant reorganization.

Powerful local control effects can be achieved with multidomain resonances. The local coordination of individual cells in a single heartbeat is one such phenomenon. Another occurs in the human brain when the elevated and synchronized firing patterns in the subconscious sensing neurons determine when to alert the conscious attention of the individual. Analysis of the characteristic scales of resonance of battlesuit technologies can identify target technologies to be enabling components of multidomain resonance.

5.4. Dynamic Systems Integration Map

The DSIM would be a powerful tool that fills the need of the basic research community in a way that will naturally feed into a DoDAF compliant architecture necessary for the deployment of a far-future battlesuit. To conform emerging ISN technologies at the basic research stage into a fully DoDAF compliant format would be counterproductive. Many of the informational categories in the DoDAF views listed above do not yet have meaning or relevance for the battlesuit. But, the DSIM sets a strong foundation for eventual smooth transition to DoDAF. DSIM is a mapping of relationships. It seeks NOT to classify and compartmentalize, but instead to identify potential relationships and interactions. As these potential interactions are explored, they will lead to the development of functional interactions between technologies, and eventually to operational interactions between components. These operational connections are the prime information that the DoDAF is equipped to manage. Thus, as discussed previously, the eventual downstream system architecture will have evolved naturally from the best leverage of the science, not from an arbitrarily enforced set of definitions.

Significant future work is required to realize full development and implementation of the DSIM. To inform future research, the tool must accurately reflect the current state of the science. It requires time and effort to obtain this information from researchers; it is not a trivial task in an organization the size of the ISN. It would be a whole masters project to acquire the necessary data and develop a cohesive database so that a software program could identify the interrelationships discussed in this chapter. The commercially available Th!nkmap® line of visualization tools (http://www.thinkmap.com/) is a potential software platform to support the DSIM. To realize the full effectiveness of such a tool requires researchers to explore the map and use scientific judgement and scientific curiosity to undertake research into exploiting these interactions. The DSIM is not expected to predict the exact nature of the interactions. A tool can organize data in such a way that a trend can be recognized. Like any tool, the DSIM cannot think, it is an aid for the creative research mind. Until future work produces the necessary support software and databases, the DSIM serves as a graphical representation of an intangible integration

paradigm that informs innovation and teaming by analysis of capabilities, component types, and characteristic time, length, and energy scales.

6. Bibliography

1. Appel, Guenter, Alexandros Yfantis, Wolfgang Goepel, Dieter Schmeisser. Highly conductive polypyrrole films on non-conductive substrates. Synthetic Metals 83 (1996) 197-200
2. Bajpai, Vardhan, Pingang He, Liming Dai. Conducting-Polymer Microcontainers: Controlled Synthesis and Potential Applications. Adv. Funct. Mater. 2004, 14, No. 2
3. Bandara, U., M. Droescher, E.L. Thomas. Solid state extrusion of thermoplastic elastomers: Structure property relationships in solid state extruded block copoly (ether ester). Colloid and Polymer Science 262:538-550 (1984)
4. Bar-Cohen, Yoseph. Electroactive Polymers as Artificial Muscles. Bellingham, WA: SPIE press. 2001
5. Barisci, J.N., R. Stella, G.M. Spinks, G.G. Wallace. Study of the surface potential and photovoltage of conducting polymers using electric force microscopy. Synthetic Metals 124 (2001) 407-414
6. Bay, L., K. West, P. Sommer-Larsen, S. Skaarup, M. Benslimane. A Conducting Polymer Artificial Muscle with 12 % Linear Strain. Adv. Mater. 2003, 15, No. 3
7. Bichot, N.P., A.F. Rossi, R. Desimone. Parallel and Serial Neural Mechanisms for Visual Search in Macaque Area V4. Science, Vol. 308, 22 April 2005.
8. Bowers, Thomas. Modeling, Simulation, and Control of a Polypyrrole-Based Conducting Polymer Actuator. MS Thesis, Massachusetts Institute of Technology. 2004.
9. Cheung, J.H., A.F. Fou, M.F. Rubner. Molecular self-assembly of conducting polymers. Thin Solid Films, 244 (1994) 985-989.
10. Couvillon, J.R.. Electroactive Polymer Actuated Heart-Lung Bypass Pumps. United States Patent Application Publication. Pub. No. US2004/0068220 A1. Appl. No. 10/262, 817. April 8 2004.
11. Davidson, R.G., L.C. Hammond, T.G. Turner, A.R.Wilsom. An electron and X-ray diffraction study of conduction polypyrrole/dodecyl sulfate. Synthetic Metals 81 (1996) 1-4.
12. Deen, William M. Analysis of Transport Phenomena. Oxford University Press, February 1, 1998
13. Deshpande, S.D., Jaehwan Kim, Sung-Ryul Yun. New electro-active paper actuator using conducting polypyrrole: actuation behaviour in $LiClO_4$ acetonitrile solution. Synthetic Metals 149 (2005) 53-58.
14. Dhanabalan A., S.V. Mello, O.N. Oliveira Jr. Preparation of Langmuir-Blodgett Films of Soluble Polypyrrole. Macromolecules 1998, 31, 1827-1832.

15. Ding, J., L. Liu, G.M. Spinks, D. Zhou, G.G. Wallace, J. Gillespie. High performance conducting polymer actuators utilizing a tubular geometry and helical wire interconnects. Synthetic Metals 138 (2003) 391-398.

16. DoD Architecture Framework Working Group. DoD Architecture Framework Version 1.0, 9 February 2004.

17. DuPont Hytrel thermoplastic polyester elastomer Product Information. plastics.dupont.com. © DuPont Company 2001.

18. Edrington, A.C., A.M. Urbas, P. DeRege, C.X. Chen, T.M. Swager, N. Hadjichristidis, M. Xenidou, L.J. Fetters, J.D. Joannopoulos, Y. Fink, E.L. Thomas. Polymer-Based Photonic Crystals. Adv. Mater. 2001, 13, No. 6

19. Figuly, G.D., A.J. Soroka, M.B. Goldfinger, R.H. Mehta, H.V. Samuelson, G.P. Weeks. Stretchable fibers of polymers, spinnerets useful to form the fibers, and articles produced therefrom. United Stated Patent number 6,548,166 B2

20. Fou, A.C., M.F. Rubner. Molecular-Level Processing of Conjugated Polymers: Layer-by-Layer Manipulation of In-Situ Polymerized p-Type Doped Conducting Polymers. Macromolecules, 1995, 28.

21. Foulger, S.H., P. Jiang, A. Lattam, D. Smith, J. Ballato. Photonic Bandgap Composites with Reversible High-Frequency Stop Band Shifts. Adv. Mat. 15, 685-689 (2003)

22. Ghandi, M.R., P. Murray, G.M. Spinks, G.G. Wallace. Mechanism of electromechanical actuation in polypyrrole. Synthetic Metals 73 (1995) 247-256.

23. Greene, R.N., G.R. Goodley, C. King. Thermoplastic Copolyetherester Elastomers. United States Patent number 4,906,729. 6 Mar 1990

24. Hara, S., T. Zama, W. Takashima, K. Kaneto. Polypyrrole-metal coil composite actuators as artificial muscle fibres. Synthetic Metals 146 (2004) 47-55

25. Hecht, Eugene, Alfred Zajac. Optics. Addison Wesley Publishing Company; 3rd edition August 1, 1997.

26. Hutchison, A.S., T.W. Lewis, S.E. Moulton, G.M. Spinks, G.G. Wallace. Development of polypyrrole-based electromechanical actuators. Synthetic Metals 113 (2000) 121-127

27. Jager, W.H., E. Smela, O. Inganaes. Microfabricating Conjugated Polymer Actuators. Science, Vol 290, 24 Nov 2000

28. Karnopp, D.C., D.L. Margolis, R.C. Rosenberg. System Dynamics, A Unified Approach, 2nd edition. John Wiley & Sons Inc; 21 Aug 1990.

29. Madden, J.D., N. Vandesteeg, P.A. Antequil, P.G. Madden, A. Takshi, R.R. Pytel, S.R. Lafontaine, P.A. Wieringa, I.W. Hunter. Artificial Muscle Technology: Physical

Principles and Naval Prospects. Oceanic Engineering, IEEE Journal of. Volume 29, Issue 3, July 2004 Page(s):706 - 728

30. Madden, J.D., R.A. Cush, T.S. Kanigan, I.W. Hunter. Fast Contracting Polypyrrole Actuators. Synthetic Metals 113 (2000) 185-192.

31. Madden, John D. W., Peter G. A. Madden, Ian W. Hunter. Conducting polymer actuators as engineering materials. The International Society for Optical Engineering Proceedings Vol 4695. Smart Structures and Materials 2002.

32. Madden, John. Conducting Polymer Actuators. PhD Thesis, Massachusetts Institute of Technology. 2000

33. Madden, P.G.A., J.D.W. Madden, P.A. Anquetil, N.A. Vandesteeg, I.W. Hunter. The Relation of Conducting Polymer Actuator Material Properties to Performance. IEEE Journal of Oceanic Engineering, Vol 29, No. 3, July 2004.

34. Madden, Peter. Development and Modeling of Conducting Polymer Actuators and the Fabrication of a Conducting Polymer Based Feedback Loop. PhD Thesis, Massachusetts Institute of Technology. 2003

35. Marshall, S.L.A. The Soldier's Load and the Mobility of a Nation. © 2002, 1950 Association of the United States Army.

36. McMahon, T.A. Muscles, Reflexes, and Locomotion. Princeton Univ Pr. 1 Mar 1984

37. Nicolae, C.A., M.P. Fontana, M. Laxxeri, G. Ruggeri. Langmuir-Blodgett films of a pyrrole derivative polymerized as a monolayer. Thin Solid Films 284-285 (1996)170-173

38. Nogami, Yoshio, Jean-Paul Pouget, Takehiko Ishiguro. Structure of highly conducting PF_6^--doped polypyrrole. Synthetic Metals, 62 (1994) 257-263

39. Park, Yun Heum, Sang Jin Kim, Jun Young Lee. Preparation and characterization of electrconductive polypyrrole copolymer Langmuir-Blodgett films. Thin Solid Films 425 (2003) 233-238

40. Quake, S.R., A. Scherer. From Micro- to Nanofabrication with Soft Materials. Science, Vol 290, 24 Nov 2000.

41. Reeves, Benjamin D., Barry C. Thompson, Khalil A. Abboud, Bruce E. Smart, John R. Reynolds. Dual Cathodically and Anodically Coloring Electrochromic Polymer Based on a Spiro Bipropylenedioxythiophene [(Poly(spiroBiProDOT)]. Advanced Materials 2002, 14, No. 10, 717-719

42. Rocchia, W., A. Mazzoldi, G. Serra, D. De Rossi. Exploiting conducting polymer fiber radial expansion for bioinspired actuation. Proc. of SPIE Vol 5051. Smart Structures and Materials 2003: Electroactive Polymer Actuators and Devices (EAPAD).

43. Sadki, S., P. Schottland, N. Brodie, G. Sobouraud. The mechanisms of pyrrole electropolymerization. Chem. Soc. Rev. 2000, 29, 283-293

44. Samuleson, Vaughn. DuPont. personal communication. Aug 2004.

45. Sapp, S.A., G.A. Sotzing, J.L. Reddinger, J.R. Reynolds. Rapid Switching Solid State Electrochromic Devices Based on Complementary Conducting Polymer Films. Adv. Mater. 1996, 8, No. 10.

46. Schmid, Bryan. Device Design and Mechanical Modeling of Conducting Polymer Actuators. BS Thesis, Massachusetts Institute of Technology. 2003.

47. Schoch, K.F. Jr., W.A. Byers, L.J.Buckley. Deposition and characterization of conducting polymer thin films on insulating substrates. Synthetic Metals 72 (1995) 13-23

48. Schrenk, W., J. Wheatley. Co-extruded Elastomeric Optical Interference Film. ANTEC 1988. 1703-1707

49. Schrenk, W.J., J.A. Wheatley, R.A. Lewis, C.B. Arends. Nanolayer polymeric optical films. TAPPI Journal Vol 7. No. 6 June 1992.

50. Schrenk, W.J., W.E. Shrum, J.A. Wheatley. Elastomeric optical interference films. USP 4,937,134. 26 Jun 1990.www.freepatentsonline.com

51. Smela, E., M. Kallenbach, J. Holdenried. Electrochemically Driven Polypyrrole Bilayers for Moving and Positioning Bulk Micromachined Silicon Plates. Journal of microelectromechanical systems. Vol. 8, No. 4, Dec 1999

52. Smela, E., N. Gadegaard. Surprising volume Change in PPy(DBS): An Atomic Force Microscopy Study. Adv. Mater. 1999, 11, No. 11

53. Spinks, G., B. Xi, D. Zhou, V. Truong, G. Wallace. Enhanced control and stability of polypyrrole electrmechanical actuators. Synthetic Metals 140 (2004) 273-280

54. Spinks, G.M., G.G. Wallace, L. Liu, D. Zhou. Conducting Polymers Electromechanical Actuators and Strain Sensors. Macromol. Symp. 192, 161-169 (2003)

55. Spinks, G.M., L. Liu, G.G. Wallace, D. Zhou. Strain Response From Polypyrrole Actuators Under Load. Adv. Funct. Mater. 2002, 12, No. 6+7

56. System Architectures for Defense Systems. Telelogic White Papers. www.telelogic.com June 2005

57. TRADOC Pam 525-66. Military Operations Force Operating Capabilities. Department of the Army. Headquarters, United States Army Training and Doctrine Command. www.tradoc.army.mil 30 Jan 2003

58. Van den Schoor, R.C.G.M., R.H.M van de Leur, J.H.W. de Wit. Synthesis of a polypyrrole film on a non-conducting substrate; the influence of the oxidant and acid concentration. Synthetic Metals 99 (1999) 17-20

59. Vogel, Steven. Life in Moving Fluids: The Physical Biology of Flow. Willard Grant Press, Boson, Massachusetts. 1981.

60. Wolfe, J. Watching Single Cells Pay Attention. Science, Vol. 308, 22 April 2005.

61. Wu, Chun-Guey, Ching-Yuh Chen. Chemical deposition of ordered conducting polypyrrole films on modified inorganic substrates. J. Mater. Chem., 1997, 7(8), 1409-1413

62. Xi, Jianzhong, Jacob J. Schmidt, Carlo D. Montemagno. Self-assembled microdevices driven by muscle. Nature Materials 4 (2005)180-184

63. Yamaura M, T. Hagiwara, K. Iwata Enhancement of electrical conductivity of polypyrrole film by stretching: counter ion effect. Synthetic Metals, 26 (1998) 209-224

64. Yamaura M., T.Hagiwara, M. Hirasaka, T. Demura, K. Iwata. Structure and Properties of Biaxially Stretched Polypyrrole Films. Synthetic Metals 28 (1989) 157-164.

65. Yang, R., D.F. Evans, L. Christensen, W.A. Hendrickson. Scanning Tunneling Microscopy Evidence of Semicrystalline and Helicall Conducting Polymer Structures. J. Phys. Chem. 1990, 94, 6117-6122.

66. Yoon, Chul Oh, Hyun Kyung Sung, Jong Hun Kim, Evgenij Barsoukov, Jong Hyun Kim, Hosull Lee. The effect of lower-temperature conditions on the electrochemical polymerization of polyipyrrole films with high density, high electrical conductivity and high stability. Synthetic Metals 99 (1999) 201-212.

67. Young, W.C., R. Budynas. Roark's Formulas for Stress and Strain. McGraw-Hill Professional. 7th edition. 13 Sept 2001

68. Zhang, Q.M., Vivek Bharti, Z. Zhao. Giant Electrostriction and Relaxor Ferroelectric Behavior in Electron-Irradiated Poly(vinylidene fluoride-trifluoroethylene) Copolymer. Science 280 (1998) 2101-2104